INFORMATION TO USERS

This material was produced from a microfilm copy of the original document. While the most advanced technological means to photograph and reproduce this document have been used, the quality is heavily dependent upon the quality of the original submitted.

The following explanation of techniques is provided to help you understand markings or patterns which may appear on this reproduction.

1. The sign or "target" for pages apparently lacking from the document photographed is "Missing Page(s)". If it was possible to obtain the missing page(s) or section, they are spliced into the film along with adjacent pages. This may have necessitated cutting thru an image and duplicating adjacent pages to insure you complete continuity.

2. When an image on the film is obliterated with a large round black mark, it is an indication that the photographer suspected that the copy may have moved during exposure and thus cause a blurred image. You will find a good image of the page in the adjacent frame.

3. When a map, drawing or chart, etc., was part of the material being photographed the photographer followed a definite method in "sectioning" the material. It is customary to begin photoing at the upper left hand corner of a large sheet and to continue photoing from left to right in equal sections with a small overlap. If necessary, sectioning is continued again — beginning below the first row and continuing on until complete.

4. The majority of users indicate that the textual content is of greatest value, however, a somewhat higher quality reproduction could be made from "photographs" if essential to the understanding of the dissertation. Silver prints of "photographs" may be ordered at additional charge by writing the Order Department, giving the catalog number, title, author and specific pages you wish reproduced.

5. PLEASE NOTE: Some pages may have indistinct print. Filmed as received.

Xerox University Microfilms
300 North Zeeb Road
Ann Arbor, Michigan 48106

THE EFFECT OF NEAR ULTRAVIOLET RADIATION ON THE MORPHOLOGY OF NYLON 66

by

Barbara Spilker Stowe

A Dissertation Submitted to
the Faculty of the Graduate School at
The University of North Carolina at Greensboro
in Partial Fulfillment
of the Requirements for the Degree
Doctor of Philosophy

Greensboro
1972

Approved by

Dissertation Adviser

Dissertation Adviser

APPROVAL PAGE

This dissertation has been approved by the following committee of the Faculty of the Graduate School at The University of North Carolina at Greensboro.

Dissertation Advisers ____________________

____

Oral Examination Committee Members ____________________

____

____

____

October 19, 1972
Date of Examination

STOWE, BARBARA SPILKER. The Effect of Near Ultraviolet Radiation on the Morphology of Nylon 66. (1972)
Directed by: Dr. Victor S. Salvin
Dr. Raymond E. Fornes

Pp. 172

Photodegradation of nylon 66 resulting from outdoor exposure and simulated weather conditions has been reported. Tensile strength losses and photochemical decomposition have been shown to occur on exposure to broad band irradiation. Physical properties of textile materials are intimately related to fiber structure. Therefore, any insights into phenomena which alter that structure, and consequently affect the expected performance of textile goods, would be useful.

This study examined the morphology of nylon 66 fibers as affected by near ultraviolet (UV) irradiation in a dry oxygen atmosphere. Ninety percent emission from the irradiation source was at 3500 ± 500 Å, a wavelength range found in sunlight at the earth's surface.

A commercial nylon 66 multifilament yarn with a 5:1 draw ratio and filament denier of approximately 6 was used. The scoured, evacuated yarn was wound in a single layer around a quartz cylinder, placed in a quartz tube, flushed with dry oxygen and sealed. The quartz apparatus was then placed in a Rayonet Photochemical Reactor where it was exposed to UV for 72, 142, and 240 hour periods. The

temperature in the reactor was approximately 52°C.

Ultraviolet exposure effects were assessed by intrinsic viscosity, acid dye take-up, density, wide line nuclear magnetic resonance (NMR), and differential scanning calorimetry (DSC) measurements.

Intrinsic viscosity and viscosity average molecular weight decreased with increasing UV exposure time. There was no evidence of gel formation after any exposure period. Viscosity average molecular weight decreased from an initial 17,100 to 10,900 on 240 hours exposure indicating considerable chain scission had occurred.

Dyeings with Anthraquinone Milling Blue BL (C. I. 122) indicated that increasing UV exposure time changed fiber molecular structure such that dye diffusion was restricted, particularly early in the dyeing process. Control yarns exhausted the dyebath in 20 minutes, but yarns exposed 240 hours did not exhaust in 45 minutes dyeing time. Dyeings with Merpacyl Blue SW (C. I. 78) indicated that on 240 hours UV exposure some amine end groups were lost by chemical change or made inaccessible to dye. However, the effect was too small to account for all the change in diffusion rate.

Density, initially 1.148 gm/ml, increased to 1.153 gm/ml on 240 hours exposure. The change corresponded to a 3% increase in crystallinity.

At the maximum UV exposure time second moment, as measured by wide line NMR, increased by approximately 1.0 gauss^2 when spectra were recorded at lower temperatures, but at

140°C there was no change from the control. This suggested there was no measurable chain disruption in original crystallites but after UV irradiation mobility in the amorphous regions was reduced. However, the restriction was not so great as to overcome all increase in mobility brought about by chain scission. The α-transition in line width of the narrow component of the NMR line was shifted to higher temperatures on prolonged UV exposure. This was taken as further evidence of decreased mobility in the amorphous regions of the fiber.

DSC thermograms for yarns exposed to UV for 240 hours exhibited lower melting shoulders on the major melting peaks. These shoulders were interpreted to be the melting peaks of small crystallites formed on prolonged UV exposure.

The study has shown that photooxidation at 3500 Å under dry oxygen atmosphere caused chain scission and an increase in molecular order in nylon 66 fibers. The findings suggest that the newly freed chain ends resulting from cleavage in the less ordered regions of the fiber relaxed into a crystalline configuration.

ACKNOWLEDGMENTS

The author wishes to express sincere appreciation to:

Dr. Victor S. Salvin, Co-chairman of the Dissertation Committee at the University of North Carolina at Greensboro, for guidance in design and completion of the research and particularly for suggesting dyeing as a measurement of ultraviolet effects;

Dr. Raymond E. Fornes, Co-chairman of the Dissertation Committee at North Carolina State University, who with unparalleled patience and skill assumed major responsibility for direction of the research;

Dr. Eunice M. Deemer, University of North Carolina at Greensboro, who with great kindness and efficiency assumed major responsibility for direction of the graduate program;

Dr. Richard D. Gilbert, North Carolina State University, who provided laboratory facilities and gave so generously of advice and counsel;

Dr. Pauline Keeney, Chairman of Textiles and Clothing at the University of North Carolina at Greensboro, for interest and guidance in design and completion of the graduate program;

Dr. Harvey Herman, University of North Carolina at Greensboro, for kindly serving as a member of the Dissertation Committee;

Professor Henry A. Rutherford, Chairman of Textile Chemistry at North Carolina State University, who extended the invitation to a most rewarding experience of inter-campus study;

American Home Economics Association for generous assistance in the form of the Ellen H. Richards Fellowship;

Chemstrand Research Center for kindly supplying the experimental yarns; and to the

E. I. duPont de Nemours Company for kindly providing experimental dyes.

TABLE OF CONTENTS

LIST OF TABLES

LIST OF FIGURES

CHAPTER I

INTRODUCTION

Nylon 66 was the first successful manmade polyamide polymer and is still used widely in textile applications. In many respects it has become quite well characterized through research efforts to solve technical production problems; through searches for new commercial applications; and through efforts to overcome practical shortcomings encountered in use. One such shortcoming is a sensitivity to sunlight and atmospheric degradation.

Outdoor exposure studies have been valuable in identifying constituent elements of the degradation process. Unfortunately, the great complexity of the degrading system termed "weather" has limited the reproducibility of results and pointed only generally to the mechanisms of deterioration.

Laboratory studies have helped elucidate the products of ultraviolet (UV) and atmospheric degradation but the effect on physical properties of polymeric materials is limited largely to the resultant changes in tensile properties. Most laboratory studies have employed broad band wave sources which include some visible and far ultraviolet as well as near ultraviolet light, the latter being found in sunlight at the earth's surface. When the effect of monochromatic UV light has been reported, it has usually been

from a low pressure mercury vapor lamp which emits at 2537 Å, a wavelength not present in sunlight at the earth's surface.

Shorter wavelength UV and high energy irradiation (x-ray, gamma, electron) of polymeric materials have been shown to produce considerable morphological change in polymers. Depending upon polymer type, irradiation energy level, and the reaction atmosphere, polymers may be predominantly cleaved, branched, or crosslinked. Irradiation reactions from widely varying energy sources are known to proceed via free radical mechanisms; consequently it is reasonable to assume some similarities may exist between irradiation effects from high energy and lower, for example, near ultraviolet, energy sources. Differences would surely be anticipated as well. Fast electrons, gamma and x-rays are capable of removing electrons indiscriminately in amorphous or crystalline regions leaving ion fragments, or of causing many secondary reactions as the high energy beam of particles is dissipated within the polymeric system. Near ultraviolet radiation is several orders of magnitude lower in energy. Energy levels are in fact of the same magnitude as some bond energies in polyamides. Near UV energy absorption, then, is far more specific and may be expected to have related but not necessarily the same effect on polymer morphology as high energy irradiation even under the same exposure conditions.

Laboratory UV studies make possible the use of controlled atmospheres so that interdependence of atmosphere and

irradiation may be detected. There is evidence, particularly on irradiation at longer wavelengths, that an oxygen atmosphere is more degrading than nitrogen as measured by loss in tensile properties, intrinsic viscosity, and decomposition products. The presence of oxygen at the site of a free radical in the polymer leads to the formation of a peroxide radical with subsequent chain scission. The presence of water in the polymer is likely to enhance oxidative degradation through the formation of hydroperoxides. The presence of TiO_2 delustrant has also been shown to accelerate photodegradation. Under nitrogen atmosphere at longer wavelengths there may be no loss of tensile strength. In fact, strength may even increase. Presumably free radicals tend to recombine, or if molecular motion is sufficient, to crosslink with radicals on neighboring polymer chains, hence the possibility of increased tensile strength.

Most weathering and UV studies appear to be carried out at ambient temperatures. One UV degradation study (2) reported temperatures up to $60^{o}C$ had little effect on the photodegradation of nylon 66.

The wide use of nylon 66 in consumer applications, particularly where exposure to sunlight is encountered, would seem to justify further understanding of the degradation process. Physical properties of textile materials are intimately related to fiber structure. Therefore, any insights into phenomena which alter that structure, and consequently affect the expected performance of textile goods, would be useful.

The effect of a narrow wave band of near UV irradiation on the morphology of nylon 66 should make a contribution to the currently existing body of knowledge of irradiation effects on fiber structure. The objective of this study then, was:

To determine the onset and course of ultraviolet effects on the fine structure of a nylon 66 yarn under dry oxygen and nitrogen atmospheres.

The hypothesis tested was:

Nylon 66 yarns exposed to 3500 Å radiation will exhibit measurable change in fine structure.

A. Nylon 66 yarns exposed to ultraviolet radiation at 3500 Å in the presence of oxygen will exhibit change sooner and at a more rapid rate than yarns exposed in a nitrogen atmosphere.

B. Nylon 66 yarns exposed to ultraviolet radiation in atmospheres of oxygen and nitrogen will exhibit increased molecular order but at different rates.

Early indications in the investigation were that irradiation of nylon 66 at 3500 Å in a nitrogen atmosphere would require unduly long exposures to detect any measurable change. Consequently, all discussion of experimental results pertains to yarns exposed to UV in an oxygen atmosphere unless otherwise denoted.

The two principal measurement techniques chosen to assess UV effects on morphology were acid dyeing rate and

wide line nuclear magnetic resonance (NMR). Certain anionic dyes have been shown to be sensitive to changes in molecular order on drawing and heatsetting of nylon. Therefore, it seemed reasonable that such dyes would detect similar effects if they resulted from UV exposure. Wide line NMR has relatively recently been applied in the study of polymeric structure. It has been successfully used to study molecular motion as affected by temperature and solvents and to assess crosslinking on high energy irradiation. It was of experimental interest to employ this technique in the measurement of UV effects on morphology of nylon 66.

CHAPTER II

REVIEW OF LITERATURE

Irradiation of Polymeric Materials

The effects of bombarding textile and plastic polymeric materials with energy of varying sources is of practical, commercial, and academic interest. High energy irradiation such as electron beam, gamma, and x-radiation has been exploited commercially to initiate polymerization and to effect desired properties such as crosslinking and grafting (62, 25). Lower energy irradiation from ultraviolet and visible light is of interest as these energy forms are constituents of sunlight and consequently affect the useful life of textile materials. Thermal energy effects are of commercial and practical interest as well but are not reviewed here.

The present work is primarily concerned with the effect of a narrow wave band of near ultraviolet energy on the physical structure of a nylon 66 yarn when exposure conditions are controlled. The experimental findings are discussed below in relation to other UV and weathering studies and to reports of higher energy irradiation effects.

Energy Levels from Various Sources

High energy irradiation usually is taken to include beams of fast electrons, fast protons, fast neutrons and electromagnetic radiation such as gamma rays and x-rays. In

the latter, high energy photons exhibit properties analogous to high energy particles. The energy carried by each particle or photon considerably exceeds the binding energy of electrons to their nucleus and bond energies between atoms.

A usual effect of high energy particles is ejection of electrons, leaving charged molecular fragments (ions). In addition to ionization, the beam of particles may excite electrons (raise them to a higher energy state without detachment from the parent atom) or cause secondary reactions as the particles lose energy to the medium. The scattered energy may be sufficient to cause secondary ionization or excitation but most energy is dissipated as thermal vibrations.

The form of ionizing energy, be it fast electrons, gamma or x-rays, matters little. The ejected electrons are captured by neighboring molecules creating (+) and (-) charged species. The energy absorbed per ion pair is approximately 34 eV, the considerable excess energy being dissipated as secondary reactions or as thermal energy (25).

Ionizing radiation particles penetrate the medium at random, indiscriminately removing electrons from molecules in the path of the beam. In turn dissipation of energy may occur from elastic collisions with electrons (Compton scattering of x-rays) or other secondary effects. For example, the probability of ionization or excitation depends on the velocity of electrons in the beam as they penetrate the medium. Early in the path when electrons are most energetic

the probability of dislocation from the medium with sufficient energy to cause further ionizations or excitations is highest.

The passage of an x-ray or gamma photon through a medium may produce one or more fast electrons and lower energy x-rays. The liberation of fast electrons causes further ionization. Thus x-rays and gamma rays are actually internal sources of electron irradiation (25).

Along the track of a fast electron, excitation and ionization occur in clusters. Each primary track may be thought of as a cylinder through which radicals have diffused at random. Magee (65) observed that a certain portion of radicals in a single track react with each other, the remainder diffuse away to give a general background which can react at random with radicals from other tracks. Additives such as I_2, which act as scavengers for radicals, when present in low concentration will react primarily with the background radicals but will be unable to compete effectively with radical-radical recombination in the dense portion of the track.

Analogously, the cage effect in solid polymers may prevent direct decomposition of excited polymers into two radical chains. Rather slow rearrangement to a more stable structure follows, rate depending upon the temperature (25).

Generally, ultraviolet radiation is sufficient to cause excitation in many molecular structures but is not energetic enough to cause ionization, with the possible exception of

the far UV. Further, the energy range of ultraviolet photons is similar to many bond energies in polymers. For this reason UV absorption is considerably more specific than high energy absorption. As with ionizing irradiation secondary reactions can occur as a result of excitation and the presence of additives or impurities in the polymeric material.

UV radiation requires more than 3.5 times as much energy to produce one macro-radical in polyethylene at 77 K as does ionizing radiation. To produce a three dimensional network requires 100 hours of intensive UV irradiation but a 92% gel can be obtained in less than 250 minutes with an ionizing dose of 70-100 Mrads (57).

Table 1 lists some bonds and associated energies found in polymers. The ultraviolet source used for the present study has a narrow wave band, 90% in the 3500 Å region. The associated energy of 3500 Å is 82.2 kcal/mole or energy sufficient to cleave C-N, C-C, and methylene hydrogen bonds in polyamides. Figure 1 indicates 3500 Å is a wavelength midway in the UV portion of sunlight which strikes the earth's surface.

Laboratory studies of ionizing irradiation effects involving exposure of textiles, fibers, or plastic films employed total doses ranging from 1 to 1.28 x 10^4 Mrads. Table 2 indicates this may be several orders of magnitudes higher than UV irradiation.

Intensity of sunlight varies with wavelength and with season, hour, and atmospheric conditions (26, 51, 100, 129).

TABLE 1

ENERGIES AND WAVELENGTHS OF SOME CHEMICAL BONDS AND A PORTION OF THE ELECTROMAGNETIC SPECTRUM

Electromagnetic Spectrum	Chemical Bond	Energy kcal/mole	Energy eV/bond	Wavelength(Å)
	C-N	65.9	2.86	4332
	C-H	71.0	3.08	4021
	CH_2	76.0	3.29	3737
	C-O	79.6	3.45	3596
	C-C	80.0	3.47	3603
	---	82.2	3.54	3500
	N-H	92.0	3.99	3106
	CH_3	98.7	4.28	2896
	ϕ-H	100.7	4.37	2836
	O-H	109.4	4.75	2609
	C=C	140.5	6.09	2035
	C=O	168.8	7.32	1695
Visible Light		41 - 71		7000-4000
Near Ultraviolet		71 - 95		4000-3000
Far Ultraviolet		95 -143		3000-2000
X-ray		953 -2.9×10^5		300- 1
Gamma ray		2.9×10^7		0.01

TABLE 2

RADIATION ENERGY UNIT EQUIVALENTS

1 megarad	= 10^6 rads
	= 10^4 mwatt·sec/gm = 10^7 watt·sec/gm
	= 2.78×10^{-3} watt·hr/g
	= 10^{15} nvt [neutrons/cm^2/sec] x [exposure time (sec)]
	= 2.389×10^{-3} kcal/gm
	= 6.24×10^{19} eV/gm = 10 joules/gm
1 eV/bond	= 6.02×10^{23} eV/mole = 23.06 kcal/mole
1 roentgen	= radiation required to produce 1 esu of ions/cm^2
rep (roentgen equivalent physical)	= absorbed radiation dose in roentgens/cm^2 of tissue

The ultraviolet portion of the spectrum is particularly affected as that radiation is scattered by constituents of the atmosphere. Generally, maximum intensity occurs on clear days in July at noon, although midday readings in June and August are quite similar to July. Figure 2 shows a spectral distribution with associated intensities recorded on an August day in Stamford, Connecticut. At this location the UV portion of total sunlight intensity ranges from less than 1% to 7% depending upon the time of day and season. The fraction of shorter wavelength UV irradiation (<3400 Å) to the total ranges from 2.5% to 16.5%.

Weathering Studies

The practical matter of deterioration of plastic and textile materials on outdoor exposure has produced many studies of the phenomena. Unfortunately, the great complexity of the degrading system termed "weather" has limited reproducibility of results and explained little about the actual mechanisms of deterioration. However, these studies have been valuable in elucidating constituent elements of "weather" and in suggesting many refinements in experimental design which have made a far better understanding of degradation possible.

Perhaps the most important element of weather is sunlight. Therefore considerable effort has been made to analyze the spectral distribution and intensity levels of sunlight. Intensity levels at different parts of the

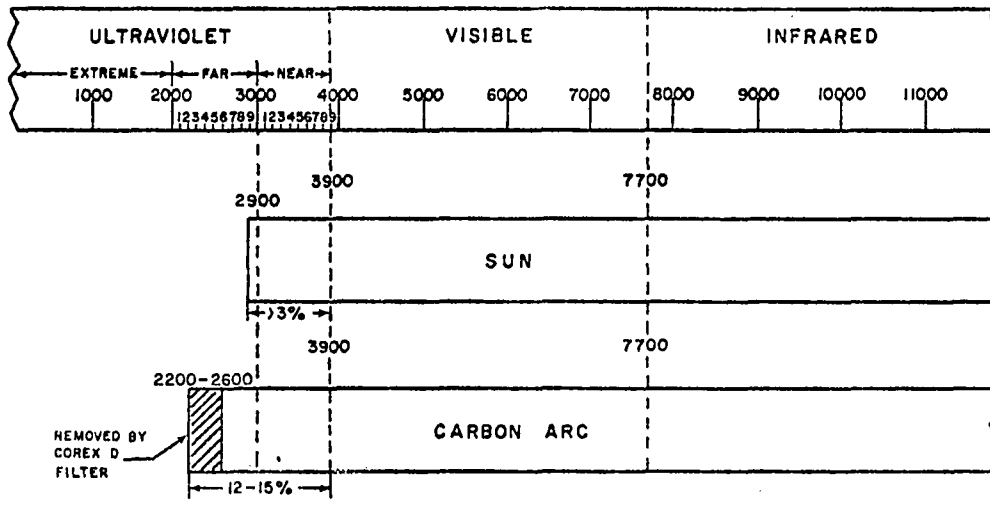

Figure 1 - Spectral distribution in Angstroms of sunlight at the earth's surface and the carbon arc (38).

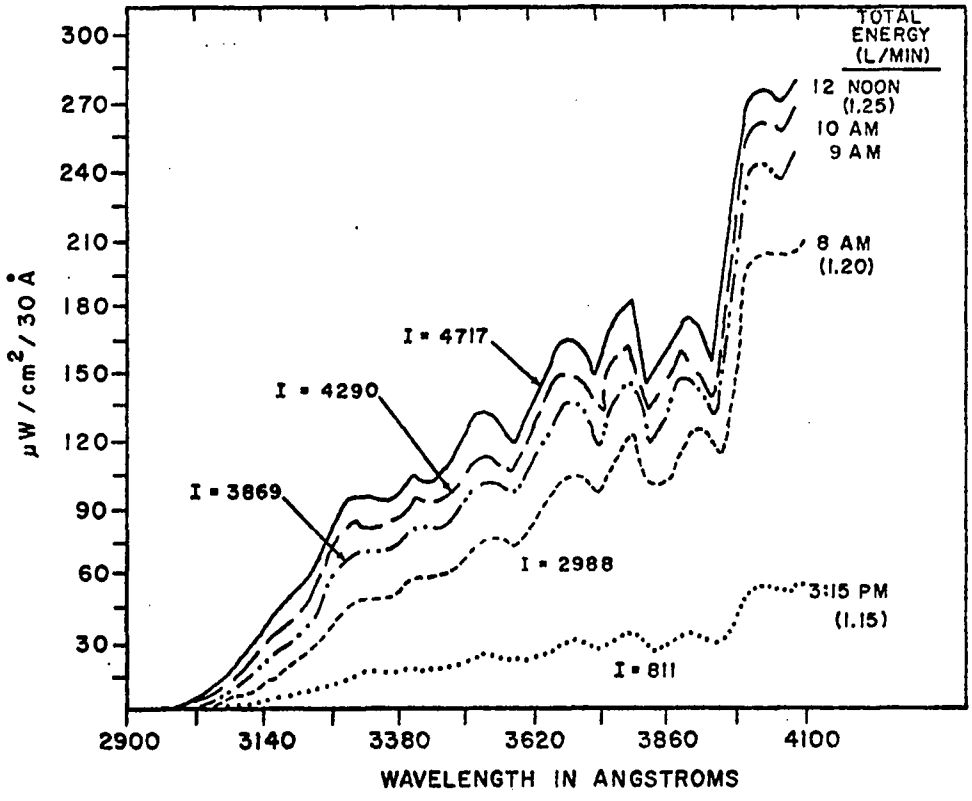

Figure 2 - Daily variation in spectral energy distribution of sunlight on August 19, 1958. Solar altitude at noon about 64°. (Clear sky, some scattered clouds at noon.) (I) integrated ultraviolet energy in microwatts (51).

spectrum have been shown to vary considerably with season, time of day, and geographical location.

Coblentz (26) collected data on intensity variations in the 2900-3150 Å range over an eight year period in the Washington, D. C. area. Maximum intensities in the range were found to occur in July.

Using strength loss of nylon, polyester, and acetate face fabrics as a measure of degradation, Singleton, et al (100) found results to vary greatly from summer to winter and from Florida to Arizona even though results were calculated on incident irradiation. However, when results were based on a ratio of Coblentz factors of UV intensity to total incident irradiation the seasonal differences were diminished. The geographical difference in results was attributed to variation in relative humidity between Florida and Arizona.

More recently Singleton and Cook (99) have attempted to broaden Coblentz' studies of spectral distribution and intensity to include more wavelengths. For comparable wavelengths, plots of UV intensity versus season were similar for Washington, D. C.; Miami, Florida; and Phoenix, Arizona. However, near UV and visible intensities varied considerably with season between the two latter sites. Strength loss of polyester, nylon, and acetate fabrics was greater at shorter wavelengths (approximately 3000 Å) in Arizona and at longer wavelengths in Florida where intensity at approximately 3200 Å radiation was much greater in July and August.

Little and Parsons (63) exposed cotton, nylon, and terylene fabrics at eight sites in the United Kingdom a total of 12 months. All fabrics were more resistant to deterioration in rural than urban areas as measured by strength loss and decrease in viscosity. Nylon deteriorated more than the other fabrics in rural areas but was superior to cotton on urban exposures.

Drapery fabrics of cotton and rayon/acetate were exposed out of doors in Tallahassee, Florida and Charleston, West Virginia during summer and winter months (86). The effect of full intensity sunlight on the rate of deterioration was evident. The polluted atmosphere of Charleston was shown to accelerate deterioration of cotton.

Despite the variations in sunlight many attempts have been made to design laboratory instruments to simulate it and other weather conditions; usually in such a way that specimen degradation rate is accelerated (115). Unfortunately, the enclosed carbon arc sources which are most used correlate least well with sunlight. Unless suitable filters are used the spectrum includes far UV which is not in sunlight at the earth's surface. Further, the intensity of several wavelengths is very different from corresponding intensities of sunlight. The Sunshine Carbon Arc is an improved version which corresponds much more closely to sunlight (51).

The xenon arc source has a spectrum most nearly like that of sunlight but is not sufficiently similar to give reproducible results. Wall, et al (129) determined from a

careful comparison of xenon arc spectra with sunlight that the xenon arc is lower in relative intensity at wavelengths greater than 3350 Å. They attributed discrepancies in nylon breaking strength between sunlight and xenon arc exposures to the fact that scissionable bonds in nylon absorb at wavelengths above 3350 Å where xenon arc intensity is lower. Results for polyester were comparable for the two sources because polyester bonds absorb at low wavelengths where sun and xenon arc have comparable intensities.

The exposure times required to obtain measurable degradative results are often inconveniently long. Therefore, attempts have been made to accelerate degradative processes. A reasonable means would seem to be to increase the intensity of the irradiation. Hirt and Searle (51) described an outdoor exposure unit fitted with a system of mirrors which increased sunlight intensity ten times. However, degradation rate increases varied from two to eleven times depending on the polymer system being studied. In a comparison of several sources on the degradation of dyed and undyed nylon yarns an American Association of Textile Chemists and Colorists Committee concluded that two hours exposure to a laser (3400 Å) was comparable to 200 hours in the Fadeometer, as measured by tensile strength retention (4).

Despite the problems encountered in weathering studies several generalizations have emerged which have provided a basis for laboratory investigations. The portion of the spectrum most deleterious to textile materials is the near

ultraviolet (3000-4000 Å) (26, 51, 76, 100). In addition, degradation is variously affected by the presence of air, moisture, heat, and fiber additives.

Laboratory Studies of Ultraviolet Degradation

Moore (76) examined the effect of sunlight and other ultraviolet sources on bright and delustered yarns of nylon 66, 610, 106, and 6 under varying conditions of atmosphere (N_2, O_2, vacuum) and humidity. The presence of moisture had very little effect on the tensile strength of nylon 66, although bright yarn lost slightly more strength under dry than wet conditions. Above 3000 Å, moisture slightly enhanced the degradation of delustered yarns. Generally, delustered yarns were more sensitive to radiation at longer wavelengths (ca 3500 Å) and bright yarns sensitive to shorter wavelengths (below 3000 Å). In all cases the presence of oxygen resulted in greater losses in tenacity. Generally, the rate of loss of tenacity and extensibility decreased with increased exposure time, delustered yarns losing strength much more rapidly than bright. Strength loss was accompanied by a progressive decrease in intrinsic viscosity and hence molecular weight. Relationships of strength loss and intrinsic viscosity were nearly linear for bright yarns and linear for delustered yarns to approximately 75% tenacity loss. Chemical analysis of the exposed yarns revealed that oxidative attack was primarily at the methylene group adjacent to the N atom of the amide group.

Achhammer, et al (2) investigated the effect of heat, ultraviolet light from an RS sunlamp, and outdoor exposure on a series of polyamide copolymer films 0.002-0.004 inch thick. Sunlamp exposures consisted of 20 hour cycles followed by four hours of fog. Outdoor exposure involved a wide variation in temperature and relative humidity, with 530 total sun hours over a period of 61 days. All samples lost tensile strength and elongation on outdoor exposure but no significant differences among films were noted. A wide range of analyses indicated that the films were degraded, chemical structure of the polymers was affected, and crystallinity was possibly affected upon exposure to the sunlamp. Temperatures up to 60°C had no measurable effect on the films nor did storage for three weeks following UV exposure. There were appreciable decreases in intrinsic viscosity with accompanying decrease in viscosity average molecular weight ($M_{\bar{v}}$) of 12,800 (from 16,300 originally) following 168 hours UV exposure. Polarized light microscopy and electron photomicrographs indicated UV exposure increased crystallinity; but x-ray diffraction, electron diffraction, and electrical property changes did not indicate increased order. Mass spectroscopy, pyrolysis, and UV transmission data revealed the loss of water on irradiation. The authors suggested the loss of water reduced plasticity and thus could have affected an increase in molecular order. The loss of the small polar molecules along with shortening of polymer chains could cause molecular rearrangement.

Egerton (34) exposed nylon 66 films to UV in the presence of oxygen and nitrogen. Atmosphere was reported to have no effect on absorption spectra. The greatest difference in exposure effects was related to wavelength. Exposure to low pressure Hg vapor light (2537 Å) produced profound changes in absorption spectra which were completely different from near UV and visible effects. It was suggested that the far UV creates free radicals which are trapped in the polymer matrix and slowly recombine on storage.

Stephenson, et al (111, 112, 113) examined the effects of ultraviolet irradiation of varying wavelengths on physical (scission and crosslinking) and chemical (degradation) properties of a group of polymer films including nylon 66 (1.0 mil thick); polyester (0.25 mil); high density polyethylene (1.0 mil); Teflon (1.0 mil), and acrylic fibers. Exposures were made in nitrogen and in vacuum with lamp intensities of 1, 6, and 7.5 mw/cm^2 at 2440, 3140, and 3690 Å, respectively. All polymers decreased in tensile strength and elongation more at shorter than longer wavelengths; 3690 Å had considerably less effect than 3140 and 2440 Å. When polymers were exposed to 2537 Å up to approximately 180 hours in vacuum and nitrogen all except Teflon decreased more in tensile strength and elongation under nitrogen than under vacuum. Several films showed initial increases in elongation and tensile strength followed by decreases. Nylon 66 film lost tensile strength continuously in vacuum. Strength increased

initially then decreased. The loss was approximately five times greater in nitrogen than vacuum at 200 hours exposure. Elongation increased initially, but decreased considerably more in nitrogen than in vacuum. It was concluded that changes in tensile properties induced by short wavelength UV were similar to changes resulting from high energy irradiation. When an intrinsic damage index (fractional decrease in ultimate elongation/joule/cm^2 of incident energy) was plotted versus photon energy it was noted no damage occurred in polyethylene, polyester, or Teflon below approximately 3.4 eV which corresponds to the energy of C-C bonds.

Possible crosslinking and chain scission (111) were examined for polymers exposed in nitrogen and vacuum at 2537 Å for periods up to 800 hours. Gels were formed in all polymers more readily in vacuum than in nitrogen, except none was formed when polyester was irradiated in nitrogen. Nylon 66 formed 70% gel in 100 hours irradiation in vacuum and a maximum of approximately 45% in 100 hours exposure in nitrogen. The authors noted crosslinking in the absence of oxygen is similar to the effect resulting from ionizing radiation. Of importance here is the fact that crosslinking, as measured by a decline in the scission to crosslinking ratio, occurs almost twice as rapidly in vacuum as in nitrogen. When off gases (113), hydrogen and methane, were monitored, considerably more H_2 was liberated from vacuum irradiation of nylon than from nitrogen. Methane liberation was comparable for the two atmospheres.

These results (113), in conjunction with scission/crosslinking ratios and tensile strength findings were taken as evidence that pressure differences are very significant in determining irradiation effects. Supposedly, pressure of the nitrogen atmosphere prevents migration of H· (created by photolysis) out of the polymer matrix and instead favors recombination, a condition which decreases the probability of crosslinking between polymer radicals. In addition, under these conditions, the -C· formed by C-C bond rupture would have a higher probability of combining with H· and hence more chain scissions would occur.

The effects of UV irradiation on nylon 6 films in vacuo were studied with ultraviolet and infrared spectroscopy and electron spin resonance (87). Films were exposed to the full spectrum of the quartz-Hg lamp and to the near UV, that is with wavelengths less than 3000 Å filtered out. Samples were evacuated in the reaction vessel for 24 hours prior to exposures from 2 to 140 hours at 30 ± 2°C. Chromatography showed that the full spectrum lamp exposure caused liberation of H_2 and CO with additional small quantities of short chain hydrocarbons. The quantity of liberated H_2 was large, 26.2 ml or 9 moles of gas/1000 polyamide chain units, after 120 hours UV exposure. Stephenson (113) reported approximately 0.2 ml H_2 evolved after 120 hours exposure of nylon 66 film to 2537 Å irradiation in vacuum. From calculations (87) of the amount of CO liberated per 1000 polymer chains for a polymer of Mw 16,000, it was determined that on 120 hours

exposure less than two C-N chain bonds were ruptured with subsequent splitting off of CO, but approximately 18 C-H bonds broke to liberate H_2. Therefore, if only a portion of the radicals formed from C-H rupture recombined, crosslinking of the polyamide would predominate over degradation. Indeed, there was an increase in intrinsic viscosity; Mv; and the Huggins constant, the latter indicating chain branching. On only five hours exposure an insoluble gel was formed, the quantity of which increased with duration of exposure. It was concluded that the formation of crosslinks was greater than chain scission but the number of crosslinks formed was relatively small.

Rafikov and Tsi-Pin (87) reported no evidence of crosslinking up to 140 hours exposure to near UV. Intrinsic viscosity decreased with exposure time. Gas evolution was predominately H_2 and CO, but quantities were much lower than obtained with full UV spectrum exposure. For example, during 50 hours exposure 0.15 ml H_2 was liberated compared to about 15 ml for a similar period of full spectrum UV exposure. Electron spin resonance measurements indicated the predominant radical formed for all wavelengths was $--CH_2-\dot{C}H-NH-CO-CH_2--$. Mechanisms of degradation were presented which are reviewed below.

Egerton, et al (33) examined the effect of temperature and atmosphere on photolytic degradation of silk, acetate, and delusterant free nylon yarns by exposure to 2537 Å with subsequent measurements of tensile strength. All fibers

retained tensile strength in both nitrogen and oxygen when exposed at temperatures below 0°C for 20 hours. However, tensile loss rose abruptly with temperature above 0°C reaching maxima at approximately 50°C. Silk and acetate lost approximately two-thirds as much strength in a nitrogen atmosphere as in oxygen. Nylon lost virtually no strength in a nitrogen atmosphere but lost 75% strength when exposed at 50°C in oxygen. The retention of tensile strength at low temperatures and in the absence of oxygen was attributed to recombination of free radicals formed on photolysis. Others suggested reactivity is inhibited by immobility of chains and radicals at low temperatures. The presence of water (100% RH) (35) inhibited strength loss on irradiation of silk and nylon but not acetate. Nylon lost considerably more strength dry than wet. It was suggested that secondary reactions between polymer and water molecules may have occurred.

Oxygen in Polymer Degradation

The presence of oxygen has been shown to be important in the degradation of irradiated polymers particularly at longer wavelengths. The use of films in irradiation studies has emphasized this and pointed to the diffusion rate of oxygen as a controlling process in photooxidation.

Maximum absorption of UV radiant energy occurs at the surface of plastics containing a uniform distribution of absorbing groups, thus thin films are especially vulnerable to photooxidation, and surface regions of thicker specimens crack, chalk, and discolor during irradiation (133).

Searle (94) reported that when films are more than one millimeter thick, ultraviolet degradation is essentially a surface phenomenon and therefore surface features such as gloss, haze, and microscopic topography may show irradiation effects before mechanical property changes are evident.

The absorption of light was almost complete in polystyrene films 0.01 mm thick (54). When oxygen was present films degraded under 3650 Å radiation. Photooxidation proceeded 40 times faster at 2537 Å.

Carlsson and Wiles (20) exposed polypropylene films 22μ thick to near UV irradiation (>3200 Å) in the presence of moving air up to 80 hours. Temperature and wavelength were carefully controlled as they were shown to greatly affect the photooxidation rate. Degradation rate was monitored by Attentuated Total Reflectance (ATR) and infrared spectroscopy bands which correspond to hydroperoxide groups (3400 cm^{-1}) and carbonyl groups (~1715 cm^{-1}); density; and elongation. With increasing exposure time, carbonyl and hydroperoxide content increased as did density, but elongation decreased to zero at 50 hours exposure. ATR analysis revealed extensive photooxidation near the film surfaces but very little oxidation in the bulk of the sample. Extensive surface oxidation had occurred prior to the considerable embrittlement of the films at approximately 30 hours exposure, but oxidation proceeded inward up to 80 hours. Since density changes can be expected to occur only in the photooxidized surface layers, observed overall density increases indicate that very

high densities (corresponding to almost 100% crystallinity) must exist in these regions. This conclusion is consistent with the fact that oxidation is normally confined to amorphous regions (limited oxygen permeability of crystallites). Therefore considerable restructuring of surface amorphous content must occur due to extensive chain scission. Evidence of this restructuring has been shown by electron micrographs where cracks are displayed. These cracks must have accounted for reduced elongation.

Zimmerman (137) irradiated nylon yarns with high energy electrons and examined the rate of oxygen diffusion following irradiation. Post-irradiation diffusion was determined spectrophotometrically as colors produced by irradiation disappear slowly in the absence of oxygen; more quickly in the presence. For filaments, its colors disappear quickly. Cross sections of thicker irradiated film showed a sharp boundary where colors existed on the interior of the film but the exterior was colorless. When apparent end group concentration (from viscosity measurements) was plotted versus fiber diameter for various irradiation doses it was shown there is a rapid decrease in extent of degradation as fiber diameter increases up to 30μ with a much smaller dependence on diameter beyond presumably because by the time oxygen has diffused to the fiber interior free radicals have terminated by other means. In an oxygen atmosphere penetration rate was approximately 15μ/70 minutes in previously irradiated samples.

A study of oxidative degradation of nylon 66 filaments in water at 80°C up to 24 hours was carried out by Vachon, et al (126). The filaments were in a 50 den/17 filament yarn which contained 0.025% and 0.015% TiO_2. Degradation as measured by intrinsic viscosity was most severe at pH 8. The authors suggest that H_2O_2 formed by the reaction acts as a degradation catalyst at pH 8. Both drawn and undrawn filaments increased in density at higher pH. Undrawn fibers showed higher increases in less time (8 hours). Density increases were expected as the molecular weight decreased. It is expected that shorter chains should have greater mobility and thus be capable of greater ordering. A further observed phenomenon was severe surface cracking of filaments exposed to aqueous oxygen systems at pH 8. The authors concluded that oxygen which initially diffused slowly into nylon formed peroxides which promoted autocatalytic degradation in line with Egerton's observations (33).

Mechanisms of Degradation

There is wide agreement as evidenced by ESR (87, 116, 127); analysis of degradation products and off gases (21, 76, 113); and model compounds (19, 67, 76, 95) that the primary free radical formed on UV or high energy irradiation of polyamides is $--CH_2-\dot{C}H-NH-CO-CH_2--$ and that chain scission occurs primarily at the methylene group adjacent to nitrogen in the chain. Table 1, page 10, indicates the C-N and methylene hydrogen bonds have two of the lowest bond energies in polyamides.

Despite the evidence for --CH_2-NH-- cleavage several workers (49, 76, 87, 113) proposed photolytic degradation at the amide linkage to account for evolved CO gas. Rafikov did find evidence in decomposition products that the cleavage could have occurred although the cleavage was not observed directly. Heuvel and Lind observed initial decomposition at the amide linkage by low temperature ESR measurements (49).

Irradiation in the near UV <u>in vacuo</u> was shown to cause chain scission according to the following mechanism as proposed by Rafikov and Stephenson (87, 113):

$$--CH_2-CH_2-\overset{O}{\overset{\|}{C}}-NH-CH_2-CH_2-- \xrightarrow{h\nu}$$

$$--CH_2-CH_2-\overset{O}{\overset{\|}{C}}\cdot \quad + \cdot NH-CH_2-CH_2--$$

$$--CH_2-CH_2-\overset{O}{\overset{\|}{C}}\cdot \rightarrow --CH_2-\dot{C}H_2 + CO$$

$$--CH_2-\dot{C}H_2 \rightarrow --\dot{C}H-CH_3$$

or

$$--CH_2-CH_2-\dot{C}H_2 \rightarrow --\dot{C}H_2 + CH_2 = CH_2$$

or

$$--CH_2-\dot{C}H_2 + --CH_2-CH_2-\dot{N}H-- \rightarrow$$

$$CH_2-CH_3 + --CH_2-\dot{C}H-NH--, \text{ etc.}$$

Moore (76) proposed the following mechanisms for photolysis at wavelengths below 3000 Å which can cause scission or crosslinking. The scission mechanism below accounts for n-pentanoic acid found on hydrolysis of irradiated nylon 66. The disproportionation reaction between polymers is less

likely due to polymer rigidity, therefore the XH in the last reaction is probably $-CH_2-$ on an adjacent chain.

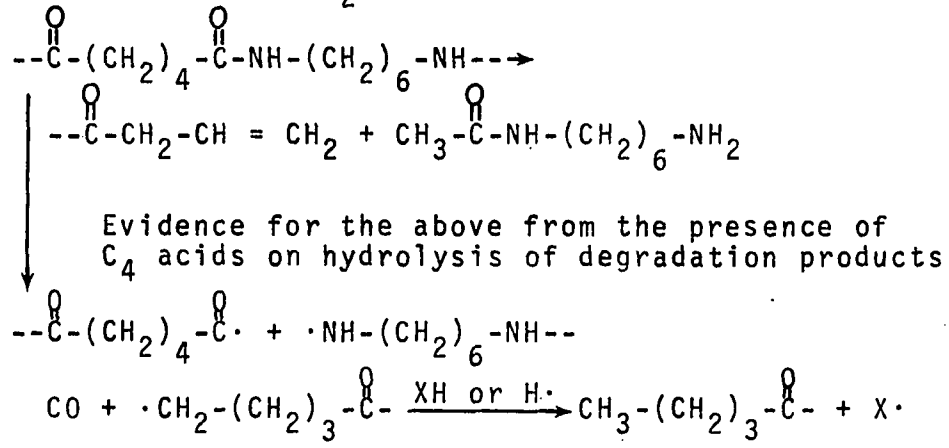

Crosslinking presumably can occur when free radicals on two adjacent chains come close enough to form a bond.

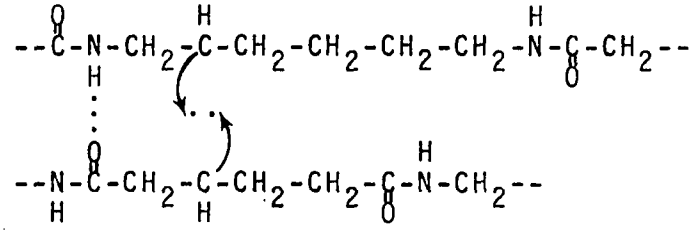

Zimmerman (137) pointed out that such crosslinking is sterically impossible when radicals occur on adjacent polymer chains which are H bonded at the amide groups. Consequently, crosslinking is not possible in crystalline regions. The probability is greater in amorphous regions where H bonds may be intermittent or temporarily broken by temperature or water and where radicals can migrate through the polymer by segmental diffusion or successive H abstraction reactions. A comparison of crosslinking propensity of a terpolymer (66/6/610)

with nylon 66 indicated the less crystalline terpolymer crosslinked much more readily. Nonetheless, the number of crosslinks produced was considerably less than expected from the number of radicals produced as measured by I_2 scavenging.

Others (31, 58, 66) have noted that nylons have a lesser tendency to crosslink under irradiation than some other polymers such as polyethylene. Majury and Pinner (66) noted for nylon as for polyethylene the most pronounced effect is hardening from crosslinking. However, the higher scission/crosslinking ratio for nylon makes irradiation stability poorer. Gel point and end group determination calculations corresponded to 290 eV as the energy dissipated per crosslink in nylon 6. This was five or six times the energy dissipated per crosslink in polyethylene.

Photooxidation Mechanisms in Polyamides

Photooxidation mechanisms have been proposed from photodegradation of model compounds, namely N-alkyl amides.

Sharkey and Mochel (95) irradiated solutions of N-pentyl hexanamide with UV irradiation ($\geqslant$3000 Å) for 285 hours at 50°C in the presence of oxygen. From reaction products of this experiment and C^{14} labelled N-pentyl-1-C^{14}-hexanamide, which established the portion of the molecule which yielded the reaction products, a mechanism was proposed. Significant portions of CO_2 and CO were derived from the methylene group next to nitrogen. From the C^{14} labelled compounds it was established that n-valeraldehyde and its decomposition products came from the amine portion of the

molecule. With this finding and the isolation of hexanamide as a product of photooxidation, oxygen attack at the methylene adjacent to nitrogen was established. Following is the proposed mechanism of photooxidation:

Initiation:

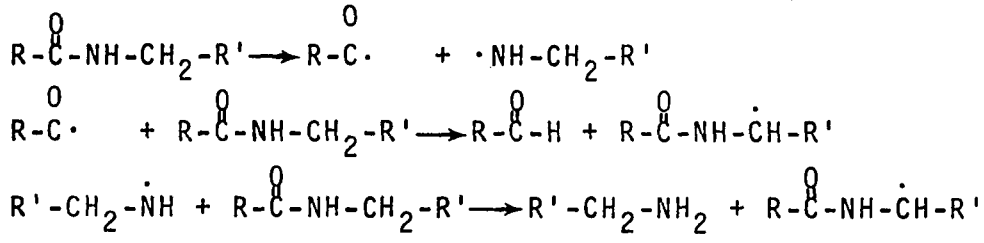

Propagation:

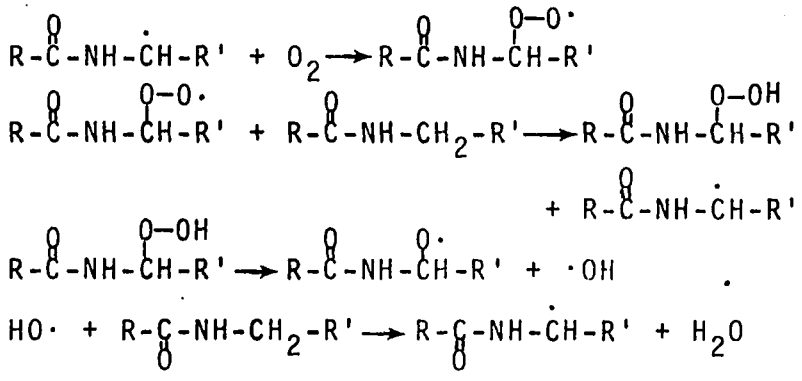

or

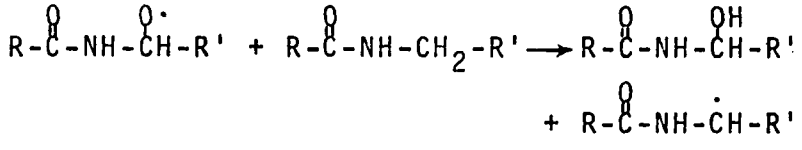

Subsequent reactions:

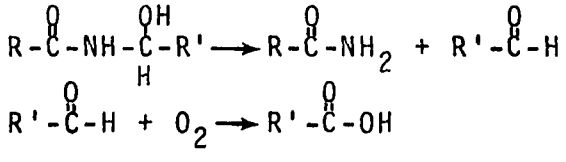

No evidence for the initial photolytic decomposition was found, but products could have been formed and subsequently oxidized to hexanoic acid and valeraldyde, two major decomposition products. Recently, however, this initial

decomposition has been observed at low temperatures by ESR (49).

Moore (76) and Burnett and Riches (19) proposed similar decomposition reactions from their studies of N-akylamides.

Photodegradation and yellowing of nylon 66 fabrics and model compounds in the presence of air and moisture were studied by Marek and Lerch (67). Exposures were made in a Fadeometer at 50°C. There was particular interest in detection of pyrroles, believed to give the yellow color to photo-oxidized nylon. The following mechanism for formation of hydroperoxides and pyrroles was proposed:

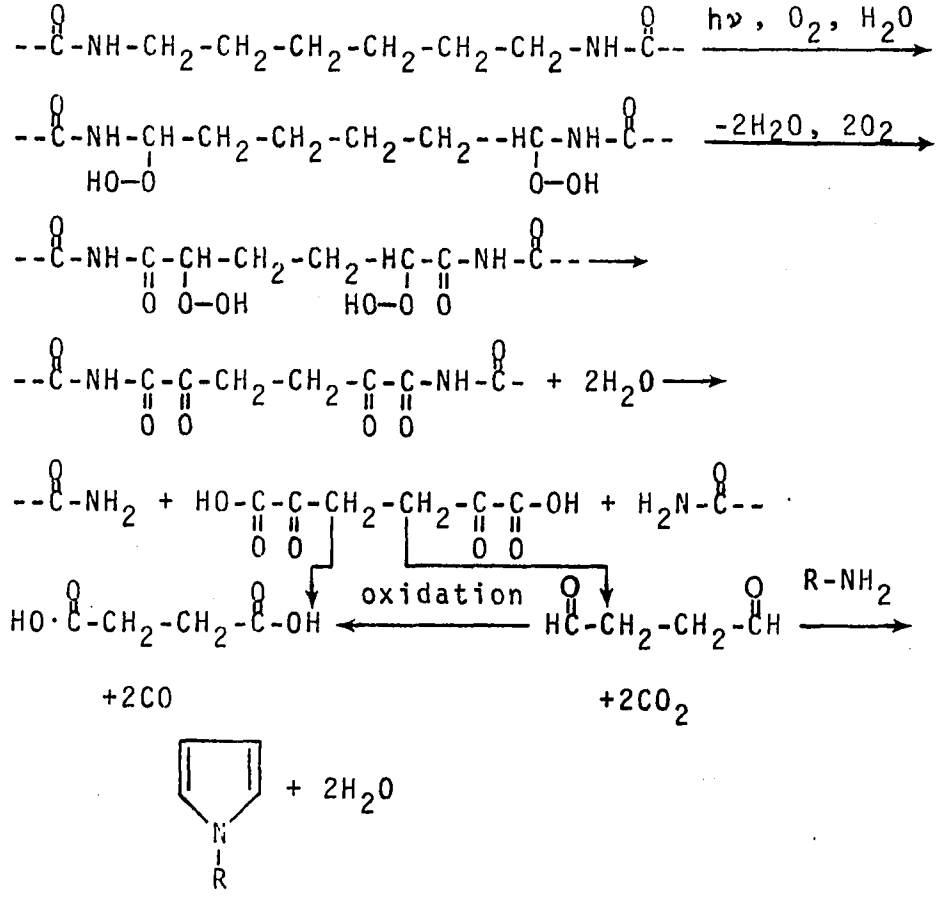

The third reaction, although it seems unlikely, was isolated. The presence of free amino groups was found essential to the formation of pyrroles, as blocking of these groups by metallic salts or acylation retarded formation.

It is apparent that the presence of oxygen, which is reactive with free radicals, favors chain degradation rather than crosslinking. Egerton and Shah (35) examined the photooxidative effect of near UV and visible light on bright and TiO_2 delustered nylon, acetate, and rayon yarns exposed to varying temperatures and relative humidities. Tensile losses were greater at higher temperatures of exposure. When yarns were stored dry in the dark at 100°C for five days, no significant changes in tensile strength occurred. Dull viscose and acetate stored in humid air lost less than 10% tensile strength. Apparently, degradation was not caused by heat alone. Nylon 66 yarns lost more strength when exposed wet than dry. Yarns which contained 0.33% TiO_2 delusterant lost considerably more strength wet than dry at higher exposure temperatures. Wet dull nylon lost 100% tensile strength in 95 hours at 75°C; at 100°C approximately 35% strength was lost for the same period. The photodegradation was attributed to H_2O_2 formed by the action of air and water on TiO_2 in a manner analogous to ZnO with O_2.

$$(ZnO) + O_2 \xrightarrow{h\nu} (ZnO)^+ + O_2^-$$

Interaction of O_2^- with water or H^+ would lead to HO_2^-, decomposition of which would lead to:

$$H_2O + O_2^- \longrightarrow HO_2^- + OH^-$$

$$2\ HO_2^- \longrightarrow H_2O_2 + O_2$$

Taylor, et al (121) studied the dependence of wavelength on the phototendering effect of TiO_2 on nylon 66 yarns. The light source was equipped to scan a spectrum 2000-5000 Å at ±10 Å increments. Intensities at all wavelengths were sufficiently low that long exposure periods of several hundred hours were necessary for measurable effects. When wavelength versus tensile strength loss was plotted for bright and TiO_2 (2%) delustered yarns it was evident that TiO_2 shifts the phototendering range to longer wavelengths. The greatest loss of tensile strength occurred at 3500 Å, in a wavelength region where peak intensities occur in sunlight. Reflectance data showed TiO_2 and dull nylon had the exact absorption curves which were maximum at wavelengths where strength loss was maximum. This indicated nylon absorption there was due to TiO_2 and TiO_2 was responsible for nylon degradation. TiO_2 probably initiates degradation by absorbing radiation, producing free radicals or peroxides which chemically attack the fiber.

Many compounds have become available for the protection of polyamides against thermal and radiation degradation. Generally, UV absorbers have groups or elements which absorb in the degradative wavelength range of fiber or dye and dissipate the absorbed energy as heat (97).

Salvin (73) exposed nylon warp face fabrics dyed with premetallized and acid dyes of high lightfastness for 100 hours in the Sunshine Arc Weatherometer. The dyes protected the fabric against photodegradation as measured by tensile strength. The protective effect was attributed to free radical scavenging by metallic ions of the premetallized dyes or selective UV absorption by the dye molecules.

Carter (22) reviewed some patents for the prevention of photodegradation:

Fr. Pat 1,546,069 ICI, Ltd.	Mn acetate, an organic phosphite, and 1, 1, 3-tris (2-methyl-4-hydroxy-5-tert-butylphenyl) butane gives good protection toward heat, light, and oxidation. A molten polyamide at 290°C showed no gel formation under water vapor after 12 hours, 25% after 16 hours. A comparable polymer containing no phosphite or substituted arylalkyl derivative showed 10% gel after 12 hours, and 61% after 16 hours.
Br. Pat. 1,036,414 BASF	Phenols, amines, and urea derivatives protect against heat, light and oxidation but more recently organic compounds which contain at least one catechol methylene ether group have been found efficient.

E. I. duPont B. P. 722,724 (17) claims the stability of linear polyamides to heat and oxygen is improved by the addition of compounds consisting of a copper compound, a halogen, and a phosphorous compound as follows:

B. P. 722,724 DuPont	Stability of linear polyamides to heat and oxygen was improved by the addition of compounds consisting of a copper compound, a halogen compound, and a phosphorus compound. Typical compounds contain 0.015-0.3% copper acetate; 0.25-2.0% KBr, KI, NaCl, NaBr, $MgCl_2$, or NH_4I; and 0.25% H_3PO_3, H_3PO_4, NaH_2PO_4,

or Na_3PO_4. Thus, 0.015% copper acetate, 0.25% H_3PO_3 and 1.0% KI based on the weight of the polyamide were added to an aqueous solution of hexamethylene diadipate. The polyamide was formed by boiling off water and successively heating in an autoclave to 250°C at 250 lb/in^2 and heating in vacuo and then under nitrogen at 275°C to drive off water. The product was spun into fibers which had heat stability at 150°C for 2000 hours as compared to two hours for unstabilized nylon. The product was stable to oxygen at 105°C for 8000 hours.

Effects of High Energy Irradiation on Polyamides

The nature of high energy irradiation (neutron, gamma, and x-radiation) has been briefly compared to ultraviolet irradiation above. The effect of high energy irradiation on polymeric materials bears some relationship to ultraviolet effects.

There is general agreement that degree of degradation or crosslinking is independent of dose rate (23, 61, 92) and perhaps source (24, 61, 92), but depends on total incident energy (24, 61).

Pile irradiation (24) of polyethylene, polystyrene, polyester, nylon, and unvulcanized rubber caused crosslinking. Polymethylmethacrylate decomposed. When polyethylene was crosslinked to a level of two crosslinks per molecule it became insoluble and no longer melted at 120°C. When exposed to higher doses polyethylene became elastic. At the highest dosage level it became stiff and amorphous. During irradiation, gases were emitted; mainly H_2, CH_4, and C_2H_6. When irradiated in air, surface oxidation occurred.

Lawton, et al (61) irradiated several polymers with high energy electrons. No effect of dose rate was found when 30×10^6 roentgens were applied at rates varying from 1 to 30 minutes. Further, no effect of temperature at which irradiation was applied was observed over a broad range ($-74^{\circ}C$ to $+193^{\circ}C$). Effects were measured by swelling. When polyethylene was irradiated the amount of H_2 evolved and the number of crosslinks formed was proportional to dose level. The number of crosslinks formed in nylon was also proportional to dose level, but the efficiency of crosslinking varied widely among polymers studied.

Little (64) irradiated nylon 66 with approximately $5 \times 10^{18} n/cm^2$. This was 50 times the dose level first shown to affect polymer solubility. Hydrogen was evolved at a rate which decreased as the dose was increased. The polymer, originally 50% crystalline as shown by x-ray diffraction, when swelled in formic acid caused crystallites to disappear. However, upon recrystallization, crystallinity reappeared at a level of approximately 30%. Dissolution was complete in a formic acid-HCl mixture. It was concluded that high energy irradiation did not cause crosslinking.

However, others have demonstrated that crosslinking predominates together with disruption within crystallites upon high energy exposure. Deeley, et al (31) irradiated nylon 66 rods of $\bar{M}n$ 17,000 and 15,600 and densities 1.150 and 1.144 gm/ml with neutron doses varying from 0.3×10^{18}nvt to 5.5×10^{28}nvt. At 0.3×10^{18}nvt the crystalline melting peak

was shifted 30°C downward. Infrared measurements showed crystallinity was decreased by 10%. Crosslinking was estimated from the slope of dynamic modulus versus temperature plots. Approximately 4% of the carbon atoms were shown to be crosslinked at this irradiation level as compared to 10% of the carbon atoms in polyethylene irradiated at the same dose. At 2.8×10^{18}nvt rubber-like behavior above 400°K indicated crosslinking was sufficient to give a network structure with approximately 9.5% crosslinked carbon atoms. Crosslinking was not found proportional to dose. With a nine fold increase in dose there was only a 2.4 fold increase in crosslinks. At the highest dose level (5.5×10^{18}nvt) there was no evidence of crystallinity as shown by melting behavior, but the crosslinking density was still 10%. Crosslinking levelled off suggesting that chain scission approached the rate of crosslinking. Mechanical loss measurements indicated an increase in amorphous fraction.

Chappell, et al (23) irradiated polypropylene film and rods of two different densities (0.899 and 0.909 gm/cc) at ambient temperature, 30-50°C, and 150°C, at an average dose rate of 3.8×10^{6} rad/sec. Samples annealed at 140°C and subsequently heated at 75°C for five hours did not change in density. At all irradiation time intervals the percent gel was higher for lower density polypropylene samples. Further, higher gel content was found in all samples irradiated at 150°C than those irradiated at 30-50°C. Percent gel content bore little relationship to irradiation dose rate. There was

evidence from this work and that of others that as irradiation of a high polymer proceeds crystallinity is destroyed making possible an increase in radical mobility which then allows an increase in crosslinking as shown by increasing gel content. Despite attempts to exclude oxygen from samples, infrared experiments showed carbonyl bands. The greater concentration of oxidation products was found in annealed rather than quenched samples. It was explained that the lower reactivity of macro-radicals towards crosslinking due to lower chain mobility in the more ordered regions results in a greater number of radicals in annealed samples. These radicals react with available oxygen diffusing into these regions. At higher doses, crystallinity is destroyed so that samples with different amounts of initial long range order compete more or less equally for available oxygen.

Zimmerman (136) irradiated polyamide films of varying composition (66, 66-610 copolymer) and thickness (0.05-0.2 mm) with 2 MeV electron beam. The films were irradiated on dry ice and stored at -78°C. Absorption spectra followed the decay of radicals by measuring color disappearance. Colors disappeared more rapidly in co-polymers and less rapidly in crystalline regions of all polymers, presumably due to relative ease of diffusion of oxygen into these regions.

Hargreaves (46) observed the effect of gamma irradiation of doses varying from 0.12×10^7 rad to 27.8×10^7 rad microscopically. Examination was at a magnification of

450 X with a polarizing microscope. Crystalline decay appeared first at fiber intersections after 13.9×10^7 rads. After 27.8×10^7 rads the filaments were completely disintegrated into small crystalline fragments.

Attention has been given to the formation, type, and location of free radicals as a result of irradiation and tensile stressing. Verma and Peterlin (127) employed ESR to study radical formation in mechanically loaded and irradiated nylon 6 fibers. Stressing fiber bundles of nylon 6 in vacuum just below the breaking point gave the same ESR spectrum as mechanically loaded nylon 66 fibers; that is --CO-NH-$\dot{C}$H-CH_2--. When the stressed samples were exposed to air a new spectrum developed slowly which was interpreted as --CO-NH-CH(O-O·)-CH_2--. In nylon 66 the radicals were trapped in amorphous regions sandwiched between crystalline blocks. Secondary radicals were formed following rupture of tie molecules with subsequent abstraction of H· from polymer chains. When samples were gamma irradiated with Co^{60} source to a total dose of 6.9 Mrad no such conversion on exposure to air occurred. This was interpreted to mean that radical formation was in different regions in irradiated polymers. That is, in mechanically stressed polymers, free radicals are formed in the amorphous phase between crystalline lamellae where oxygen can diffuse easily. In gamma irradiated samples radicals are formed in crystalline regions where diffusion of oxygen is inhibited.

Similarly Szöcs, et al (116) examined free radical formation in irradiated and stressed nylon 66 and 6 fibers of 2×10^{-2} mm diameter and $M\bar{W}$ 20,000. Samples were irradiated in vacuum at 77°K with 1 Mev electron beam to 10^7 rads. Strained samples were elongated 17% at 290°K in dry nitrogen. After treatment samples were transferred to the cavity of the ESR spectrometer. As found by others the predominant radical formed was on the methylene carbon next to nitrogen. When radical concentration was plotted versus temperature radical decay was shown to obey second order recombination kinetics in the temperature region studied. Activation energies of recombination for strained polyamides were 22 kcal/mole (nylon 6) and 29 kcal/mole (nylon 66). Recombination rate constants were quite different for irradiated polyamides and varied considerably with temperature.

Polymer	Temp (°K)	Activation Energy (kcal/mole)
6	77-180	0.1
	180-250	1.2
	270-320	12.0
66	140-190	0.1
	190-270	1.1
	270-320	14.5

The findings correlated with low frequency dynamic mechanical measurements in a similar temperature region. The differences in activation energies of recombination between strained and irradiated fibers were related to molecular mobility. Radicals in strained polyamides were in regions where molecular mobility was higher and hence recombination was facilitated.

Rutherford reviewed high energy irradiation studies on textile materials (92). At equal calculated radiation doses, reactor radiation or gamma rays alone have similar effects on cotton, rayon, and acetate as measured by changes in tensile strength, elongation, and viscosity. Further, for textiles the dose rate mattered little, the effect being a function of total dose. The effect of irradiation on polyamide, polyester, and acrylic fibers was compared. These fibers tended to crosslink, but on prolonged exposure deteriorated. When nylon (66, 6, 6HT) and polyester tire cord were exposed to gamma irradiation, all fibers lost more strength as the dose was increased in air. All nylons lost approximately 60% tensile strength exposed in air to 10×10^6 rads. In vacuum, nylon yarns lost approximately 10-15% tensile strength. Polyester lost only 17% tensile strength when exposed to 10×10^6 rads in air. Nylon and polyester melting points were unchanged by the highest level of exposure. In another study of parachute fabrics, nylon lost more tensile strength at lower irradiation dose than acrylic and polyester. Rutherford generalized that those fibers which tend to crosslink on high energy irradiation include: modacrylic, acrylic, polyester; and those which deteriorate include: cotton, rayon, acetate, and wool. Nylon irradiated in air exhibits intermediate behavior.

Polyamides exposed to a low dose level of irradiation (30 mCi of radium) for a prolonged period (up to 5 months) absorbed a total of 10^{16} quanta. The exposure caused a sharp

decrease in second moment of the NMR line which was taken to mean very few crosslinks were formed, probably because of the very low probability of simultaneous action of two quanta on two neighboring polymer chains (108).

The relative propensity for crosslinking under irradiation was studied by Karpov, et al (58). Polyethylene, polypropylene, polyacrylonitrile, and polyamide filaments were irradiated with 0.162 Mrad/sec up to 500 Mrad in vacuum and in air at 20°C. Generally, all fibers lost tensile strength more rapidly in air than in vacuum with increasing dose.

Polyamide filaments lost little strength when irradiated in vacuum. Measurable gels were formed in polyacrylonitrile, polyethylene, and polypropylene at 15, 45, and 100 Mrad, respectively. Nylon did not gel when irradiated in air as shown by continuously decreasing viscosity. When exposed in vacuum, viscosity increased at 100 and 200 Mrad but decreased when filaments were irradiated with 300 Mrad.

Several workers have compared the effects of ultraviolet and higher energy irradiation sources on polymeric materials. Charlesby (25) states that many reactions induced by high energy irradiation can be initiated by UV which can only produce radicals, not ions. Where similar reactions are observed there is good reason to believe that radical reactions occur via excited states. The ions produced by high energy irradiation may recapture primary electrons to give further excited species, increasing the total yield. By contrast, the radical initiation efficiency (in quanta) at

3100 Å is 0.001 for styrene, 0.12 for polymethylmethacrylate, and 0.003 for vinyl acetate, all considerably lower than high energy initiation yield.

Nylon 66, high tenacity nylon 66, heat resistant nylon (Nomex), semidull nylon 6, and sunlight resistant nylon 66 fibers were exposed to thermal radiation (up to 1000°C), UV irradiation at 2537 Å (3.02×10^{-2} watt·hr/in^2) and to gamma irradiation (1.16 to 0.82×10^6 rads/hr) under vacuum, nitrogen, air and humidity (47). Off gases were collected for analysis. There was a decrease in viscosity when nylon 66 was exposed to UV and UV plus gamma irradiation. However, when nylon 66 was irradiated with 1.72×10^8 rads in air, viscosity increased. Nylon 66 melting point decreased slightly with UV irradiation but decreased more with UV plus gamma irradiation in nitrogen. Melting behavior observed on a hot stage microscope showed the fibers shrink and curl as the core melts leaving the skin intact. Then the skin melts and the fibers flow together. Melting behavior was not visibly changed with irradiation. Analysis of off gases of gamma irradiated nylon 66 indicated CH_4, CO_2, and CO were evolved from irradiation in air; CO_2 and CO from irradiation in nitrogen; and CO from irradiation in vacuum. When nylon 66 samples were UV irradiated in air at 6.04×10^{-2} watts, CO_2 and CO were evolved. Infrared spectra of the irradiated residues showed little change in fiber chemistry. Microscopy with polarized light showed gamma irradiation destroyed crystallinity in nylon 66. Nomex was resistant to gamma and

thermal degradation but was degraded by ultraviolet light.

An attempt to substitute UV energy for ionizing radiation as a crosslinking source for polyethylene was made by Kachan, et al (57). Unstabilized films (0.06 mm thick) of high, medium and low pressure polyethylene were irradiated with 2.0 MeV linear beam and UK-70,000 Co unit. Other samples were exposed to UV irradiation (2537 Å) in air, helium, and vacuum. Electron paramagnetic resonance signals of the UV irradiated polyethylene at 77°K consisted of two superimposed curves.

(I) $--CH_2-CH_2\cdot$ (II) $--CH_2-\dot{C}H-CH_2--$

The spectrum of ionizing irradiated samples consisted almost entirely of II, thus suggesting that UV irradiation causes mainly degradation of polyethylene whereas ionizing irradiation promotes crosslinking. Because ionizing irradiation exceeds bond energies radiation is absorbed more generally and more macro-radicals are produced. In the presence of air crosslinking efficiency of ionizing radicals fell rapidly due to the formation of peroxide and hydroperoxide radicals which cause chain scission. The effect may continue over time as oxygen continues to disperse to trapped radicals. Crosslinking can occur in UV irradiated polyethylene in the presence of air as a smaller number of radicals are formed at one time so that recombination is presumably inhibited.

The studies reported above indicate that high energy irradiation destroys crystallinity and usually favors crosslinking. Ultraviolet irradiation can promote crosslinking in

vacuum but generally in air chain scission occurs. Under certain circumstances polymer crystallinity may be increased.

Crystallinity (101) can be increased in polymers that undergo scission because of less restraint on the shortened molecules. The freed chain ends can then be more easily oriented in the crystalline structure.

Winslow, et al (132) observed oxidative crystallization on prolonged heating of linear and branched polyethylenes at 100°C. Both types of these films remained unchanged in density after 300 hours at 100°C in nitrogen, but density increased 0.06 g/cc when samples were heated in oxygen. X-ray diffraction patterns of the latter samples revealed only mere traces of amorphous material. Most of the initial density increase (which was rapid) apparently arose from chain cleavage followed by reordering of the freed chains and adjacent segments. The gel fraction of the crystallized samples was less than 1%. Oxidative crystallization was suppressed by dense crosslinking but proceeded readily in branched polyethylenes.

Thermal and photooxidative reactions in branched and linear polyethylenes were compared (134). Films 0.01 inch thick were irradiated at 2800 and 2537 Å under oxygen. Thermal oxidation (as observed by O_2 uptake and density measurements) passed through an induction period before oxygen uptake levelled off at 40 ml/g. Oxidation at 2537 Å proceeded linearly with time to an uptake of 50 ml/g in 800 hours. Photooxidation was apparently oxygen diffusion controlled.

Photooxidative crystallization was inhibited by extensive crosslinking during initial stages of the reaction, the gel fraction being 18% after oxygen uptake of 2 ml/g. Scission reactions gradually reduced the gel content on continued exposure.

Polyethylene crystallized from the melt (133) consists of crystalline lamellae interlaced with tie chains in a disordered arrangement. Since tie chain concentration rises with molecular weight, thermal annealing under the most favorable conditions proceeds exceedingly slowly in an ultra-high molecular weight linear polymer. Yet, exposure of such a polymer to oxygen at elevated temperatures or UV irradiation produces a rapid rise in crystallinity. As chains break in the amorphous regions freed fragments relax into a more compact arrangement.

The effect of wavelength on photooxidative processes in polyethylene film was observed by Heacock, et al (48). Films of 0.919 g/cc density were exposed to broad band UV irradiation centered around 2750 Å and 4000 Å for periods up to 240 hours. Exposures were at 50°C and 90°C. Crosslinking was initiated at 4000 Å. At 2750 Å density increased (above oxygen uptake) and x-ray measurements indicated crystallinity had increased. Oxidation was shown to occur in amorphous regions primarily at branch points.

Acid Dyeing of Nylon

The amine and amide groups which can carry a positive charge make it possible to dye nylon with acid dyes; dyes which usually contain one or more sulfonic acid groups in their structure. Dyeing is usually accomplished from a solution of the sodium salt of the dye in an acidified aqueous bath. The bath may contain a buffer effective in the pH range chosen for dyeing and a surfactant to assist in wetting out nylon which is relatively hydrophobic. Generally, acid dyeing occurs by the adsorption of hydrogen ions from the acidic medium onto available amine end groups in amorphous regions of the fiber, creating positively charged species. An equivalent number of dye anions will then be adsorbed to obtain electrical neutrality. The ionic attraction between fiber and dye probably accounts for adsorption but not substantivity. The latter is more likely a result of interaction between the large dye molecule and the polymer (72, 130).

Practical problems of obtaining deep shades, level dyeing (14, 78, 84), and predictable results from dye mixtures (9, 125) have encouraged study of the acid dye process (52, 73). Diffusion rate of certain anionic dyes is so sensitive to the molecular order and orientation of nylon fibers that considerable interest in the dye diffusion process in relation to fiber structure has resulted in several studies (9, 32, 72, 78). Peters and Turner (83) classified a large number of dyes according to their sensitivity to

physical and chemical structure of nylon 66. Indeed, dyeing has been used as a diagnostic procedure for fiber treatments such as drawing (29, 78, 117) and heatsetting (84, 130). The relationship of high energy irradiation and fiber dyeing properties has been reported for cellulose (123).

The dyeing process is not a simple one. Both equilibrium take-up and diffusion rates are dependent upon a number of variables including the nature of the fiber, chemical structure of the dyestuff, composition of the dyebath, and the dyeing conditions.

Briefly, equilibrium dye take-up may be a function of:

1. Available amine end groups in the fiber
2. pH of the dyebath
3. Concentration of dye in the bath if it is below amine end group saturation
4. Basicity of the dye
5. Size and configuration of the dye molecule

Dye diffusion rate may be dependent upon:

1. Molecular order in the fiber
2. Size, structure, and basicity of the dye molecule
3. pH of the dyebath as it affects surface adsorption and the electrical potential gradient in the fiber
4. Temperature at which dyeing is carried out
5. Available adsorption sites in the fiber

It has been well established that the principle adsorption sites for acid dyes are the available amine end groups, although adsorption may occur at amide sites at low dyebath pH (128). Studies of equilibrium dye take-up on nylon fibers altered by acetylation for amine content (85) and correlation of amine content (determined by acid titration) with dye results establish this point. The Peters

study on the effect of dyebath pH is illustrated in Figure 3.

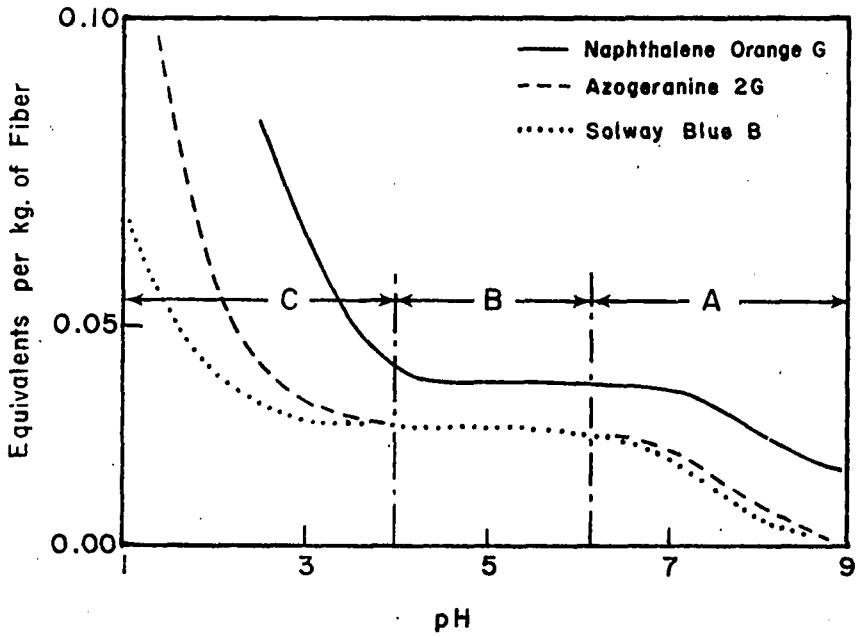

Figure 3 - Adsorption of acid dyes on nylon yarn at different pH values at 60°C (128).

Very little dye adsorption occurred at pH above 7. Approximately at pH 6 all amine end groups had associated dye ions. Between pH 3 and 5 little additional adsorption took place. Below pH 3 adsorption on amide groups occurred. When the study was repeated with acetylated nylon the adsorption curves were similar but correspondingly lower. The great increase in adsorption at low pH may be a result of new amine end groups arising from acid hydrolysis of the polyamide chains (29, 128). A study of desorption of dye in 0.1 N sodium chloride showed that when dye content was less than 0.02-0.04 equivalents/kg of fiber, chloride ions could displace little of it. However, any dye in excess of this amount was readily displaced. The study showed that dye is

first strongly adsorbed on amine end groups, but when these are saturated, amide groups become dye sites. During desorption the solutions from more heavily dyed fibers became strongly acid indicating hydrogen ions were desorbed as well as dye ions (128). The implication is that adsorption on amide groups must be adsorption of free dye acid, which is reversed in salt solution, the dye leaving to increase acidity of the desorbing solution. Evidence from these two studies suggests, then, that if dyebaths contain less than enough dye to combine with amine end groups, no adsorption occurs on the amide groups, and on desorption little or no dye leaves the fiber showing that the dye has high affinity for amine end groups in the pH range 3-5.

If amine end groups are oxidized or otherwise lost by some fiber treatment such as heatsetting or drawing the equilibrium dye take-up is reduced (29, 84, 130). Conceivably, dye take-up could be reduced if amine end groups became inaccessible to dye due to increased molecular order. Munden and Palmer (78) found that there was slightly lower equilibrium take-up of a dibasic and a tribasic dye if the draw ratio of the nylon yarn was increased. Peters and White (84) did not believe decrease in dye take-up could be attributed to masking of the amine end groups by increased molecular order because although acid dye take-up was limited by steam heatsetting treatments, metal complex dye take-up increased. It is interesting to note that when they plotted dye rate versus increasing temperature of heatsetting for a

metal complex dye (C. I. Acid Red 220), the dye rate decreased more rapidly than the amine end group content.

Discrepancies in stoichiometry between sulfonic acid groups in dyes and amine end groups as shown by dye studies may be due to amine end groups which are buried in the complex fiber structure and hence inaccessible (52).

Atherton and Peters (9) studied the practical problem of incompatibility when two or more dyes are applied from the same dyebath. They observed the dyeing rates of the dyes applied individually and in binary mixtures and found that competition is determined by dyebath concentration, diffusion coefficients, basicity of each dye and its relative affinity for the fiber. Rate determinations showed that tribasic dyes had lower affinity for nylon than dibasic dyes. When relative affinities were determined by desorption measurements, the results were opposite. The following explanation was given for this apparently contradictory behavior. Kinetic experiments were performed under conditions which provided dye saturated fiber surfaces. Because of the bulk of dye molecules, tribasic dyes usually being larger than dibasic, there can be stoichiometric deviations between dye take-up and available amine sites. Desorption conditions involve dye levels below saturation but involve small chloride ions which can conceivably saturate all unoccupied amine end groups and displace dye molecules by ionic exchange. Large dye molecules must also compete for the hydrophobic areas within the fiber for attachment. Trisulfonic

dyes are more hydrophilic than those of lower basicity so conceivably they could be displaced more easily from hydrophobic surfaces. If this were true, desorption by chloride ions would apparently (and perhaps falsely) show polysulfonated dyes to have a higher fiber affinity.

On steric considerations, although all sulfonic acid groups in a dye can react with amine groups, the more functional groups on the dye the less likely they will all be adjacent to amine end groups. Consequently, dyes of lower basicity can be more easily accommodated (1, 9). The more negatively charged dibasic dyes do not "level" easily and emphasize physical irregularities in the fiber (125).

Munden and Palmer (78) studied the effect of draw ratio on the number of available amine sites. Equilibrium dyeings with three ionic dyestuffs (di, tri, and tetrasulfonated) showed slightly higher dye take-up at low draw ratios when di and trisulfonated dyes were used. However, there was a lower take-up of the tetrasulfonated dye at all levels of draw ratio.

Studies in Dye Diffusion

Much has been learned about the mechanism of transfer of dye from bath to fiber substrate from kinetic studies of the dye process. Vickerstaff (128) identified three stages of diffusion as follows:

1. Diffusion of dye through an aqueous medium to the fiber surface

2. Adsorption of dye on the outer surface of the fiber
3. Diffusion of the dye inside the fiber from the surface inward

Stage 2 is virtually instantaneous if the dyebath concentration is sufficient to saturate the fiber surface. Stage 3 is much slower than Stage 1 as diffusion into the fiber substrate is impeded by the charged molecular structure. Hence, the third stage is rate controlling under usual dyeing conditions (71).

It has been well established that molecular order of the fiber strongly influences the rate of dye diffusion into the fiber although it may have little or no effect on equilibrium take-up (12, 29, 52). Rate of dyeing curves generally show a rapid initial rate followed by leveling off at a concentration of dye approximately equal to the number of charged groups in the fiber. Apparently, as electroneutrality within the fiber is approached there is a restriction of dye sorption (72).

Generally, anionic dyeing is believed to occur in regions of low molecular order where amine end groups are available. The rate of diffusion will be controlled by the resistance the internal molecular arrangement provides for the bulky dye molecules and the extent of adsorption of dye on the polymer surfaces. Orientation and molecular packing then become critical.

The effect of fiber fine structure on dye site

accessibility has been recognized by Bittles, and others (14). Fibers with the same amine end group content but unlike diffusional properties exhibited different dyeing behavior as the amount of available dye was varied. Unlevel dyeing resulted when excess dye was in the bath because accessible dye sites saturated first. When the dye was added slowly so that the concentration at any one time was well below amine end group saturation level dyeings were obtained.

Recently it has been proposed that where increased molecular order has created voids with large interior fiber surface more dye molecules can be adsorbed on those surfaces where they are then held by Van der Waals forces (130).

It is not difficult to visualize on steric considerations that large dye molecules whose structures may deviate from planarity will have restricted mobility and may be restrictive to passage of other molecules. In addition, dyes with greater numbers of sulfonic acid groups in their structures will have restricted mobility. For example:

1. A larger number of sulfonic acid groups will increase the probability of interaction with the ionic polymer and thus slow diffusion.
2. Fewer polysulfonated dye molecules can be adsorbed by the fiber with limited sites. The result will be a lower concentration gradient within the fiber which slows diffusion (78).

Trommer (125) listed "level" dyes, those with good "transfer" properties, as having one carboxylic or sulfonic

group in their structure. "Reserving" dyes, those which do not transfer easily and which emphasize yarn irregularities, usually have a strong negative charge because of two sulfonic acid groups in their structure.

Hopper, et al (52) compared diffusional properties of two similar acid dyes; one monobasic, the other tribasic. When dye concentration was controlled to a level of half saturation of the amine end groups, the dye of lower basicity penetrated farther into the fiber than the other for a given dyeing time. These authors concluded that the mathematical expression adequate to describe diffusion behavior had to include a basicity term.

Correlations between dyeing behavior and fiber treatments such as drawing and heatsetting are well established. Takagi (117) examined dye diffusion in cross sections (lateral and longitudinal) of nylon 6 filaments of varying draw ratios. Examining dye penetration constant differences he determined dye diffusion rate depends on molecular structure especially as amorphous areas become more compact and oriented with the fiber axis.

In a similar examination of dye concentration at various points in the fiber cross section, Bell et al (13) determined that the distance of penetration for a given time is a function of polymer physical structure whereas dye concentration in the region near the fiber surface is determined by amine end groups. Another study of the dependence of dyeing rate and equilibrium take-up on fiber orientation showed the

greater dependence to be on dyeing rate, particularly when nylon is dyed with anionic dyestuffs (78).

Hopper et al (52) found diffusion coefficients to be 100 times greater for undrawn than for drawn films. The rate of diffusion was dependent on polymer structure, especially orientation, and not on dye concentration in the fiber if the fiber structure was homogeneous. Heterogeneous films (those which were more crystalline near the surface) showed a dependence of diffusion coefficient on dye concentration in the film.

Varying conditions of heatsetting such as temperature, duration of treatment, and moisture content are known to influence the way these treatments modify the fiber structure (84, 130). Dyeing behavior reflects the differences among heatsetting treatments. Generally, dry heatsetting (195-240^{o}C) reduces dye take-up rate and may reduce equilibrium take-up if oxygen is not excluded from the system. When correlated with other measurements such as density, moisture regain, end group analysis, x-ray, and birefringence reduced dye take-up was taken as evidence of an increase in lateral order and a loss of amine end groups.

Warwicker (130) found that yarns heatset a 250^{o}C under seven grams tension became much more dye receptive, increasing in both rate and equilibrium take-up. At this setting temperature, density and birefringence also increased. X-ray data indicated increased lateral order between lamellae, but decreased order within, perhaps due to the onset of melting.

Moisture regain decreased. Warwicker gave the following explanation for his findings. Rather than viewing the fiber fine structure as crystallites imbedded in a more or less amorphous array he views the structure as fibrillar ribbons or sheets spiraling about the fiber axis. In this model increased lateral order and density, without decreased volume can only lead to voids within the fiber. The voids can accommodate large dye molecules held to the fibrillar surfaces by Van der Waals forces. Hence, dye take-up can increase even though crystallinity also increases. Water can only be held at available amide groups. If these become less available due to increased crystallinity then moisture regain decreases. Thus more void space leads to a loss of sites for water.

Steam heatsetting tends to increase dyeing rate. Amine end groups are apparently not affected if oxygen is absent. When analyzed with other measurements it seems that steam increases density and crystallinity but decreases orientation of crystallites. Dye is accommodated in voids created by increased crystallinity (84).

Davis and Taylor (29) found that boiling nylon yarns in water for 24 hours increased density and crystallinity (apparently calculated from density) by 3%. When boiled and unboiled yarns were dyed at varying temperatures there were marked differences in diffusion. Diffusion was faster in unboiled yarns dyed at 102^{o}C; the same for both yarns dyed at 80^{o}C; and faster in boiled samples dyed at 60^{o}C. Diffusion

behavior at 102°C was explained on changes in density. The apparent inconsistency of increased diffusion rate with increased density for samples dyed at 60°C and 80°C was explained. Apparently heatsetting occurred at the 100°C boil which created voids as some amorphous material took on crystalline order. Any thermal motion at 60°C or 80°C dye temperatures was not adequate to create sufficient free volume to enhance dye diffusion. Consequently the voids already created in the boiled yarn favored diffusion more than any small amount of free volume which might have been created in the unboiled yarns at low dye temperatures.

Dye Diffusion Mechanisms

A general view of anionic dyeing of nylon 66 has been outlined above. Rate of transport can be expected to be influenced by:

1. The tortuosity of flow path through the polymer matrix
2. The existence of localized charge in the polymer which would tend to impede the flow of oppositely charged dye molecules
3. The concentration gradient of dye in the fiber
4. The electrical potential gradient within the fiber, a result of the different mobilities of the acid anions which are replaced by dye anions as diffusion progresses in the fiber

Dye rate has been shown to be lower when the number of NH_3^+ groups is limited. When the dyebath pH is high enough to limit H^+ which associate with amine end groups the dye rate is slower. Similarly, the measured diffusion coefficient has been shown to be lower when the dye concentration

within the fiber is lower (72). The usual shape of sorption isotherms indicate a rapid initial dye take-up which levels off as the number of available amine end groups decreases.

Davis and Taylor (29) predicted a relationship between the diffusion coefficient and the fraction of occupied amine sites. A plot predicted diffusion to increase initially but decrease as more dye sites were occupied, the curve maximum occurring when 0.5 sites were occupied. Their experimental values fit the curve exactly at the maximum point.

Although these studies are evidence that the number of available amine end groups has a pronounced influence on diffusion it is probably secondary in importance to molecular order, especially orientation.

Hopper et al (52) recently developed expressions for the diffusion coefficient which take into account the following parameters: 1) diffusion in the fiber "pores," 2) basicity of the dye, 3) fraction of unsaturated dye sites, 4) fraction of inaccessible dye sites, and 5) the electrical potential gradient. Experimental data were adequately described by the derived expression, but the electrical potential gradient term probably was of minor importance.

Attention has also been given to segmental motion with accompanying increase in free volume as the driving force of diffusion (89). It was proposed that segmental motion in polymers controls rate of dye diffusion as it does rate of creep and relaxation phenomena. At dyeing temperatures above polymer Tg free volume swept out by segmental rotation forms

"holes" which can accommodate dye molecules. The energy of diffusion may depend not only on the hole formation but, in ionic systems the binding energy of dye to polymer; a factor influencing release of the dye molecule to enter the "hole" formed.

Bell (11) demonstrated the relationship between dye diffusion and fiber mechanical properties in experiments on acid dyeing of nylon. A diffusion constant was calculated and related to time dependent mechanical properties. The experimental results were linear as predicted but the slope was higher than expected. The discrepancy probably resulted because:

1. Dye motion is mostly lateral whereas mechanical stress and relaxation are largely axial
2. Electrostatic interaction exists between dye and fiber.

Quantitative Analysis of Dye Diffusion

A fundamental expression for dye diffusion is Fick's law: Existence of a concentration gradient causes dye to diffuse towards the center of the fiber at a rate proportional to the gradient (128).

Dyeing experiments have shown repeatedly that this simple expression does not adequately explain the complexity of the diffusion process. Therefore, numerous studies have been accompanied by derivations of complex mathematical expressions to adequately describe the observed phenomena (28, 52, 128).

However, a simple expression used by Hill (50) for describing diffusion into or from a plane surface of a semi-infinite solid has been widely used to approximate the diffusion coefficient under certain dyeing conditions (11, 12, 13, 32, 71, 78, 91).

The expression is derived from:

$$D\left(\frac{\delta C}{\delta x}\right)_{x=0} = \frac{DC_o}{\sqrt{\pi Dt}}$$

that is, the rate of transfer of a diffusing substance from or into a semi-infinite medium when the surface concentration is zero (28). The total amount of the diffusing substance which has entered the medium is given by integration of the expression on the right with respect to (t):

$$M_t = 2C_o\sqrt{\frac{Dt}{\pi}}$$

where:

M_t = amount of dye diffusing across the surface in time (t)

C_o = concentration of dye in the bath

D = apparent diffusion coefficient

Providing the time (t) of diffusion is short enough so that only a thin surface layer is penetrated, many semi-infinite solids with surfaces other than plane may be adequately treated by this expression.

Calculation of the apparent diffusion coefficient for fiber dyeing must include a term for fiber volume (V). The

following expression holds where a linear plot of the fraction of total available dye on the fiber at time (t) versus the $\sqrt{t}$ obtains:

$$\frac{\frac{C_t}{C\infty}}{\sqrt{t}} = \frac{2}{\sqrt{\pi}} V\sqrt{D}$$

where: C_t=conc. of dye on fiber at time (t)

$C\infty$=conc. of dye on fiber at fiber saturation*

and $\frac{C_t}{C\infty}/\sqrt{t}$ gives the slope

$V = 2\pi rl$

where:

r = filament radius
l = length/gm of filament

then: $$\frac{\left(\frac{C_t}{C\infty}\right)^2}{t} = \frac{4}{\pi} 4\pi^2 (rl)^2 D$$

$$\frac{\left(\frac{C_t}{C\infty}\right)^2}{t} \left[16\pi(rl)^2\right]^{-1} = D$$

The above expression is subject to the following assumptions:

1. Dye concentration available to the fiber surface is at all points constant
2. Dye penetrates only a surface layer of the fiber and surface concentration remains constant
3. Concentration of dye on the fiber surface and inside is zero initially.

Obviously, these conditions would obtain only in early stages of dyeing.

*Anthraquinone Milling Blue BL dyebaths did not contain excess dye. Therefore the term $C\infty$ in the expression used to obtain the slope of the line was defined as the concentration of dye on the fiber at dyebath exhaustion.

Wide Line Nuclear Magnetic Resonance

Principles of Nuclear Magnetic Resonance

Nuclear magnetic resonance (NMR) spectroscopy (8, 21, 98) is a tool for studying the structure of matter by capitalizing on the fact that certain atomic nuclei possess angular momentum (spin) and an associated magnetic moment. The angular momentum of the "spinning" nucleus is described in terms of spin number (I) which is the resultant spin of protons and neutrons in the nucleus. Atomic isotopes for which the number of protons or neutrons (or both protons and neutrons) is odd possess magnetic moments. The generated magnetic moment ($\vec{\mu}$) of these dipoles is a vector quantity, having both magnitude and direction. The proton is the most commonly studied magnetic nucleus. It has spin I = ½.

When a magnetic nucleus is placed in an external magnetic field ($\vec{H}_0$) it can assume a certain number of discrete orientations, given by (2I + 1). For the proton with spin number I = ½, the number of possible orientations is 2. These orientations are parallel and antiparallel to the external magnetic field ($\vec{H}_0$) and are designated as + ½ (lower energy state) and - ½ (higher energy state), respectively. A change from one orientation to the other is accompanied by absorption or emission of a discrete quantum of energy (ΔE). The change in energy (ΔE) depends upon the external magnetic field ($\vec{H}_0$) and the magnetic moment ($\vec{\mu}$) of the spinning proton according to the following relationships:

$$E = -\vec{\mu} \cdot \vec{H}_0$$

where E equals the dot product of the projection of the magnetic moment ($\vec{\mu}$) on the external magnetic field ($\vec{H}_0$)

$$= \frac{\gamma h}{2\pi} I \cdot \vec{H}_0$$

h = Planck's constant

γ = gyromagnetic ratio, $\frac{2\pi\mu}{hI}$

$\vec{I} = \pm \frac{1}{2}$

$$= \pm \tfrac{1}{2} \frac{\gamma h \vec{H}_0}{2\pi}$$

$$\Delta E = E_{-\frac{1}{2}} - E_{+\frac{1}{2}}$$

$$= \frac{\gamma h \vec{H}_0}{2\pi}$$

Equating the energy of an electromagnetic wave to ΔE, we obtain

$$\Delta E = h\nu_0 = \frac{h}{2\pi}\omega_0 = \frac{\vec{H}_0}{2\pi}$$

where ν_0 = frequency in cps

ω_0 = angular frequency.

Thus the proton may be pictured as precessing with velocity ω_0 in the field $\vec{H}_0$. The corresponding frequency for $\vec{H}_0$ of 14,092 Gauss is approximately 60 MHz which is in the radio-frequency range.

If, then, an applied radio frequency (ω_1) equal to the proton precessional velocity (ω_0) is introduced at right angles to $\vec{H}_0$, creating an associated magnetic field $\vec{H}_1$, a resonance condition occurs. Nuclei absorbing electromagnetic radiation from the radio-frequency (RF) source will flip to

the high energy state absorbing discrete quanta of energy. Nuclei reverting to the lower energy state will emit a discrete quanta of energy which can be recorded as a peak on chart paper. The absorption or emission of energy occurs only when the resonance condition exists. The resonance condition is shown schematically in Figure 4.

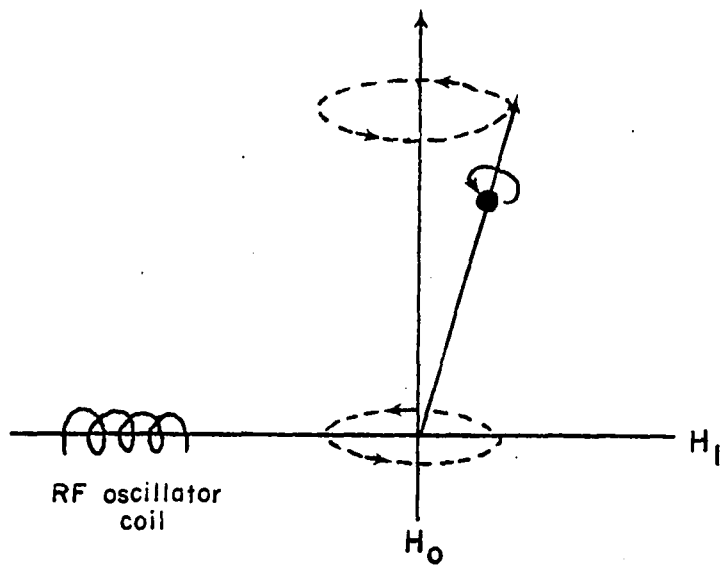

Figure 4 - Schematic representation of the nuclear magnetic resonance condition.

The above describes the hypothetical case of an isolated proton in an external magnetic field. In real systems, neighboring protons will interact altering the resonant condition. The proton is in proximity to other magnetic fields created by neighboring nuclei in the molecule. In solids, these fields are approximately static, but in liquids they are in vigorous translational and rotational motion. The excited proton can dissipate its energy to the system and

return to the lower energy state. Energy dissipation of this type is designated spin-lattice relaxation (T_1).

In order that NMR signals may be recorded the populations of the two spin states cannot be the same. The exciting field created by the RF circuit and internal magnetic fields promote spins to the upper energy state, but dissipation of energy to the surrounding lattice returns them to the lower state. The probability of transition upward in unit time is less than the probability of transition downward. Therefore, in the equilibrium state, as governed by Boltzmann statistics, the lower level will have the higher population. Due to inequality of populations of the energy levels and the equal probability of transitions induced by the exciting field ($\vec{H_1}$), the number of transitions in unit time from the lower to upper level will be greater than the number of transitions from upper to lower. If, however, the exciting field ($\vec{H_1}$) is too great, an excess of spins will be promoted to the higher energy state so that the populations are more nearly equal (108). This situation, termed resonance saturation, will distort the NMR signal.

Nuclear Magnetic Resonance in Solids

It has been stated above that in the hypothetical case of the magnetic dipole ($\vec{\mu}$) of a single proton in an external magnetic field that the quantum of energy emitted from a transition from the excited state downward can be recorded as a single line peak. If two nuclei with magnetic dipoles are situated in close proximity there may be dipole-dipole

interaction creating a magnetic field with a different resonant frequency than either dipole possesses alone.

The magnetic field ($\vec{h}_1$) produced by the magnetic moment $\vec{\mu}_1$ of nucleus (1) at the point in space of $\vec{\mu}_2$ of nucleus (2) is shown schematically in Figure 5.

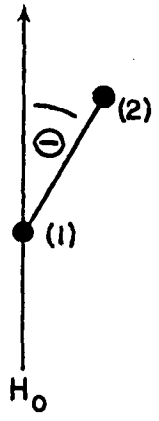

Figure 5 - Schematic representation of interacting magnetic moments of an isolated pair of nuclei.

The magnetic field produced by the interacting pair of nuclei is given by the following expression:

$$h_1 = \pm 3/4\sqrt{\hbar}r^{-3}(3\cos^2\Theta - 1)$$

where r is the distance between nuclei

Θ is the angle between the unit vector and (H_o)

The total energy for a system of two interacting nuclei is given by:

$$E = -\vec{\mu}_1\cdot\vec{H}_o - \vec{\mu}_2\cdot\vec{H}_o - \left[\frac{3(\vec{\mu}_1\cdot\vec{r}_o)(\vec{\mu}_2\cdot\vec{r}_o) - (\vec{\mu}_1\cdot\vec{\mu}_2)}{r_o^3}\right]$$

Further, if the dipoles act as a coupled system, a different transitional frequency may be required. It follows then that in a real solid there will occur a broad range of resonant frequencies resulting from the internal magnetic fields created by the large number of interacting dipoles oriented at various directions in space. To record a range of resonant frequencies, the external field ($\overrightarrow{H_0}$) is varied over a narrow range. Below are typical line shapes which might be recorded (Figure 6).

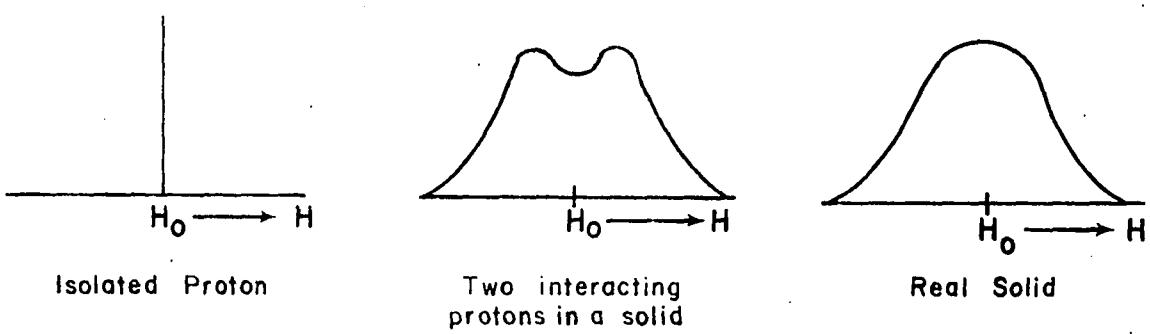

Figure 6 - Typical NMR line shapes for an isolated proton, interacting proton pair, and multiple proton interactions in a real solid.

Nuclear Magnetic Resonance of Polymers

Two particular aspects of polymeric solids make them suitable subjects for broadline NMR study. First, rather than being homogeneous solids, drawn or otherwise oriented systems are anisotropic having regions of close molecular packing where dipole-dipole interaction could be maximal and the internal magnetic fields fixed in space. Recorded spectra of such regions would give a broad line. In addition,

polymeric systems contain regions of disorder where internuclear distances would be greater and dipole-dipole interaction is reduced, especially at high temperatures where thermal motion would average out the interaction. Recorded spectra of such regions give a much narrower line which is superimposed on the broad line of the rigid fraction giving an overall complex line shape.

Second, systems of linear polymers give different line shapes depending upon the orientation of the polymer sample in the external magnetic field. This is because in the rigid fraction of a drawn polymeric sample such as a fiber, most of the polymers are oriented parallel to the fiber axis which fixes a large number of interacting dipoles in space.

Olf and Peterlin (80) studied molecular motion of oriented nylon 66 fibers with 5:1 draw ratio. They determined that the best resolution of the two phases of the complex wide line occurred when $\cos^2\theta$ in the expression which gives the magnetic field strength for an interacting pair of protons was 1; that is when the fiber bundle was oriented parallel to $\vec{H}_o$. They determined $\overline{\cos^2\theta} = 0.97$ for their drawn nylon sample when fiber axes were parallel to H_o.

Recording and Analysis of Wide Line Spectra

Figure 7 illustrates a typical two-phase NMR line for a polymer sample and the first derivative of that line. Spectrometers typically record the first derivative of the line because a more favorable signal to noise ratio is obtained.

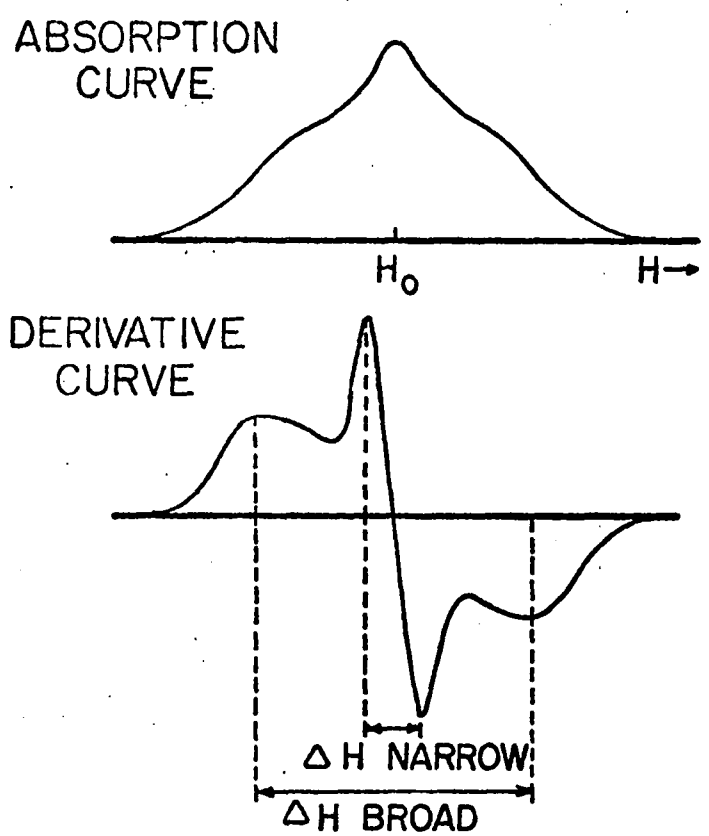

Figure 7 - Typical NMR absorption curve and first derivative of that curve for a polymer. Determination of line width (ΔH) is shown on the derivative curve.

Two measurements of the line are usually used to analyze phenomena measured by NMR. The second moment (ΔH^2) is the mean value of the square of the internal magnetic field strength. The first moment (moment of inertia) is not used because the distribution of frequencies is symmetrical so the total contribution to the moment would be zero. The second moment is useful because it can be used for theoretical calculations for a system to be measured. The expression used was derived by Van Vleck (108) in a study of CaF_2 crystals.

For a perfect crystal the result is readily obtainable from the following:

$$\Delta H^2 = 3/4\gamma^2 \; I\,(I+1)\; 1/N \sum_{i=1}^{N} \sum_{\substack{j=1 \\ (i\neq j)}}^{N} \left[1 - (3\cos^2\Theta_{ij})/\vec{r}_{ij}^{\,3}\right]^2$$

where Θ_{ij} describes the vector projection relative to (H_o) and

$\vec{r}_{ij}$ is the vector from dipole i to j

To calculate the second moment from half the derivative curve, the following integral applies:

$$\Delta H^2 = \frac{\int_{H_o}^{\infty} (H-H_o)^3/3 \; f'(H)dH}{\int_{H_o}^{\infty} (H-H_o) \; f'(H)dH}$$

where f'(H) = derivative function recorded by the spectrometer.

The second measure of the NMR line is line width (ΔH), here defined as the distance between maxima and minima on the derivative curve as shown in Figure 7.

The areas under the curves of the complex NMR line are proportional to the number of nuclei in the molecular fraction represented by the curve. The shape of the NMR line, the ratio of areas under the superimposed curves of the complex line, and second moment can elucidate information about a compound such as the ratio of mobile to immobile fraction (that is, amorphous to crosslinked or crystalline fractions), major transition temperatures, specific molecular motions within the polymeric structures, and the presence of "impurities" and their effect on molecular motion (8, 74, 79, 108, 110).

Interpretation of Wide Line Spectra

The two phase character of NMR lines resulted in early attempts to measure polymer crystallinity by this method. Wilson and Pake (131) reported degree of crystallinity of polyethylene and Teflon. Using the Wilson and Pake method of phase separation which involves drawing a straight line from the minima of half of the derivative curve to the origin, Collins (27) found crystallinity values of polyethylene to agree with x-ray values within 1.8%. Determination of crystallinity by the NMR method was questioned by others (39). When Fuschillo, et al (38) attempted to determine polyethylene and nylon crystallinity from spectra obtained over a wide temperature range, they found wide disagreement with

x-ray measurements. Further, when samples were irradiated to levels known to reduce x-ray crystallinity to zero, a high rigidity index was still obtained.

Correlation time is the time required for a molecule to reorient or assume any one of its possible equilibrium positions in the crystal lattice. Its value is temperature dependent. When the reorientation rate is of the order of the frequency line width, the resonance line narrows (8). The NMR method for determining crystallinity is based on the assumption there exists a temperature at which the average correlation time for motion in the crystalline region is $\tau cc \gg 10^{-4}$ sec; and in the amorphous region it is $\tau ca \ll 10^{-4}$ sec (107). However, the relationship between τcc and τca varies with temperature. At low temperature τcc and $\tau ca \gg 10^{-4}$ sec for a polyethylene sample. As the temperature was varied $\tau ca \cong 10^{-4}$ sec but $\tau cc \gg 10^{-4}$ sec. At sufficiently high temperatures both lines narrowed and $\tau cc \gg 10^{-4}$ sec $\gg \tau ca$ obtained. Unless a temperature can be found where this final combination exists, separation of phases, even in an arbitrary way, is not possible. Motion in polymers measured by NMR is not necessarily associated with molecular order. For example, crosslinks or entanglements of branched polymers can cause constraints on motion which bear no relation to crystallinity. The authors cautioned that crystallinity determined by NMR must be verified by other methods of measure.

McCall and Anderson (69) suggested that it is more accurate to consider the broad and narrow components

as measures of rigid and mobile fractions, respectively. This concept is valuable as it is the mobile fraction which dominates the mechanical properties of polymers. McCall and Anderson were concerned, as were others (38, 107) with the arbitrary separation of the complex line into mobile and immobile fractions. The straight line was found more accurate than a curve when values for the immobile fraction of polyethylene were compared with values obtained for a 100% crystalline sample. The ratio of mobile or immobile fractions to the total area under the NMR line, then, gives some information about polymer structure, but it does not describe the shape of the curves which may provide insights as well.

When polyethylene (69) was swelled with carbon tetrachloride, the narrow peak intensity increased but the integrated intensity did not change. Further, no change in shape of the broad peak occurred. This was taken as evidence that solvent enters only the amorphous regions of the polymer.

Plots of the second moment (ΔH^2) and line width (ΔH) of the NMR line versus temperature provide information about molecular structure. Treatments known primarily to crosslink certain polymers (37, 44) and those known to increase crystallinity (105) affect the second moment and line width plots in ways which can elucidate which process has affected molecular immobilization. Gupta (43) irradiated isotactic polypropylene with neutrons and calculated (ΔH^2) and (ΔH) from the spectra recorded from 77^{o}K to 375^{o}K. Increased neutron dosages caused a decrease in (ΔH^2) and (ΔH) at low

temperatures and an increase in these parameters at higher temperatures. The effect was one of diminishing the transition near 275°K. Although the trends were the same (ΔH) changes with neutron dose were much greater than ΔH^2 changes. The decrease in (ΔH) and (ΔH^2) at low temperatures was attributed to disruption of crystallites and a loss of H_2 through free radical formation. Increase in (ΔH) and (ΔH^2) at high temperatures indicated crosslinks were formed, primarily in the amorphous regions.

Fujiwara, et al (37) irradiated polyethylene film with a deuteron beam for 30 seconds. The film lost 2% H_2 and gained 1.03% in weight due to adsorption of O_2. Second moment and line width were similar to Gupta's findings for polypropylene.

High energy irradiation effects on polyethylene were evaluated by density, x-ray and NMR (106) measurements. In agreement with other findings, irradiation decreased crystallinity and caused crosslinking. The amorphous halo of x-ray patterns increased at the expense of crystalline regions. Density and x-ray Bragg spacings decreased at low irradiation doses; then increased as the dose increased. The authors attributed the greater density to space contraction in the amorphous regions due to introduction of crosslinks. Nuclear magnetic resonance was found to be less sensitive to irradiation effects than other measurements. One crosslink per 50 carbon atoms caused change detectable by tensile and solubility tests, but was not sufficient to

affect molecular motions measured by NMR. Dose levels as high as 5.0×10^8 reps caused no change in the portion of the resonance line associated with amorphous regions. Line narrowing was observed in the 150 - 250°K region indicating irradiation had reduced constraints in the crystalline fraction. At dosages sufficient to cause considerable cross-linking there was little NMR line narrowing well above the usual melting point for polyethylene.

Stark rubber is a crystalline product obtained by compressing rubber at low temperature over a long period of time. Crystallinity was confirmed by x-ray and NMR measurements (105). Narrowing of the NMR line occurred at higher temperatures for stark rubber than for untreated rubber. At low temperatures (to - 100°C) the NMR line was broader for the crystalline rubber as a result of closer chain packing.

The importance of vigorously drying samples before NMR measurements is generally recognized (40, 80, 135). The relatively unrestrained protons in water can cause a sharp intensity peak in the NMR spectrum which can distort the narrow portion (74). Under controlled conditions, the effect of water on the NMR line has been used to study the plasticizing effect of water on molecular motion in polymers. Woodward, et al (135) compared (ΔH) and (ΔH^2) for several polyamides with 0, 1.7, 7.0 and 7.5% water content recorded from 80 - 300°K. The effect of water generally was to decrease the (ΔH^2) and shift the (ΔH^2) transitions to lower temperatures. At 7% moisture content (saturation) the

transition occurred 150°K lower than for dry nylon 66. A similar effect was observed for line width where the transition occurred 100°K below that for dry nylon. Lowering of the transition which is associated with segmental motion in the amorphous phase, was attributed to rupture of hydrogen bonds in the polymer followed by association with water molecules. Since the equilibrium amounts of water absorbed were proportional to polymer amorphous content, the plasticizing effect of water was believed to occur primarily in those regions (41).

Olf and Peterlin (81) verified that the mobile polymer line of the NMR spectra for nylon 66 recorded at 28°C in the presence of water was associated with the alpha transition by observing an analogous mobile line when spectra for dry nylon were recorded at 120°C. These workers also observed that in atmospheres below 20% relative humidity (which corresponds to 0.7% moisture regain) no sharp water peak was seen in NMR spectra.

Statton (110) examined the effect of heating and moisture on molecular motion of several polymers, relaxed and under tension. Drawn nylon 66 measured under tension gave a broader NMR line than relaxed. Boiling the sample in water relaxed the yarn, restoring the original NMR line. It was concluded that soaking nylon 66 fibers in water at room temperature has a "loosening" effect on the molecular structure similar to dry heating at 200°C.

Several workers (43) have associated the transitions in plots of (ΔH^2) and (ΔH) versus temperature with specific molecular motions. Transitions observed in NMR lines have also been related to transitions observed by dynamic mechanical loss measurements (31, 59). The two methods compare favorably although the temperatures at which transitions occur do not always coincide.

Three transitions have been identified (alpha, beta and gamma) as arising from motions in the amorphous regions. In nylon 66 the alpha transition (50 - 80°C) is associated with the onset of coordinated segmental motion in the aliphatic chain segments. It is usually referred to as the glass transition temperature, although the designation is questioned because of the fairly wide range over which it is found to occur (74, 80). The alpha transition in polymers has been found to vary with draw ratio (75), length of paraffinic segments (102), and presence of moisture (40). The beta and gamma transitions occur at low temperatures, beta being associated with the presence of water or other low molecular weight impurity (59). The gamma transition, in NMR experiments found near -100°C (80), is associated with rotation of methylene groups.

Motion in crystalline regions of polymers has been identified by NMR studies (74, 79, 80). It was observed that carefully prepared crystalline samples gave a complex NMR line similar to lines obtained from two phase polymer systems. The narrow line of polymer crystals has been

attributed to lattice defects (42). With carefully controlled experiments, Olf and Peterlin (79) were able to attribute the gamma transition in polyethylene to motion in chain folds at the lamellar surfaces of the crystallites. At temperatures above the alpha transition, but below the melting point, motion has been observed in the rigid fraction of nylon 66 fibers (74, 80). The (ΔH^2) transition is observed most clearly when samples are oriented with molecular axes parallel to the magnetic field. Olf and Peterlin (80) have shown that the motion at 180°C is characteristic of a 60° oscillation (termed 60° "flip-flop") of the amide groups between the hydrogen bonded plane and the van der Waals plane in the crystallites. At this temperature there is also torsional oscillation of high amplitude in the aliphatic chain segments (74, 80, 102).

Gupta (45) employed broadline NMR to study the orientation of hydrogen bonds in several polymers by relating line width to sample orientation in the magnetic field. Hydrogen bonds in nylon 66 were found to be oriented perpendicular to the chain axis; an orientation favorable to intermolecular bonding.

CHAPTER III

EXPERIMENTAL PROCEDURES

Experimental Yarn

Selection

A multifilament nylon 66 yarn was obtained from the Chemstrand Research Center. Information from the manufacturer identified the yarn as their type A05, 630 denier, 104 filament yarn with a ½ Z twist. The yarn contained copper, iodine, and titanium dioxide in undisclosed form and quantities. From patent literature (17) it was deduced that the additives were probably thermal antioxidants added to the hexamethylene diadipate prior to polymerization as copper acetate and potassium iodide. The titanium dioxide is a well known delusterant commonly added to polyamides and other transparent polymers.

The experimental yarn was of the same description and source, though probably not the same merge number, as that used by Olf and Peterlin (80) for NMR studies of drawn nylon 66 fibers. They obtained information from the manufacturer relative to yarn draw ratio and molecular weight. Density and crystallinity measurements obtained from density data were made. Table 3 shows yarn data reported by Olf and Peterlin and that obtained by measurement of the yarn used in this study.

TABLE 3

PARAMETERS OF CHEMSTRAND NYLON 66 YARNS OF THE SAME DESCRIPTION AS REPORTED FROM TWO LABORATORIES

Parameter	Olf and Peterlin (80)	This Study
Draw Ratio	5:1	---
Molecular Weight		
$\bar{M}_n$ (End Group Analysis)	17.5×10^3	
$\bar{M}_w$ (Light Scattering)	34.4×10^3	
$\bar{M}_v$		17.1×10^3
Density (gm/cc)	1.144	1.148
Crystallinity (%)*	53	52.4
Filament Denier	---	6
Filament Diameter (μ)	---	29
Removal of Spinning Finish and Storage	Extracted 2 days in ether. Evacuated at 10^{-4} Torr at 100°C for 4 weeks	Aqueous nonionic scour; 6 rinses; air dried at room temp.; evacuated until use

*The apparent discrepancy in percent crystallinity from density measurements must arise from a slight difference in calculating procedure. See p. 138.

Removal of Spinning Finish

The supplier reported the yarn to have a 1% (owy) finish which could be removed by a 30 minute extraction in carbon tetrachloride. Gravimetric analysis of carbon tetrachloride extracted residue and yarns suggested that solvent was being retained by the yarn. When the residue was analyzed 1.09% weight loss was calculated. However, when the extracted yarns were weighed, a 0.34% weight loss was recorded. The discrepancy was beyond experimental error. Further, retained chlorine could act as a free radical initiator and/or scavenger under UV irradiation. It has been shown (55) that the presence of solvents in polyamide films is influential in UV degradation reactions. The sodium fusion test for halogens (16), modified to distinguish Cl^- from I^-, confirmed the presence of chlorine on the yarns. Consequently, the solvent extraction procedure was abandoned.

Gravimetric analysis revealed that a 15 minute aqueous scour in a nonionic surfactant was sufficient to remove the 1% spinning finish. However, the yarn shrank approximately 3.5% when placed in distilled water at $130^{o}F$ for 15 minutes; approximately 2% under similar conditions at room temperature.

To insure adequate removal of the spinning finish and surfactant with minimum change in the yarn the following scouring procedure was formulated and carried out in the pilot finishing plant in the School of Textiles. All experimental yarn required for the study was scoured at one time.

A surface layer of yarn was removed from the manufacturer's bobbins and discarded. A total of 327 grams of yarn was mechanically reeled from the bobbins and divided into four skeins. Each skein was leased in six places, wrapped in clean white cheesecloth, and tied four times. The skeins were soaked in distilled water at room temperature. The soak was followed by a 20 minute hand agitated scour in a distilled water solution of 0.1% Triton X-100 at 125°F. Triton X-100, a Rohm and Haas product, is a nonionic surfactant with general chemical formula:

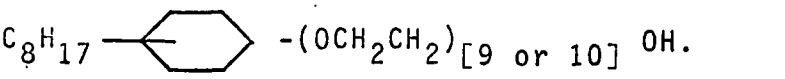

Six distilled water rinses of 5 to 10 minutes each were used. All rinses were at room temperature except the second which was at 100°F.

The skeins were air dried. Each was then wound mechanically with minimum tension onto a perforated stainless steel package and stored under vacuum in a darkened dessicator until use.

Ultraviolet Exposure

Apparatus

All UV exposures were made in a Rayonet Photochemical Reactor manufactured by the Southern New England Ultraviolet Company. The apparatus is an insulated circular chamber with highly reflecting interior surface. Sixteen lamps are spaced evenly around the chamber wall. The apparatus is equipped

with a fan which reportedly maintains an interior temperature of 44°C. However, monitored temperature averaged 52°C.

Sixteen 24-watt RPR-3500 lamps with 90% of the wavelengths at 3500 ± 500 Å were mounted in the Rayonet Reactor. Intensity at the center of the reactor was reported to be 9200 μwatts/cm^2 (Figure 27, Appendix).

The manufacturer suggested discard of the lamps following 2000 hours use due to decrease in intensity. Lamp intensity was monitored with a photocell. New lamps were installed following the preliminary work and 72 hour exposures.

Sample Preparation

All sample preparation was done under dry nitrogen gas atmosphere to prevent adsorption of moisture onto the scoured evacuated yarns. All apparatus which would contact the yarn was oven dried and cooled in a nitrogen atmosphere prior to yarn handling.

Yarn was carefully wound with minimum tension in a single layer around a quartz tube with 35 mm outside diameter. The quartz tube could accomodate enough yarn for at least one replicate of each analytical procedure. Records were kept so that all analyses could be identified with the appropriate UV exposure period.

The yarn wound tube was inserted into a quartz exposure flask with 45 mm inside diameter and closed with a rubber stopper fitted with two stopcocks. The sample was flushed with dry oxygen gas for 30 minutes when that test atmosphere

was used. The stopcocks were then closed and the stopper sealed in place with paraffin wax.

The quartz exposure apparatus (Figure 8) was lowered into the center of the Rayonet Reactor, the lamps and exhaust fan turned on. The apparatus was operated continuously for designated exposure periods. Preliminary exposure periods of 20 and 48 hours were insufficient to cause detectable change by measurements employed. Consequently, data were reported for 72, 142, and 240 exposure periods. Three replications of each exposure period were obtained.

Following each exposure period, the apparatus was immediately opened under nitrogen atmosphere, NMR samples prepared, and the balance of the exposed yarn placed in clean dry darkened bottles. Dye and viscosity measurements were made within 24 hours; NMR measurements within 48 hours.

Dyeing Procedures

Sample Preparation

Half-gram samples of control and UV exposed yarns cut in approximately one inch lengths were placed in separate beakers, covered with 60 ml of distilled water, and stirred occasionally over a 1 to 1½ hour period until all air bubbles were removed and yarns appeared wetted out. Excess water was carefully drained from the samples and they were dropped into preheated dyebaths with vigorous stirring.

ULTRAVIOLET EXPOSURE
APPARATUS

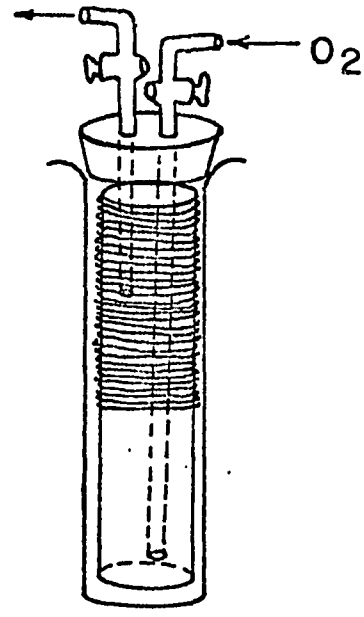

Figure 8 - Quartz assembly for UV exposure of yarn under a controlled atmosphere.

Dyebath Preparation

Two acid dyes were used, one to characterize differences in amine end group content and the other to determine differences in fiber structure as exemplified by dyeing rate.

1. Amine end group content - Merpacyl Blue SW

(C. I. Acid Blue 78)

Merpacyl Blue SW is a monobasic sulfonic acid dye of the following chemical structure:

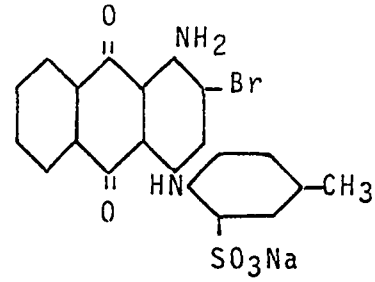

The dyeing procedure was a modification of DuPont diagnostic dyeing for capacity uniformity (124).

Dye Formula

0.05	g/l	Merpol S. E. (surfactant)
5.0	g/l	monosodium phosphate
10.0	%	sodium hydroxide to bring the bath to pH 6.0
1.0	%	Merpacyl Blue SW (owf)

2. Rate of dyeing - Anthraquinone Milling Blue BL

(C. I. Acid Blue 122)

The procedure was a slight modification of the DuPont diagnostic dyeing procedure for structural uniformity of nylon 66 (124). The chemical structure of this dye is not published. However, it is probably a dibasic sulfonic acid dye (125).

Dye Formula

0.005 % Merpol SE (owf)
3.0 % ammonium sulfate (owf)
Glacial acetic acid to a bath pH 3.7 ± 0.1%
1.0 % Anthraquinone Milling Blue BL (owf)

For either dye, a one liter solution of all additives was made up and pH adjusted using a pH meter. A 100 ml portion was removed as a blank for spectrophotometric determinations. The blank was subsequently handled in the same manner as the dyebaths. Dye was added to the remaining solution and stirred until dissolved. Dissolution of the Anthraquinone Milling Blue BL was excellent, making straining of the solution unnecessary. The Merpacyl Blue SW dissolved less readily but on warming with stirring, solution was obtained. The pH of dyebaths was checked after addition of dyes, but in no case was adjustment necessary.

Well stirred dye solution was measured in 100 ml volumetrics and transferred to 100 ml beakers. In this manner a 200:1 dyebath for each 0.5 gm fiber sample was prepared.

The dyebaths were covered with watch glasses and placed in a constant temperature oil bath so that the dyebath level was below that of the oil. The temperature was brought to 97°C and the fibers entered with vigorous stirring. Anthraquinone Milling Blue dyeings were carried out for 60 minutes (or until dyebath exhaustion) at constant temperature with intermittent stirring. Five milliliter aliquots were removed after 5, 10, 20, 45, and 60 minutes dyeing time for spectrophotometric analysis. Merpacyl Blue dyeings were

carried out for 90 minutes; 5 ml aliquots being removed after 5, 20, 45, 60, and 90 minutes for analysis. Aliquots were taken from control dyebaths (those containing no fibers) on reaching 97°C and at the end of the dyeing time to be used as a spectrophotometric reference and to detect any occurrence of dyebath evaporation.

Evaluation of Dye Data

Optical density of serial dilutions of both diagnostic dyes showed them to obey Beer's law (Appendix Figure 28.) A Beckman DK Recording Spectrophotometer was used to record spectral absorbence of dyebath aliquots in the 400nm to 750nm range. The maximum absorbence peak for both dyes occurred at 620nm. Consequently, all absorbence data was taken from this point. Calculations of percent dye on the fiber were made as follows:

$$100 - \left[\frac{\text{Sample dyebath absorbence at time (t)}}{\text{Original dyebath absorbence}}\right] \times 100 =$$

Percent dye on the fiber at time (t)

Experiments were run with the Anthraquinone Milling Blue to determine the effect of four weeks storage on the dye take-up of yarns exposed to UV up to 142 hours and the effect of vacuum drying versus air drying on the dye take-up of yarns exposed to UV for 72 hours. There was no observable dyeing effect resulting from yarn storage or vacuum drying so these experiments were discontinued.

Equilibrium Dyeing with Anthraquinone Milling Blue BL

Two 5 gm lengths of yarn, one control and the other exposed to UV for 240 hours, were coiled and loosely tied; identified; and wet out in 0.005% Merpol SE solution for approximately one hour.

A 900:1 bath to yarn ratio of the following formulation was prepared (all percentages owf):

0.005% Merpol SE
3.0 % ammonium sulfate
Glacial acetic acid to a bath pH 3.75
4.5 % Anthraquinone Milling Blue BL

The bath was covered with a watchglass, brought to 88°C in a constant temperature oil bath, and the yarns entered with vigorous stirring. Yarns were dyed with occasional stirring at 88°C for three hours.

Dyed samples were removed from the bath, rinsed in distilled water, and air dried. Evaluation of dye adsorption and fiber penetration was visual and microscopic.

Reporting of Dye Results

Percent dye on the fiber at time (t) was plotted versus dyeing time. Apparent diffusion coefficients (D) were calculated according to the modified procedure for diffusion into a plane semi-infinite medium.

$$D = \frac{\left[\frac{C_t}{C_\infty}\right]^2}{t} \left[16\pi(rl)^2\right]^{-1}$$

where: $\frac{\left[\frac{C_t}{C_\infty}\right]^2}{t}$ gives the slope of the line

$r = 14\mu$; the radius of the filament
l = length/gm of a 6 denier filament

Nuclear Magnetic Resonance Procedures

Sample Preparation

All samples were prepared in a dry nitrogen atmosphere immediately following designated UV exposure periods. The control samples were prepared under nitrogen following at least 24 hours evacuation.

Figure 9 illustrates the device used for winding oriented NMR samples. Yarn was removed from (a), perforated package (control) or the quartz tube from the UV exposure apparatus, by passing it through eyelet guides (b) and Teflon guide (b'), then around Teflon posts (c) by manually turning turntable (d). Guide (b') could be adjusted to insure even parallel distribution of the yarn as it was looped around the posts. A small plastic spacer (e) was used to keep the posts erect during winding. It was determined that 420 complete revolutions would provide a 0.5 gm finished sample.

The looped yarn sample was secured with a separate tie and drawn carefully through opening (b) in the 3/8" Teflon rod sample holder shown in Figure 10. A slit from the bottom of the holder to opening (b) allowed expansion of the opening to prevent undue stress on the sample as it was fitted snugly into the holder. Sleeve (c) was slipped over the end of the sample holder to hold the yarns firmly in place. Excess yarn was removed with a razor blade, cutting the yarn flush with the sample holder. Yarn cuttings were stored in dry bottles in the dark to be used for other analyses. Finally, a thin Teflon sleeve (d) was slipped over the end of the sample

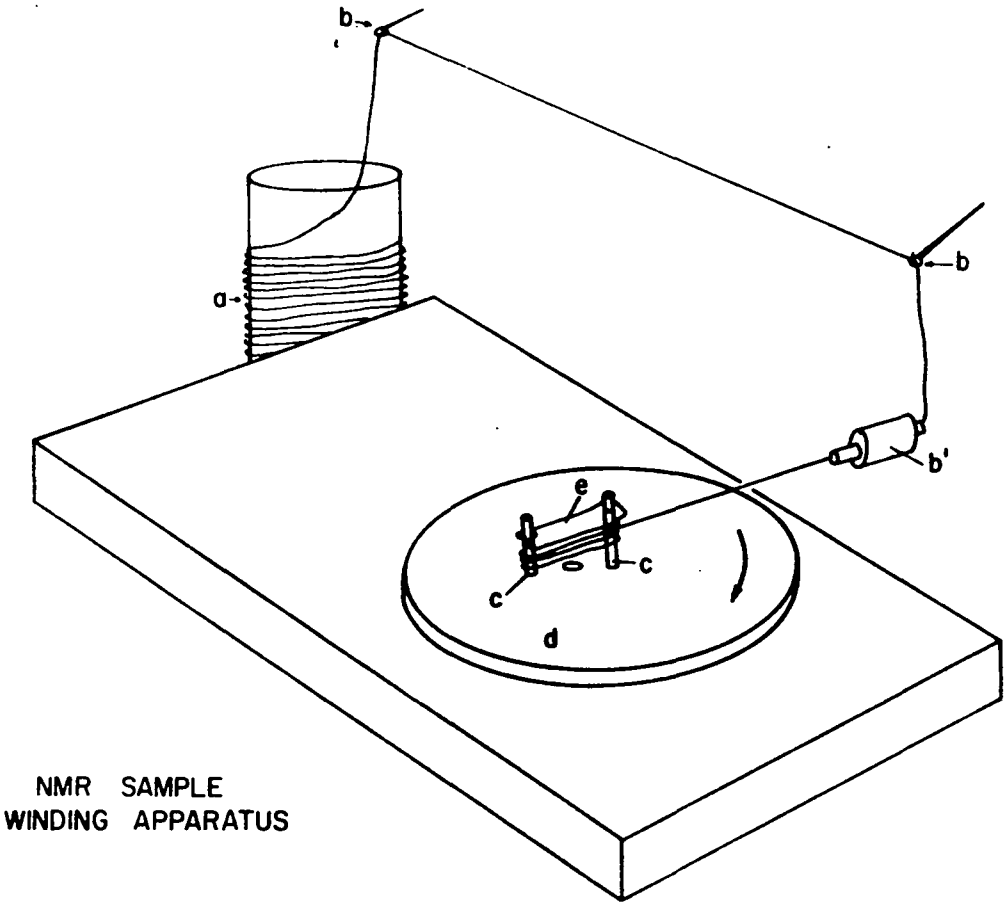

Figure 9 - Apparatus used for winding oriented yarn samples for NMR analysis.

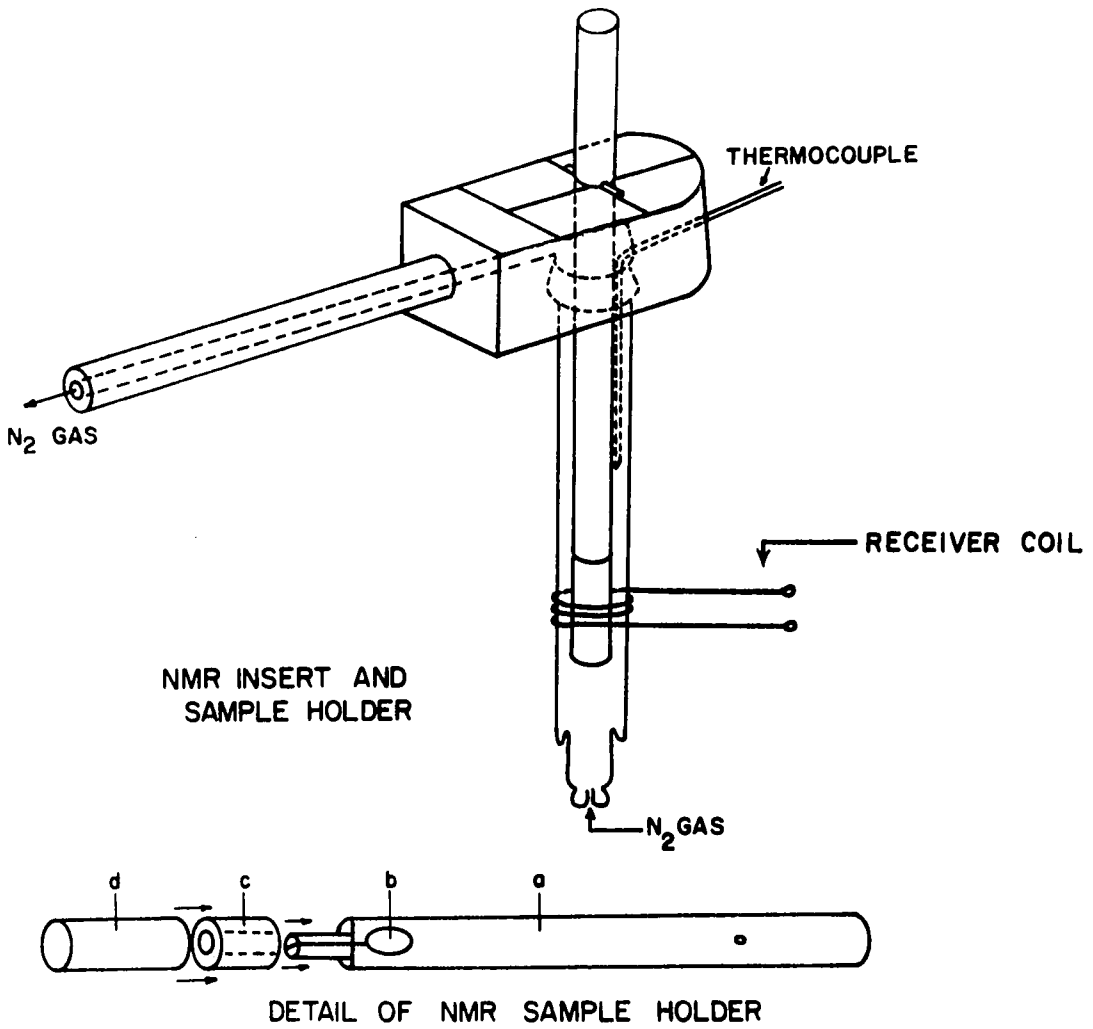

Figure 10 - NMR insert assembly showing yarn sample holder placement and detail of yarn sample holder.

holder covering the yarn. The holder with sample was evacuated at 10^{-4}mm Hg for at least 24 hours before NMR spectra were recorded. This procedure was adequate to prevent interfering proton signals from absorbed water.

Recording Wide Line Spectra

A Varian Model DP 60 with fixed radio frequency of 58.6 MHz was used to record NMR spectra. The glass insert of the variable temperature probe shown in Figure 10 was fitted with a Teflon cover which allowed positioning of the sample at a known orientation in the magnetic field, accomodation of a thermocouple, and escape of nitrogen gas which had been passed over the sample. All spectra were recorded with fiber axes oriented at 0 ± 5^{o} to the magnetic field ($\vec{H}_o$).

High temperature control was obtained by adjusting voltage of a heater attached to the spectrometer and adjusting rate of nitrogen gas flow. Low temperatures were obtained by adjusting rate of nitrogen gas flow as it passed through a copper coil immersed in liquid nitrogen prior to passage over the sample. Temperature was monitored by positioning a thermocouple inside the glass insert as near the sample as possible without interfering with the RF circuit. Temperature was read out on a digital thermometer. Spectra were recorded at approximately 10^{o}C intervals. At least 15 minutes equilibrium time was allowed following temperature change. Spectra were recorded in the following sequence: room temperature to -100^{o}C; then room temperature to $+140^{o}$C.

Due to limitations of the temperature control system it was not always possible to obtain readings at 140°C.

All spectra were recorded at RF field strength below saturation at attenuation of 15 or 20 dbs. Modulation amplitudes of 2.14 or 1.70 gauss at 40 cps were used. Field sweep rate was approximately 0.1 gauss/sec and the response was 1.

First derivative curves were simultaneously printed out and stored on 512 channels of a Varian Associates C-1024 Computer of Average Transients (CAT). When possible data were read out from the CAT onto tape using a Tally 420 Perforator (Tally Register Corporation, Seattle, Washington). When mechanical difficulties or excessive noise made use of the CAT and Tally impossible data were extracted manually from the derivative curves.

Analyses of Wide Line Spectra

Calculation of second moment--The following expression was used for the calculation of second moment:

$$\Delta H^2 = \frac{\int_{H_0}^{\infty} (H-H_0)^3/_3 \, f'(H)dH}{\int_{H_0}^{\infty} (H-H_0) \, f'(H)dH}$$

where $(H-H_0)$ is the distance from center to either extreme of the base line of derivative curve

$f'(H)$ is the function of the derivative curve

The denominator of the expression is a normalizing term.

Data points for the manual calculation were obtained by drawing a base line, overlaying halves of the curve, averaging the two halves, and recording points at small intervals

from (H_o) to (H). Data were punched on IBM cards and calculations made by computer. The function f'(H) was obtained by linear approximation of the slope of the line at the small intervals. In the case of manual analysis the intervals were 0.24 gauss. When data points were recorded by the CAT intervals were approximately four times smaller.

Data recorded on tapes were fed directly to the computer by teletype. In this case all analysis of a spectrum was obtained by computer. A "base line" was established by averaging over all recorded points. The function f'(H) was defined by recording the difference between recorded points and the average "base line"; the slope at each interval thus could be obtained by linear approximation as above.*

The second moment versus temperature curves were plotted by computer using a least squares fit of a cubic equation.**

Line Width--Line width for both the broad and narrow components of the NMR curves were obtained by measuring peak to peak distance in gauss as shown in Figure 7. In the temperature range where the two phases were not clearly defined accurate determination of peaks was difficult, hence the point scatter.

Area Ratios of Mobile Fraction to Total Area--Area ratios were calculated from the average of two halves of the

---

*Fortran programs written by Dr. R. E. Fornes, School of Textiles, North Carolina State University.

**SAS Stepwise Regression Procedure, Triangle Universities Computer Center (TUCC), Research Triangle Park, N. C.

spectra recorded at 125°C and above. Only at elevated temperatures are the mobile and immobile fractions of the curve distinguishable.

A straight line was constructed from the minima where the phases are separable to the origin. The lower right hand curve of typical spectra illustrated in Figure 11 shows this minima.

Points were recorded from the two portions of a curve at 0.24 gauss intervals. By computer, area ratios were determined according to the following relation:

$$\text{Mobile fraction} = \frac{A_m}{A_m + A_i}$$

where: A_m is the area of the mobile fraction of the spectrum

A_i is the area of the immobile fraction of the spectrum.

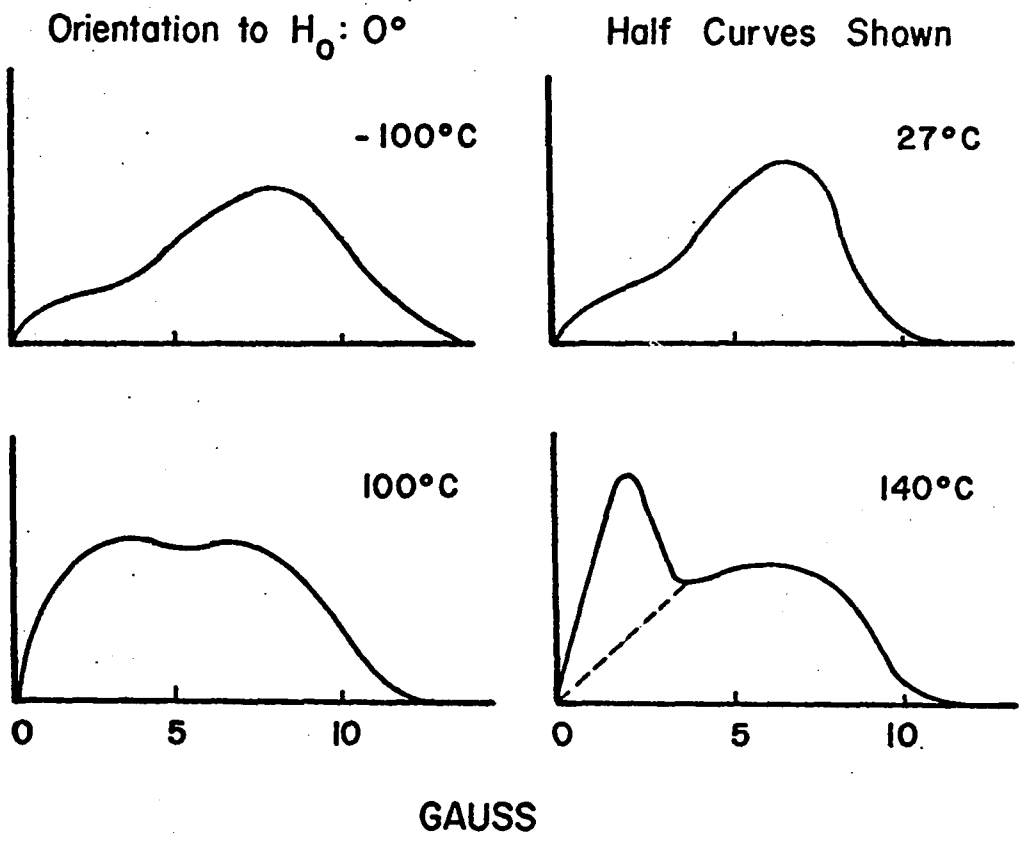

Figure 11 - Typical NMR derivative curves for nylon 66 yarns.

CHAPTER IV

RESULTS AND DISCUSSION

Dyeing Experiments

Acid dyeing, generally, is a matter of diffusion of mono or polybasic dyes from an acid medium into the amorphous regions of the nylon fiber. Rapid moving cations from the acid associate with amine end groups which then attract acid anions. These are then displaced by slower moving dye anions. If UV irradiation increased molecular order and/or changed the number of available amine end groups either by rendering them inaccessible or photochemically decomposed these changes should be detectable by diffusion rate and equilibrium take-up of certain acid dyes applied under carefully controlled conditions.

Dyeings with Merpacyl Blue SW

Merpacyl Blue SW (C. I. Acid Blue 78) is a monobasic sulfonic acid dye which under favorable dyebath conditions is more sensitive to available amine end groups than to morphologic structure of the fiber. Rate of dyeing curves could be expected to be similar in shape and any differences in equilibrium take-up would reflect changes in amine end group level in the fiber. Figure 12b shows rate of dyeing curves for control samples and yarns exposed for 72, 142, and 240

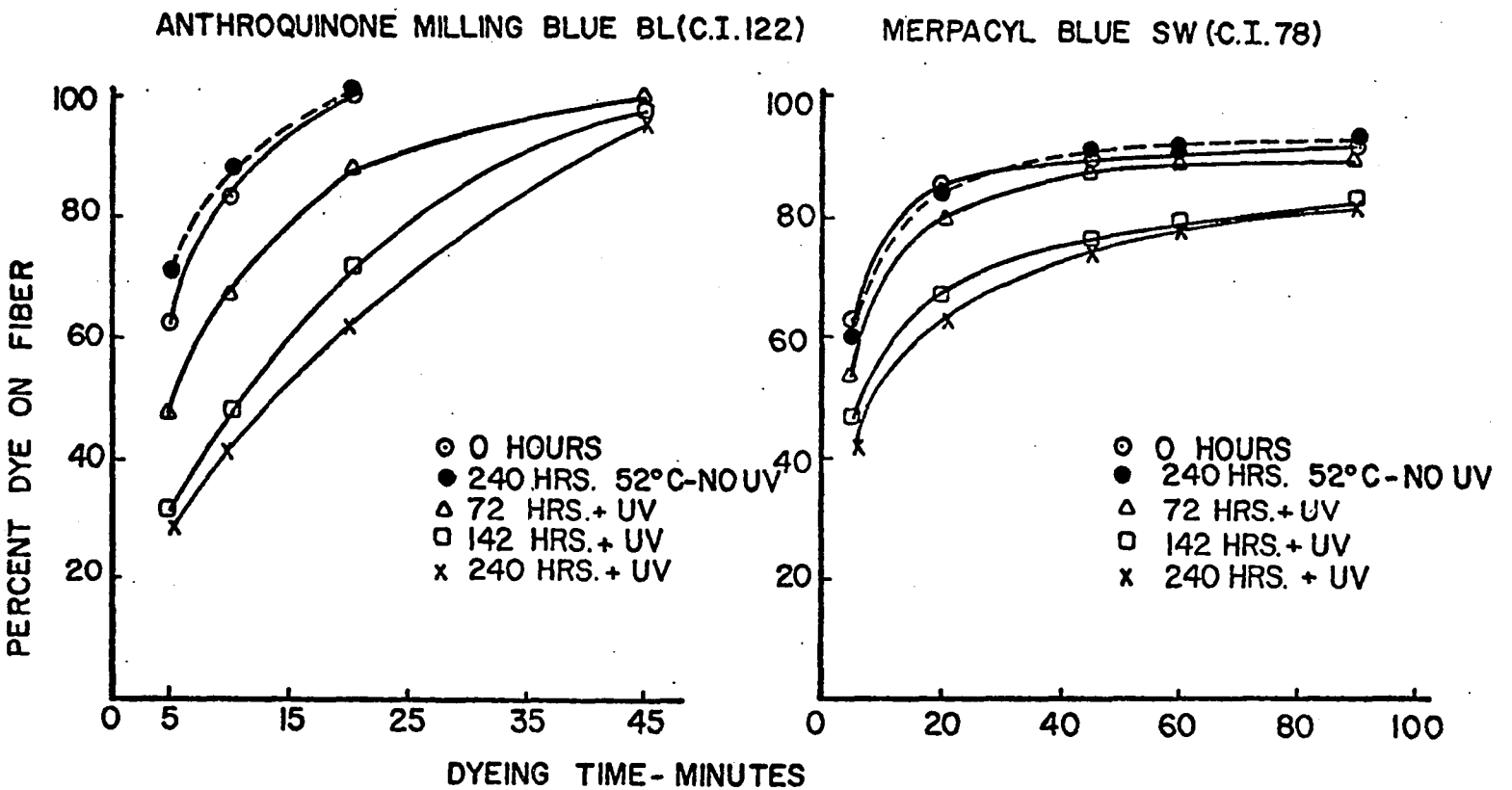

Figure 12 - Rate of dye take-up for UV exposed nylon 66 yarns dyed with (a) Anthraquinone Milling Blue BL and (b) Merpacyl Blue SW.

hours to near ultraviolet radiation. The temperature in the ultraviolet exposure chamber was approximately 52°C. The overlapping control and temperature exposure curves indicate that 240 hours at 52°C in a dry oxygen atmosphere had no effect on amine end group content in these experiments.

In the early stages of dyeing there were slight differences in curve shape between the control and UV exposures. These differences were probably due to increases in molecular order which could be expected to have at least a small effect on diffusion of Merpacyl Blue SW. However, these small differences disappeared as equilibrium take-up was approached. The most significant effect appeared to be the difference in dye take-up between 72 hours and 142 hours UV exposure. This difference may be exaggerated as new lamps were installed in the UV apparatus following the 72 hour exposures.

After 90 minutes dyeing time there was 7% more dye on the control yarns than on those exposed 142 or 240 hours. The controls had very nearly reached equilibrium dye take-up. Although the samples exposed 142 hours and 240 hours were continuing to adsorb dye at 90 minutes dyeing time, the rate was greatly attenuated and was the same for both exposures. This was interpreted to mean that upon 142 hours exposure to 3500 Å irradiation in dry O_2 atmosphere a measurable number of amine end groups were changed by photochemical oxidation, or were made virtually inaccessible to dye by an increase in molecular order. The oxidative effect was probably predominant. Additional exposure to UV beyond 142 hours had little

effect on the number of available amine end groups. Figure 24, page 132 shows that UV exposure caused considerable chain scission. Dyeings with Merpacyl Blue SW clearly show that the scission was not primarily depolymerization which would have created new amine end groups. The photochemical decomposition of amine end groups has been reported by others (67, 76).

Figure 13 shows dyeing rate of Merpacyl Blue SW to be non-Fickian when quantity of dye on the fiber was plotted versus the square root of dyeing time. When apparent diffusion coefficients (D) were calculated (Table 4) for the dyeing time intervals between 5 and 20 minutes there was no discernible trend in the results. If an effect of UV irradiation was to change polymer morphology at the fiber surface under conditions of relatively long dyeing times these results could be expected.

McGregor and Peters (71) observed nonlinear behavior of such plots which they attributed to diffusional properties of the boundary layer next to the fiber surface which are different from diffusional properties of the medium at the fiber surface. They showed that the plot varies with amount of stirring of the dyebath; amount of stirring affecting the thickness of the boundary layer. As dyeing time is prolonged, stirring no longer affects diffusion as the rate becomes dependent on the dye already in the fiber.

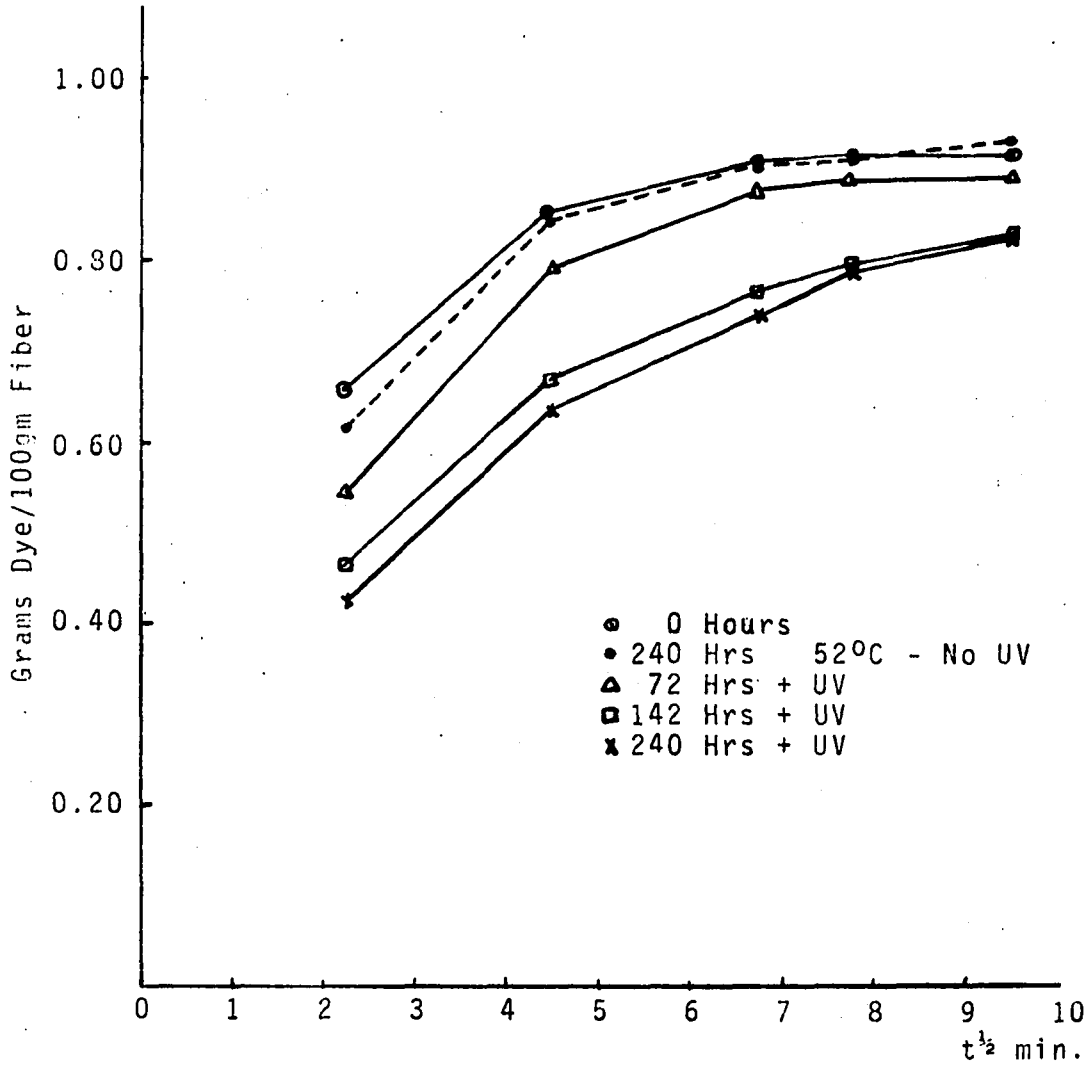

Figure 13 - Grams Merpacyl Blue SW adsorbed per 100 grams of nylon 66 yarn as a function of time$^{\frac{1}{2}}$ and UV exposure.

TABLE 4

APPARENT DIFFUSION COEFFICIENTS (D) FOR CONTROL AND ULTRAVIOLET EXPOSED YARNS DYED WITH ANTHRAQUINONE MILLING BLUE BL AND MERPACYL BLUE SW

Hours Exposed at 52°C	D x 10^8 cm^2/min Anthraquinone Milling Blue BL	Merpacyl Blue SW*
0	2.80	0.35
72	1.51	0.54
142	1.38	0.37
240	1.01	0.40
240 (No UV)	1.51	0.46

*Calculated for 5 to 20 minute intervals only.

Dyeings with Anthraquinone Milling Blue BL

Dye experiments with Anthraquinone Milling Blue BL (C. I. Acid Blue 122) were carried out under conditions which would accentuate differences in dyeing rate and favor amine end groups as sites. Dyebath concentration (0.05 gm/l) was apparently below the level of saturation of available amine end groups as control fibers and those with minimum UV exposure rapidly exhausted the dyebath. The bath pH of 3.7 ± 0.1 was within a range which favors amine end groups rather than amide groups as dye sites and assures no further formation of amine end groups by acid hydrolysis of the polyamide (73, 128). Dyebath temperatures were above the

glass transition temperature (Tg), a factor shown to be critical in the diffusion process (29, 89).

Figure 12a indicates that as the duration of ultraviolet exposure was increased the yarn was modified to reduce rate of dye take-up. Control yarns exhausted the bath in less than 20 minutes, but all dye was not adsorbed in 45 minutes by yarns exposed to UV for 142 hours. The yarn held at 52^{o}C adsorbed slightly more dye than the control, but the difference is not significant. It does show clearly that decreased dye adsorption following UV exposure was a real effect and not solely a thermal one.

The largest decreases in dye take-up occurred following 72 hour and 142 hour exposure periods. When these data were compared with the Merpacyl Blue SW dyeings it became apparent that the decrease in dye take-up after 72 hours exposure was largely due to an increase in molecular order as there was little change in amine end group content. Similarly, the decrease in dye adsorption following 240 hours UV exposure was greater than could be accounted for by loss of dye sites.

Reference to Figure 12 indicates that the greatest differences in amount of dye adsorption among the UV exposures appeared to occur in the early stages of dyeing, that is in 20 minutes or less. The first five minutes of dyeing would involve initial adsorption on the fiber surface. The amount of dye adsorbed then depends to a considerable extent on the available adsorption sites (78). The trend in adsorption behavior was similar for both acid dyes suggesting that there

was little additional loss of amine end groups beyond 142 hours UV exposure.

In every instance except one after five minutes dyeing time there was more Merpacyl Blue SW on the fiber than Anthraquinone Milling Blue BL, the difference being greater at higher UV exposures. This was probably not a function of dyebath concentration because at five minutes both dyebaths contained sufficient dye to saturate the fiber surface. Both sulfonic acid groups in the latter dye could be expected to react with available amine sites. However, the probability of the dye molecules obtaining steric alignment favorable for attachment would diminish as the fiber molecular structure became more constrictive. Conversely, monobasic dyes such as the Merpacyl Blue, which are usually smaller molecules, are less restricted in movement by the fiber molecular arrangement (78). This could account for differences in percentage adsorption between the two dyes and was taken as further evidence that UV exposure under these experimental conditions increases fiber molecular order.

It has been previously observed (20, 137) that ultraviolet irradiation effects are essentially surface phenomena. The dye data seem to imply that the fiber surface which the dye must penetrate has become increasingly resistant to diffusion after 240 hours UV exposure.

When the amount of Anthraquinone Milling Blue BL adsorbed was plotted versus the square root of dyeing time the relationship was linear. This was to be expected under the

conditions of low dyebath concentration and short dyeing times (Figure 14).

Calculation of apparent diffusion coefficients (Table 4) amplified the foregoing observations. The control fiber had the highest apparent diffusion coefficient as expected. The reason for the smaller value for the temperature control is less easily understood. There was no decrease in amine end group content and slightly higher dye take-up at 5 and 10 minute dyeing times. Further, there was a slight increase in intrinsic viscosity, with accompanying increase in $M_{\bar{v}}$ (Figure 24, page 132). The effect of 240 hours at 52°C may have been to cause some crosslinking. That could be expected to reduce diffusion rate, but not necessarily affect amine end groups.

The greatest reduction in diffusion rate occurred in the first UV exposure period. A much smaller change occurred with 70 additional hours of exposure, but diffusion rate decreased further as a result of the last exposure period.

The reduction in apparent diffusion coefficients does not reflect changes in amine end group content as shown in Table 4. This was expected of the Anthraquinone Milling Blue BL. Any reduction in diffusion coefficients due to decrease in chemical potential gradient should be minimized under the experimental conditions, that is low dye concentration and short dyeing time. If the effect of polymer segmental motion at dyeing temperatures above Tg is to increase diffusion rate,

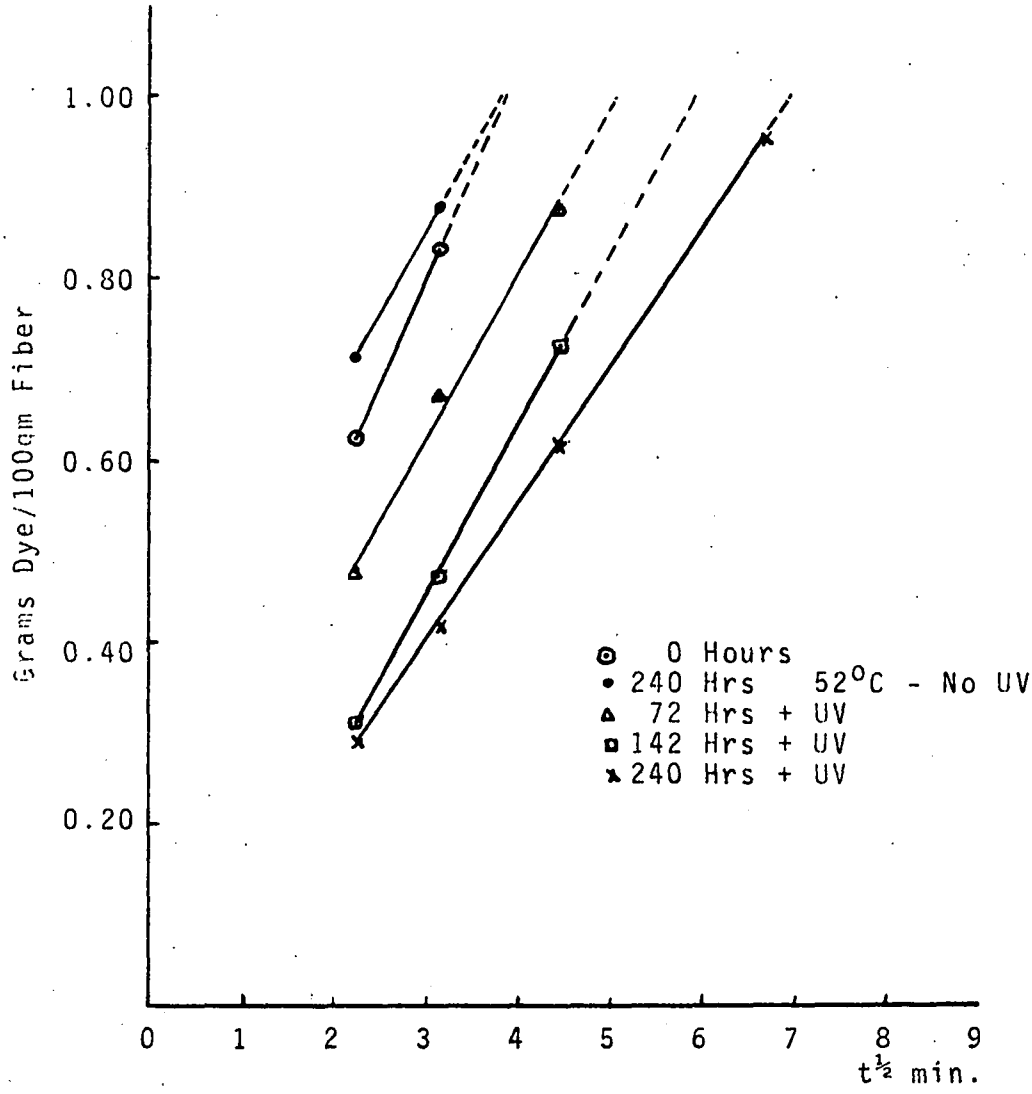

Figure 14 - Grams Anthraquinone Milling Blue BL adsorbed per 100 grams of nylon 66 yarn as a function of time$^{\frac{1}{2}}$ and UV exposure.

as segmental motion is restricted due to increased molecular order in the amorphous phase, diffusion rates should decrease. (See Figure 22, page 120.)

The dyeing experiments suggest that prolonged exposure at 3500 Å ultraviolet irradiation in dry O_2 atmosphere increased molecular order but rendered ineffective some amine end groups either by photochemical decomposition or masking in newly ordered regions.

Equilibrium Dyeing with Anthraquinone Milling Blue BL

Control yarns and those exposed to UV for 240 hours were dyed together in continuous filament form in an infinite dyebath for 2 hours, 50 minutes. The UV exposed sample visibly absorbed less dye although dye penetrated approximately 4 microns into the surface of all fibers. These results support other evidence that UV irradiation eliminated or rendered amine end groups inaccessible near the fiber surface. Similar results have been reported following heat-setting and drawing treatments (13, 117).

The fact that dye penetrated all fibers to essentially the same depth was not expected in view of other evidence of change in molecular order. It would seem that for the same dyeing time the dye should have penetrated further in the control fiber than in the exposed fiber which had a lower apparent diffusion coefficient. However, it has been reported (13, 29, 52) that although dye may penetrate fiber substrates at different rates the equilibrium take-up will

be the same. Hopper, et al (52) found there was a dependence of diffusion coefficient on dye concentration in heterogeneous films, that is those shown to be more crystalline near the film surface. Additional study is needed to satisfactorily explain the observed phenomena.

Nuclear Magnetic Resonance Experiments

The nylon 66 fiber studied was from the same source and of the same description as that reported by Olf and Peterlin (80). The effect of yarn pretreatments and NMR sample preparation on the second moment (ΔH^2) were examined by comparison with their data. Removal of spinning oils with carbon tetrachloride gave second moments which compared most favorably. However, the CCl_4 treatment was abandoned in favor of an aqueous scour with yarns in a relaxed condition for reasons described above (Figure 15). The slight increase in (ΔH^2) following aqueous scour is not understood; however, the data were sufficiently similar to consider the treatments comparable.

Effect of Ultraviolet Irradiation on Second Moment

A cubic equation of (ΔH^2) as a function of temperature calculated by the least squares method was found to best fit the data. The second moment for unexposed nylon 66 decreased gradually (and almost linearly) from approximately 23 gauss^2 at -100^{o}C to approximately 11 gauss^2 at 140^{o}C. At 72 hours exposure to UV in an oxygen atmosphere there was practically no change in second moment. There appeared to be an increase

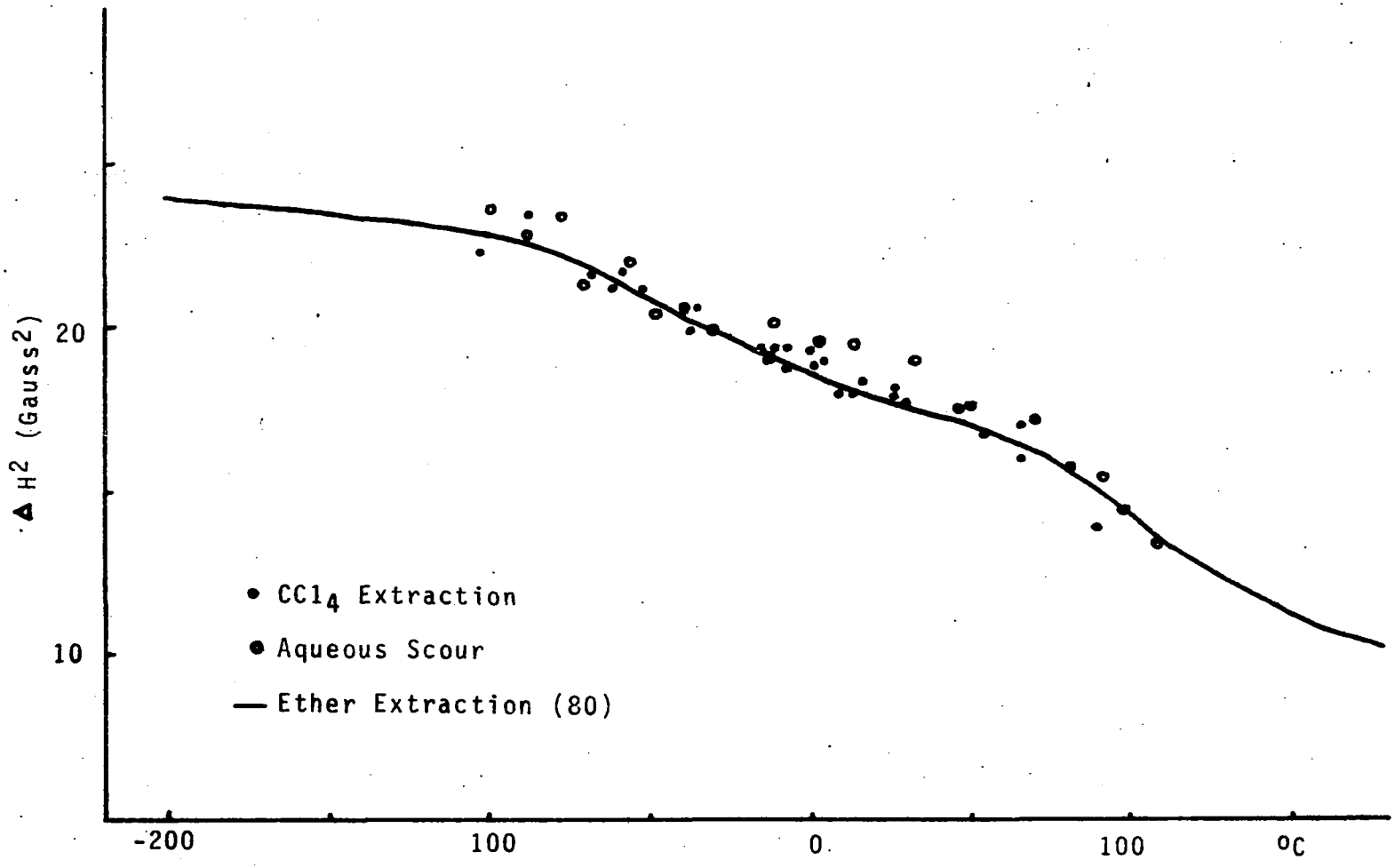

Figure 15 - Second moment for nylon 66 yarns of the same description recorded in two laboratories.

in second moment between -80°C and 40°C and a slight decrease from 40°C to 120°C as a result of 142 hours UV exposure. The scatter of data points casts doubt on the reality of this change. Samples exposed for 240 hours decreased from 24 gauss^2 at -100°C to 11 gauss^2 at 140°C. Second moment versus temperature plots are shown in Figures 16 to 19.

Within the temperature range studied at least one transition in (ΔH^2) should appear and possibly two. Both dynamic mechanical measurements (31) and NMR (56, 74, 80, 103) have detected a low temperature transition near -100°C, called the γ transition, which is characteristic of methylene group rotation about the chain axis in the amorphous regions. The α-transition, sometimes called the glass transition, usually occurs between 50°C and 90°C in nylon 66. It is indicative of coordinated segmental rotation of the aliphatic portion of the chains in amorphous regions. The γ-transition was not detected. The α-transition was not apparent in any of the second moment curves but did appear clearly when line width was plotted versus temperature as shown in Figures 20 and 21.

Figure 23 clearly indicates that 240 hours UV irradiation caused a small but measurable increase in (ΔH^2) of approximately 3/4 gauss^2 at low temperatures to 1 gauss^2 at 40°C followed by a disappearance of any difference at 140°C. An increase in (ΔH^2) indicated that UV irradiation had introduced constraints on molecular mobility but at sufficiently high temperatures the constraints were either masked or

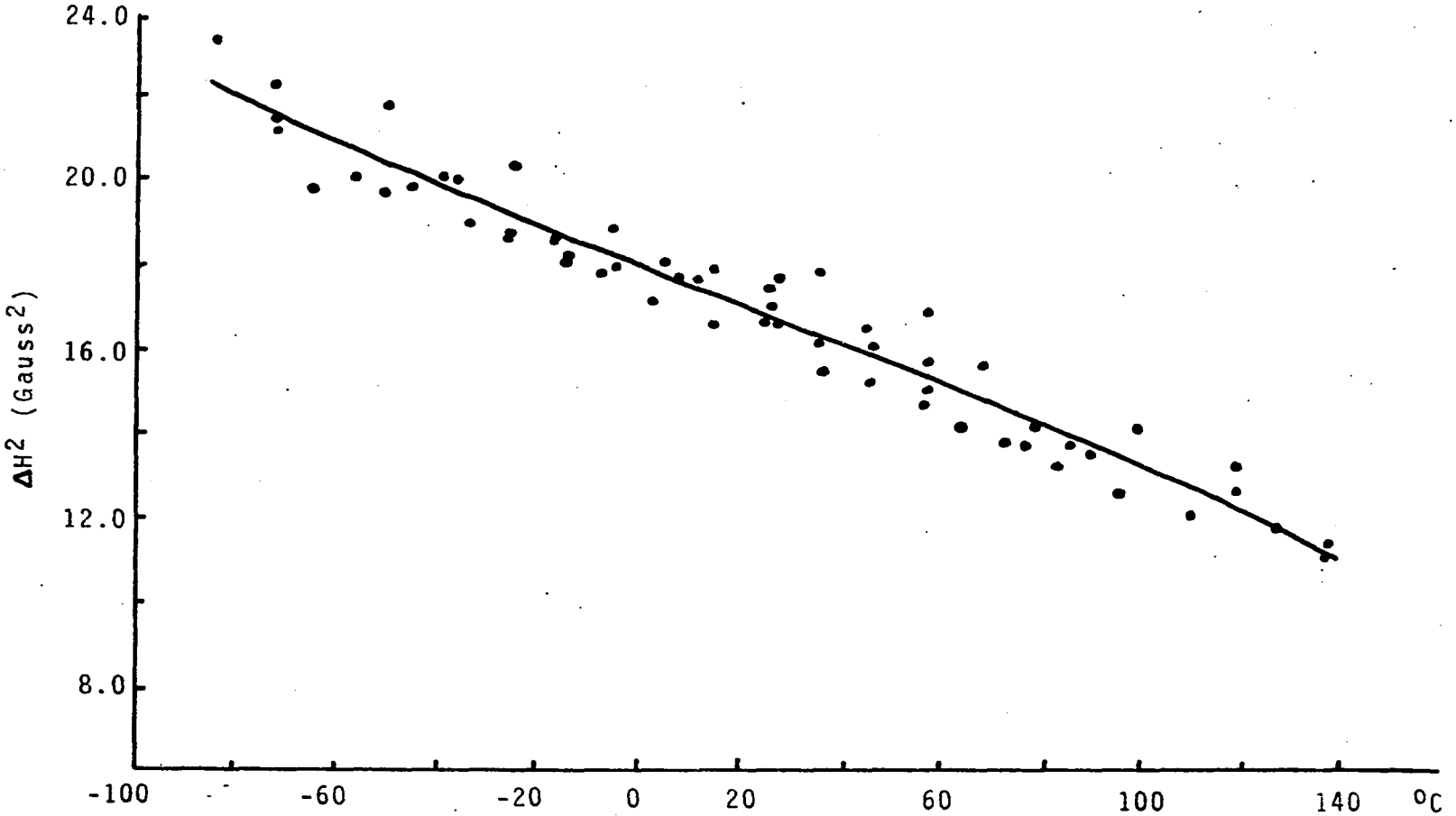

Figure 16 - Second moment for nylon 66 yarns exposed to UV for 0 hours.

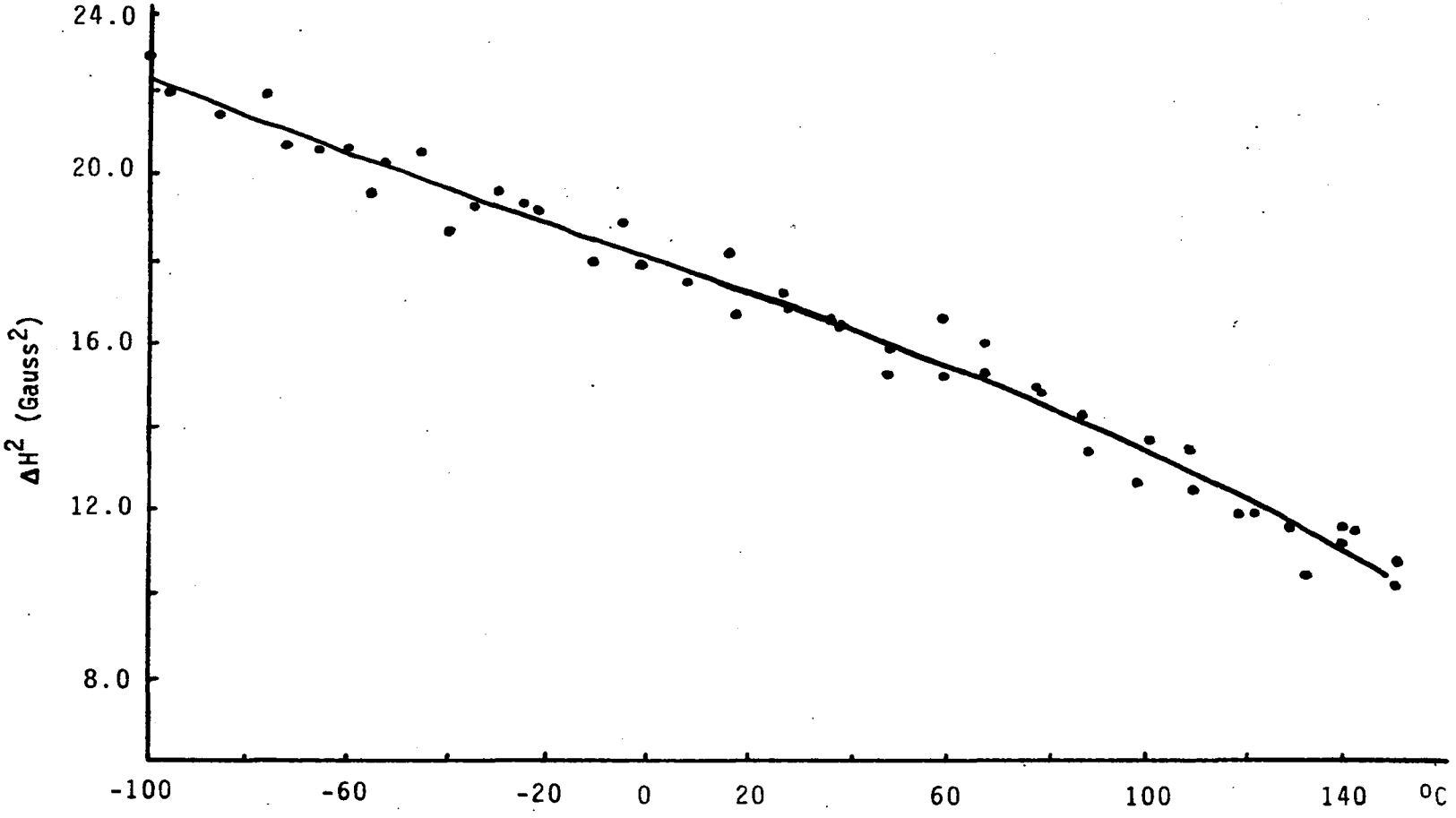

Figure 17 - Second moment for nylon 66 yarns exposed to UV for 72 hours.

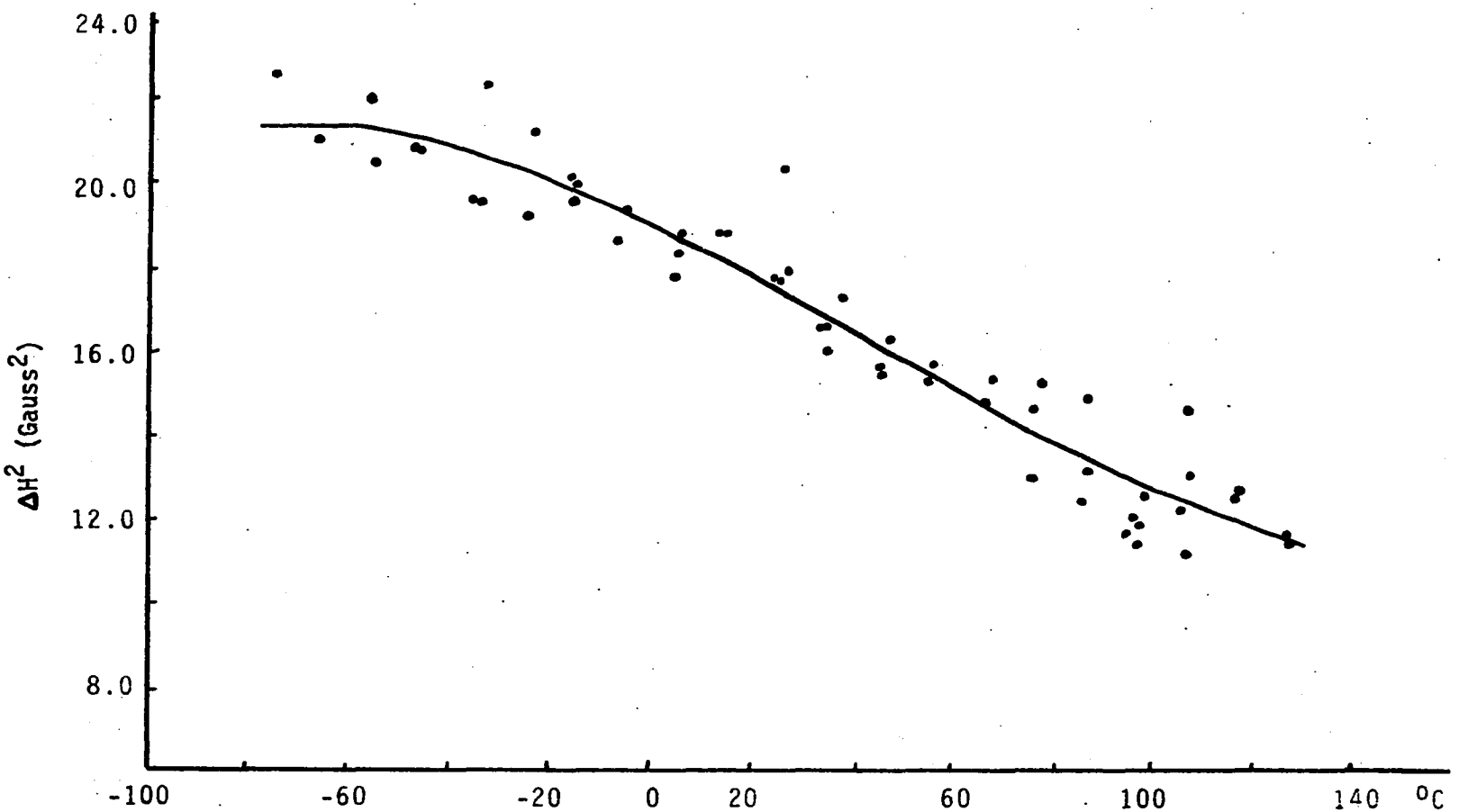

Figure 18 - Second moment for nylon 66 yarns exposed to UV for 142 hours.

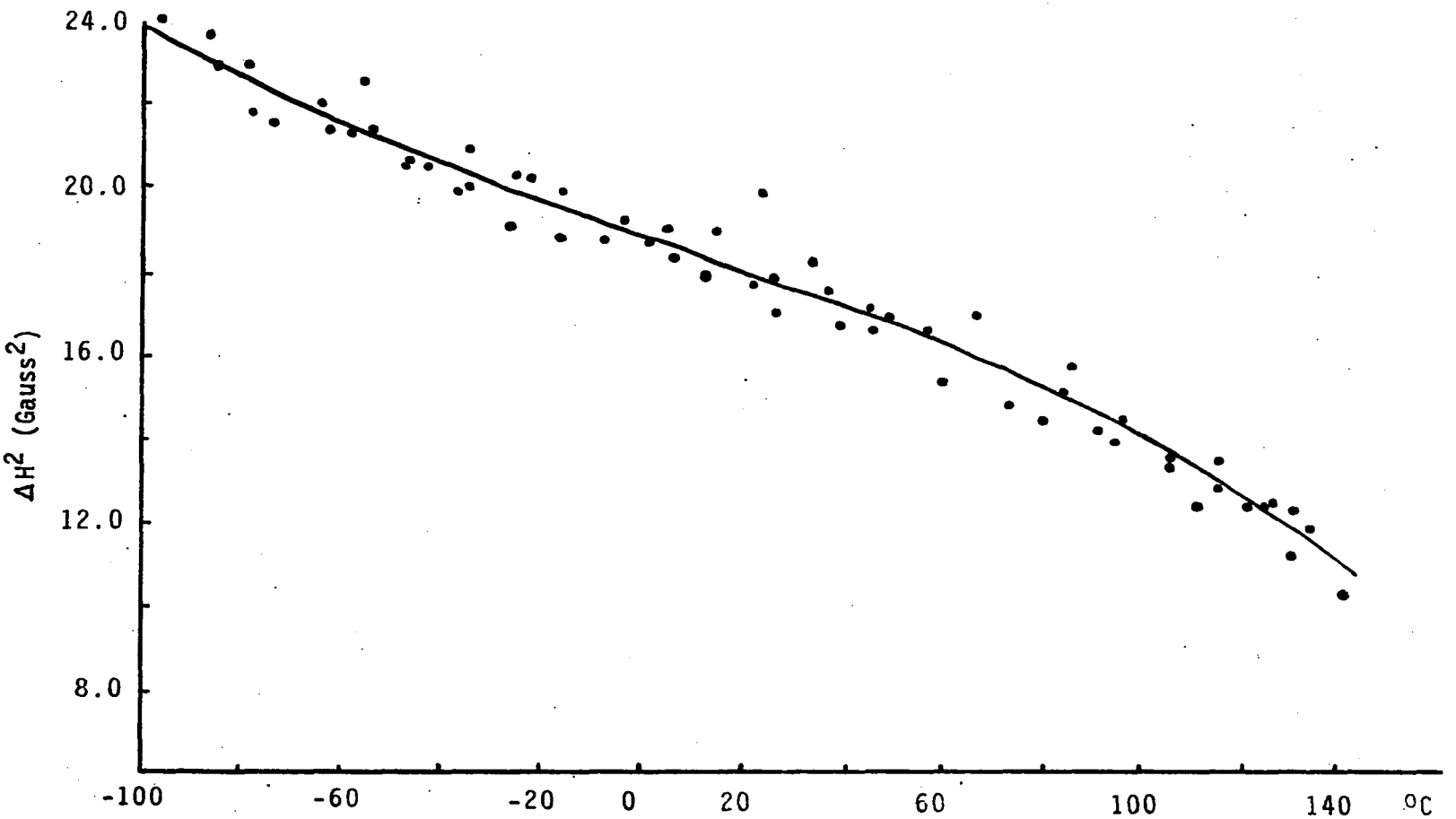

Figure 19 - Second moment for nylon 66 yarns exposed to UV for 240 hours.

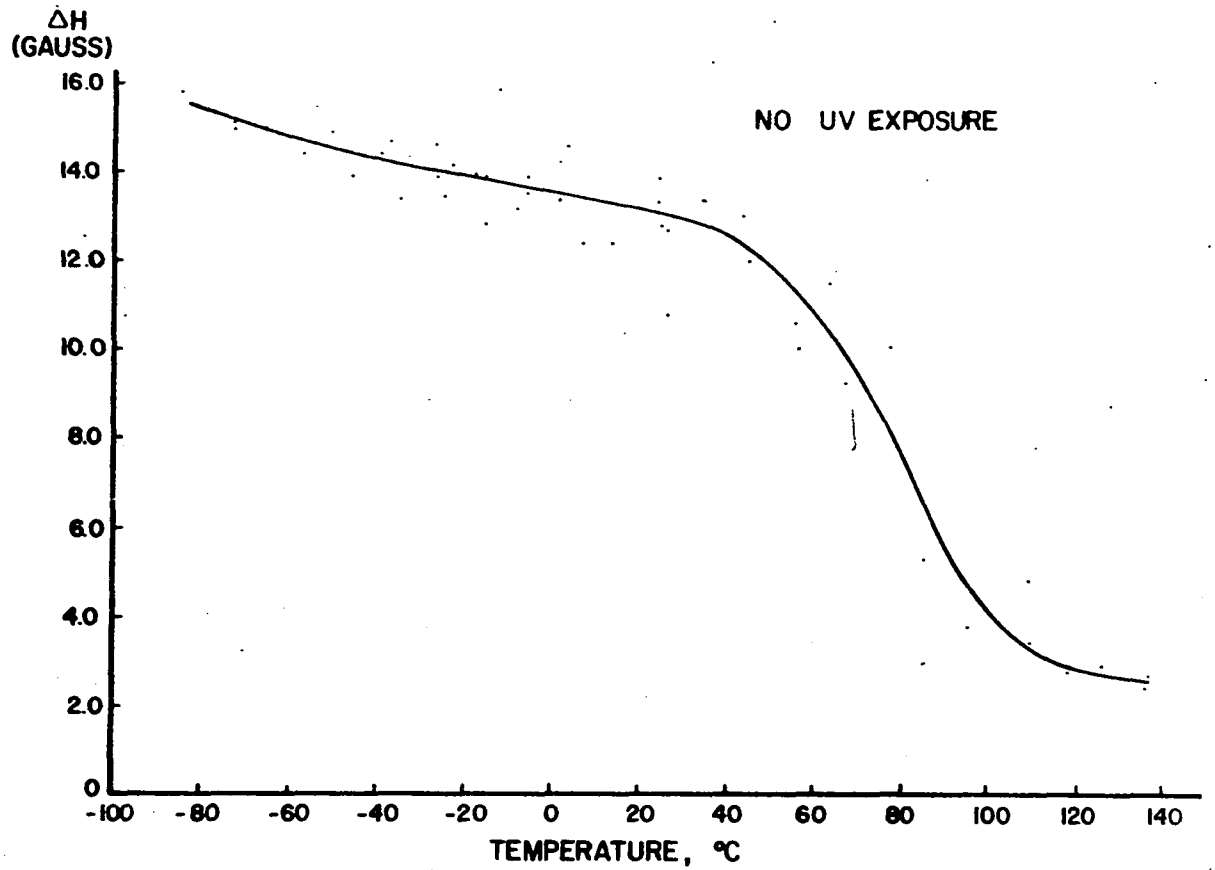

Figure 20 - Line width for nylon 66 yarns exposed to UV for 0 hours.

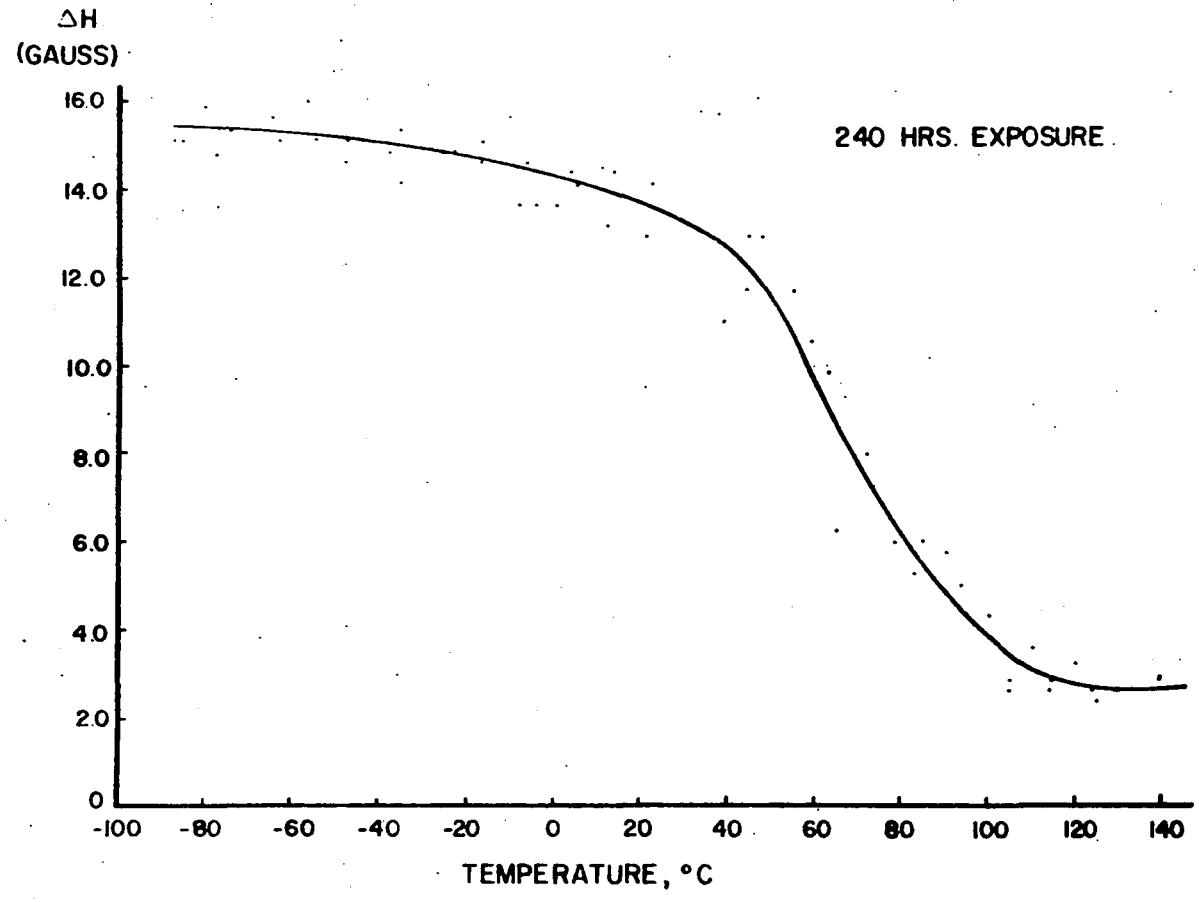

Figure 21 - Line width for nylon 66 yarns exposed to UV for 240 hours.

otherwise overcome by the increase in polymer mobility resulting from chain scission.

Effect of UV Irradiation on Line Width

Line width is a measure of peak to peak distance between maxima and minima on the derivative curve of the NMR spectra. In the complex NMR line of polymers, peak maxima for the rigid fraction are most easily obtained from spectra recorded at low temperatures and maxima for the mobile fraction from higher temperature spectra. There is considerable uncertainty in obtaining line width information from spectra recorded at temperatures where the rigid and mobile fractions are not clearly distinguished. Because UV effects were small and point scatter excessive only (ΔH) for the 240 hour exposures was compared with the control. Plots for (ΔH) versus temperature clearly show the α transition occurring between 50°C and 90°C. No significance can be attached to apparent differences between (ΔH) for unexposed and 240 hour exposed yarns due to difficulty in obtaining accurate values.

Line width of the broad component (ΔH_{wide}) was plotted versus temperature for the above described samples as shown in Figure 22. In both cases there was a decrease from approximately 16 gauss at the lowest temperature to 11 gauss at the highest. Any real difference in curve shape may be obscured by the wide limits of experimental error. (See Appendix Figures 29 & 30). There appears to be a detectable trend toward more rapid line narrowing on UV exposure in the temperature range above 35°C. This suggests irradiation may

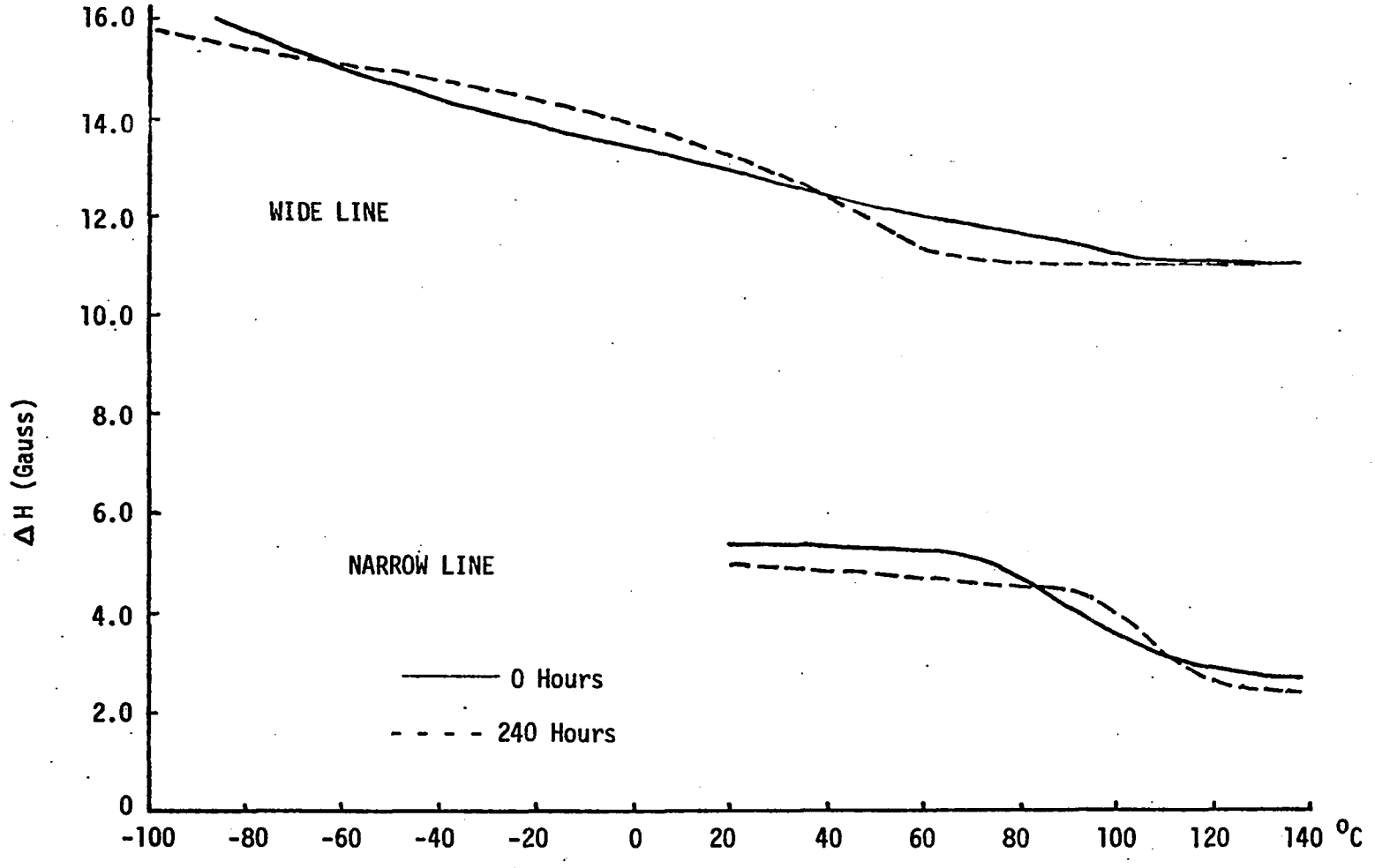

Figure 22 - Line width of the wide and narrow components of the NMR line for nylon 66 exposed to UV for 0 and 240 hours.

have caused some chain disruption in crystallites. The (ΔH_{wide}) values are similar to data reported (80) for this fiber, except at high temperatures where line narrowing was greater than previously reported.

Figure 22 compares (ΔH_{nar}) of the mobile fraction of the unexposed and irradiated samples. There was a very gradual decrease in line width from 5.9 gauss at lower temperatures to approximately 2.6 gauss at high temperatures for both samples. However, in the temperature range where a transition occurred it was apparent that it was sharper and shifted to higher temperatures (90°to 120°C) following 240 hours irradiation. The transition range for the control sample was from 70° to approximately 110°C. The transition shift to higher temperature suggests that UV exposure has caused some restraint on molecular mobility in the amorphous regions. The (ΔH_{nar}) values for unexposed samples compare favorably with those reported by Olf and Peterlin (80).

Area Ratios of the Two-Phase System

Areas under the NMR derivative curves are proportional to the number of nuclei in the sample. If the two phase spectra can be resolved estimates of the relative proportion of nuclei in the mobile and immobile fractions can be made.

Arbitrary separation of two phase spectra recorded at 125°C and above was obtained as described above and ratios of the mobile fraction to the total area were calculated. Table 5 reports average area ratios for unexposed and UV exposed samples. No differences beyond experimental error

among UV exposures or between unexposed and UV exposed samples were observed by this method of measurement.

TABLE 5

AREA RATIOS (MOBILE FRACTION/TOTAL AREA) FROM NMR DERIVATIVE CURVES FOR NYLON 66 YARNS EXPOSED TO ULTRAVIOLET IRRADIATION AT 52°C

Hours Exposed	NMR Spectrometer Temperature (°C)	Area Ratio (%)	
0	126.3	14.58	
	136.7	16.39	
	136.9	15.50	
			15.49
72	131.5	18.52	
	128.6	15.56	
	138.6	15.96	
			16.68
142	127.0	15.56	
	127.0	17.81	
			16.68
240	130.0	16.07	
	133.0	15.29	
	124.6	17.58	
	139.6	16.49	
			16.36

Discussion

Changes in nylon 66 morphology resulting from 240 hours UV irradiation seem smaller than expected when NMR findings are compared with the dye experiments and viscosity data. It may be that opposing effects such as chain scission (shown by viscosity decrease) and increased crystallinity were occurring simultaneously, and thus effectively cancelling one

another. It has been reported (106) that NMR was less sensitive to high energy irradiation dose levels than tensile and solubility tests.

Nevertheless, (ΔH) and (ΔH^2) measurements indicated there was an overall decrease in molecular mobility when nylon 66 was exposed to 3500 Å irradiation for 240 hours. Molecular constraint can be caused by crosslinking, crystallization, or chain entanglement. Several studies of ionizing irradiation effects on polyethylene, polypropylene and polyamides have shown the predominant effect is crosslinking. However, when irradiated, polyamides crosslink less readily than the other two fibers (58, 137). Deeley, et al (31) found 0.3×10^{18}nvt disrupted crystallites and increased the rubberlike behavior of polyamides. Similarly, when polyethylene and polypropylene were irradiated (23, 37, 44, 106) it was concluded that crystallites were disrupted and crosslinks formed as shown by NMR and x-ray (106).

It was noted that (ΔH^2) and (ΔH) decreased with increasing irradiation dose at low temperatures and increased at higher temperatures, having the effect of diminishing the transition near 300^{o}K. These authors (23, 34, 44) attributed the decreases in (ΔH^2) and (ΔH) at low temperatures to disruption of crystallites. The high temperature increases in (ΔH) and (ΔH^2) were caused by creation of crosslinks primarily in the amorphous regions.

Slichter (106) also reported a decrease in (ΔH) at lower temperatures which was attributed to freedom of

constraints in the crystallites. Further, x-ray measurements verified the loss of crystallinity. Increasing the neutron dose caused the amorphous halo to become more sharply defined as the crystalline features decreased in intensity and definition.

The presence of increased crystallinity modifies the NMR line in ways distinguishable from crosslinking although both have constraining effects on the molecular structure. Stark rubber is a crystalline product obtained by compressing rubber and storing it at low temperature for a period of time. Slichter (105) reported that stark rubber showed a crystalline x-ray pattern and that NMR line narrowing occurred at higher temperatures than for untreated rubber. Further, at low temperatures (to -100°C) the NMR line was broader for the crystalline rubber because the chains were more closely packed.

In the present study it appears that low energy UV irradiation had quite a different effect on the morphology of nylon 66 from high energy irradiation of polymers. Figure 23 shows 240 hours UV irradiation caused an increase in (ΔH^2) at low temperature and no change at high temperatures. Line width changes were less decisive; however, the (ΔH_{nar}) transition of the irradiated yarn was shifted to higher temperature and became sharper. Apparently, low energy UV irradiation causes an increase in crystallinity primarily in the amorphous regions. The considerable chain scission as shown in Figure 24, page 132 must release constrained molecules in

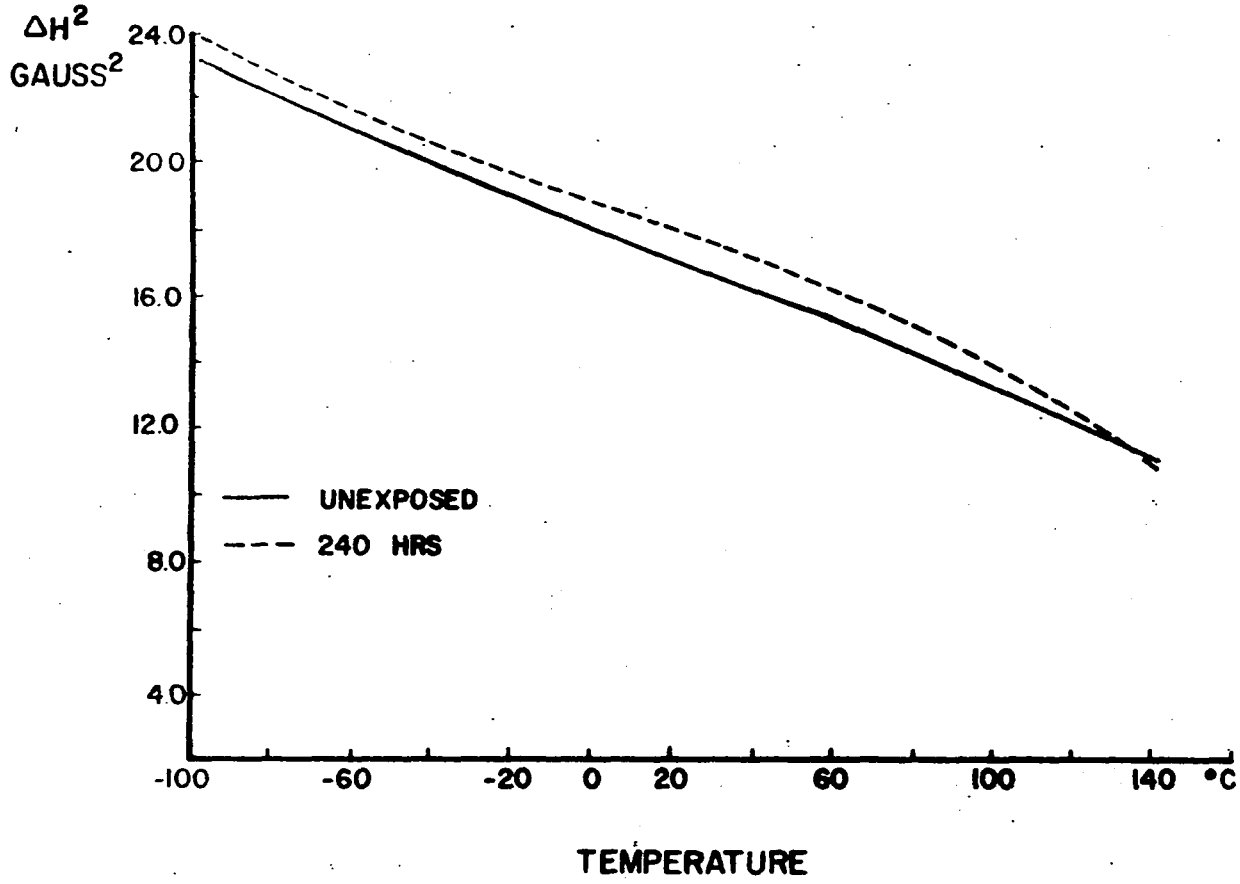

Figure 23 - Comparison of second moments for nylon 66 yarns exposed to UV for 0 and 240 hours.

the less ordered regions of the drawn polymer freeing them to assume a crystalline arrangement under the exposure conditions. The decrease in second moment at high temperatures suggests that chain scission which removed constraint in the amorphous phase exceeded the restraining effect of any newly formed crystallites. The shift of (ΔH_{nar}) to higher temperature, accompanied by no significant change in (ΔH_{wide}) is further evidence that UV irradiation effects occurred primarily in the amorphous phase.

It was considered that annealing which could occur in the spectrometer as NMR spectra were being recorded might account for increases in (ΔH^2). However, spectra were recorded at low temperatures first where annealing would not occur. At high temperatures annealing could be expected to increase (ΔH^2), but such an effect was not observed.

CHAPTER V

ADDITIONAL EXPERIMENTS

Viscosity and Viscosity Average Molecular Weight

The use of dilute solution viscosity to characterize molecular weight of linear high polymers was first recognized by Staudinger (36). The higher the molecular weight within a series of linear polymer homologs, the greater the increase in viscosity produced by a given weight concentration of polymer in an appropriate solvent at constant temperature. Appropriate solvents are those which completely dissolve the polymer but do not react with it to cause degradation.

Broadly, viscosity may be regarded as internal friction of a fluid. Direct measurements, then, involve rate of lamellar flow of liquid layers past one another under a known force, in this case gravitational. As viscosity is directly proportional to flow rate, viscosities are calculated from flow times.

Listed below are commonly used viscosity (η) relationships. Currently recommended, although not widely accepted, terms are in parentheses (8).

Relative viscosity (Viscosity ratio)	$\eta_r = \eta/\eta_o \simeq t/t_o$	the ratio of the solution to the solvent
Specific viscosity	$\eta_{sp} = \eta_r - 1$	expansion of relative viscosity in a power series, neglecting all terms after the first; c = conc. in gm/dl

where

$$\eta_r = 1 + A_o c + A_1 c^2 + A_2 c^3 + \ldots$$

Reduced viscosity (Viscosity number)	$\eta_{sp/c}$	specific viscosity per unit concentration
Inherent viscosity (logarithmic viscosity no.)	$\ln\left(\eta_{r/c}\right)$	natural logarithm of relative viscosity per unit concentration
Intrinsic viscosity (limiting viscosity no.)	$[\eta]=\left(\eta_{sp/c}\right)_{c=o}=\left[\ln\left(\eta_{r/c}\right)\right]_{c=o}$	reduced and inherent viscosity at infinite dilution

Intrinsic viscosity values may be obtained by plotting reduced and inherent viscosities, each at at least three concentrations, and extrapolating to zero concentration. Thus inherent viscosity becomes independent of concentration, but is dependent on the solvent.

Staudinger (36) suggested that reduced viscosity of dilute solutions of polymers was proportional to polymer molecular weight. The Staudinger relationship $\left(\frac{\eta_r - 1}{c}\right)_{c\to o} = KM$ gave molecular weights which were too low and did not take into account the distribution of molecular weights in a given sample.

The expression $[\eta] = K'M^a$ attributed to Mark (53) appeared to describe more accurately the relation between viscosity and molecular weight. K' and a are constants which vary with polymer type, solvent, and temperature. Where molecular weights of fractionated homologs of a linear polymer may be obtained a linear log-log plot of $[\eta]$ versus $M_{\bar{w}}$ can provide the constants; K' and a being the intercept and slope, respectively. A linear relationship of this type has

been amply demonstrated for many polymer-solvent systems (18, 36, 53).

Viscosity average molecular weight was a designation proposed by Flory (53) as this average molecular weight determined by viscosity differs from number average and weight average determined by other methods. Viscosity average molecular weight has been shown to be closer to weight average than is number average (20) and hence is more sensitive to larger molecules in a distribution of molecular weights. Taylor demonstrated, however, that viscosity of nylon solutions in 90% formic acid are linearly related (on a log-log plot) to M_n derived from end group determinations (119).

Experimental Procedures

Viscosity measurements were obtained for unexposed nylon 66, yarns exposed to UV at 52°C under dry oxygen atmosphere for 72, 142, and 240 hours, and for yarns exposed 240 hours under the same conditions but without UV. Viscosity determinations for 72 hour UV exposures under nitrogen atmosphere were also recorded. ASTM method D 2857-70 was generally followed (7).

Yarn samples of 0.1250 gm were chopped in approximately half-inch lengths, placed in clean dry stoppered 25 ml volumetric flasks, covered with approximately 20 ml of 90% formic acid and swirled gently to facilitate dissolution. Mechanical shaking was avoided to prevent breaking any gels possibly present in irradiated samples. All determinations were made in the same Ubbelohde viscometer, dichromate

cleaned, dried, and conditioned at 30 ± 0.05°C in a constant temperature bath. Volumetric flasks containing samples were conditioned in the same constant temperature bath for at least 30 minutes, then the volume brought to 25 ml with 90% formic acid also at 30°C. The sample was filtered through a 300 gauge stainless steel screen into the viscometer. The screen was examined for any gel.

Flow times, recorded on a digital electric timer, were taken until at least three readings agreed within ± 0.3 sec. Flow times of three dilutions of each sample were recorded for calculation of intrinsic viscosity. Flow times of the formic acid solvent were taken periodically during the course of viscosity experiments.

Relative, specific, reduced, inherent, and intrinsic viscosities were calculated using formulas and procedures described above. All reported values were an average of three replications. Typical plots of reduced and inherent viscosities extrapolated to zero concentration are shown in Appendix, Figures 31 through 35.

Viscosity average molecular weights ($M_{\bar{v}}$) were calculated according to $M_{\bar{v}} = K'[\eta]^a$, where $K' = 1.3 \times 10^4$ and $a = 1.39$. The constants were those derived emperically by Taylor (119) from $[\eta]$ and $M_{\bar{n}}$ determined by end group analysis for nylon 66 in 90% formic acid at 25°C.

Results and Discussion

Table 6 and Figure 24 report viscosities for control

and UV exposed yarns. Viscosity decreased with increasing UV exposure time. In no case was any gel observed following sample irradiation nor were any erratic flow times observed. This would suggest that chain scission was predominant on UV exposure in the presence of oxygen. If any crosslinking occurred it was below the detectable gel point. Decreases in viscosity of polyamides on UV exposure have been observed by others (2, 55, 76, 87). Gel formation has been observed (111), when nylon 66 was exposed to far UV (2537 Å) under nitrogen and *in vacuo*. In this study exposure in nitrogen up to 72 hours caused no measurable change in viscosity.

Nylon yarns held at 52°C for 240 hours had slightly increased viscosity values. There may have been a small amount of branching or crosslinking below the gel point but there was no evidence of chain scission as a result of the irradiation temperature.

There was a decrease in $M_{\bar{v}}$ upon increased photooxidation from an initial 17,100 to 10,900 on 240 hours UV exposure. These values, calculated from Taylor's constants as determined by $[\eta]$ and $M_{\bar{n}}$ (end group analysis), are thus approximations of $M_{\bar{n}}$. Olf and Peterlin (80) reported $M_{\bar{n}}$ of approximately 17,500 as determined by end group analysis for nylon 66 of the same source and description as the experimental yarn used in this study.

$M_{\bar{v}}$ increased slightly when yarns were held at 52°C for 240 hours in oxygen. Some crosslinking or branching could account for the increase.

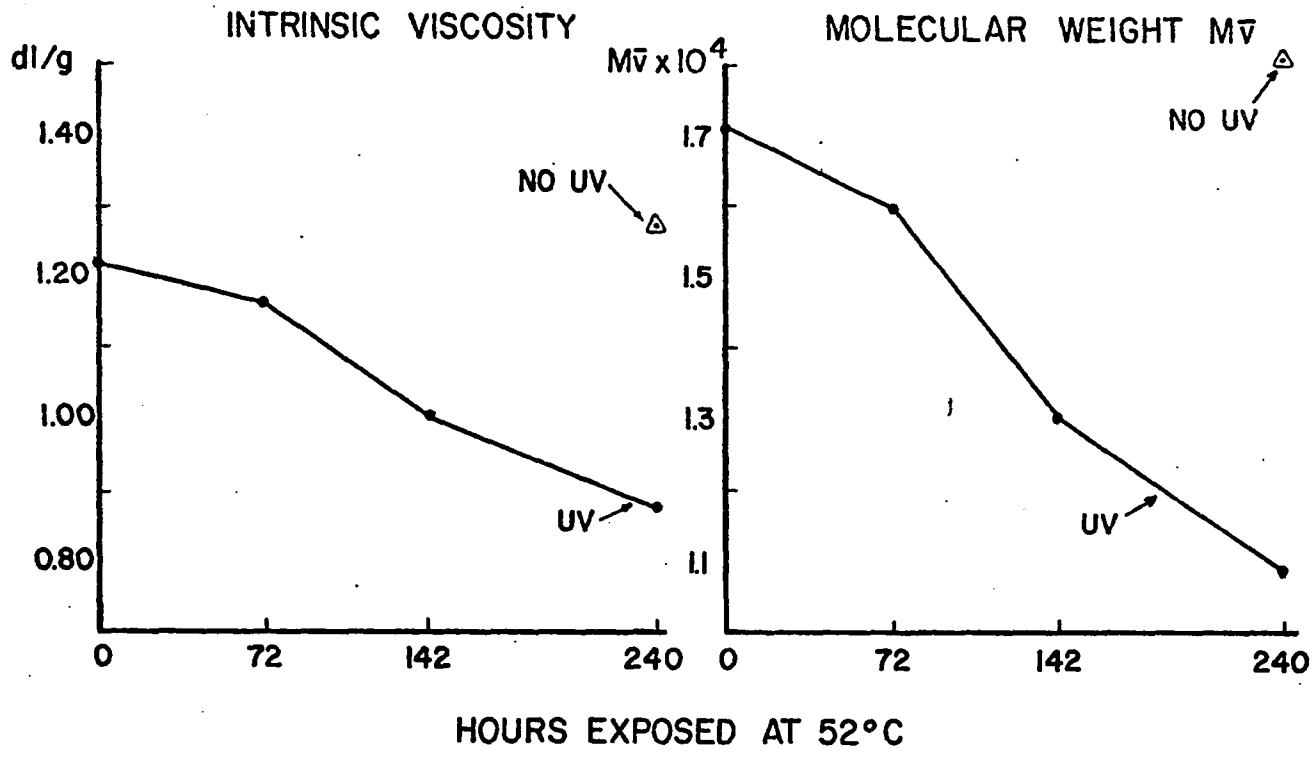

Figure 24 - Intrinsic viscosity and M_v for nylon 66 yarns exposed to UV.

TABLE 6

INTRINSIC VISCOSITY AND VISCOSITY AVERAGE MOLECULAR WEIGHT FOR NYLON 66 YARNS EXPOSED TO ULTRAVIOLET IRRADIATION AT 52°C

Hours Exposed	Intrinsic Viscosity (dl/gm)	Viscosity Ave. Molecular Weight ($M_{\bar{v}}$)
0	1.220	1.71×10^4
72	1.163	1.60
142	1.007	1.32
240	0.878	1.09
240-No UV	1.272	1.81

Density and Crystallinity

Density measurements of control and UV exposed nylon 66 fibers were made by the linear density gradient method. The method involves partial mixing of two liquids of different density. Fibers, free of occluded air, will float at the level in the column where the mixed liquid density is the same as that of the fiber. The method has been known applicable to textile fibers (122) for some time. It is reliable and reproducible relative to other methods of determining density such as hydrostatic weighing and pycnometer measurements (95).

Experimental Procedures

A jacketed graduated column 76 cm tall with approximately 50 mm inside diameter was prepared by ASTM Method D 1505-68, Method C, using a carbon tetrachloride (density 1.59 gm/cc)-toluene (density 0.87 gm/cc) mixture (6). The column was prepared to cover a measured density range of 1.1198 to 1.1802 gm/cc. Calibration of the column was obtained with the introduction of four glass floats of known densities: 1.1198, 1.1398, 1.1598, and 1.1802 gm/cc. Linearity of the column is shown in Figure 36, Appendix. The column was maintained at 23 ± 2°C by circulating water from a thermostatically controlled reservoir through the jacket.

Yarn samples were prepared from approximately one inch lengths of yarn; each sample tied loosely with an identifying knot. Care was taken not to tie so tightly as to occlude air or introduce strain. Samples were prepared from control and exposed yarns which had been stored in dark capped bottles, but not under vacuum. Prepared samples were immediately placed in a solution of the least dense of the test liquids for 15 minutes before introduction into the column. During the 15 minutes soak samples were observed for release of any air bubbles. None was observed.

Samples reached equilibrium level within 5 days after which all readings were taken. Sharma and Mandelkern (95) observed in measurements of polyethylene there is a well defined time interval before density reaches equilibrium, the value of which is then maintained constant for two or three

weeks. All readings of float and sample levels were determined with the use of a cathetometer; cross hairs being centered at the center of the identifying knot of the sample.

Density was calculated according to the following formula:

$$\text{Density at } x = a + \left[\frac{(x-y)\ (b-a)}{z-y}\right]$$

where: a and b are densities of two standard floats

y and z are distances of a and b, respectively, bracketing the unknown measured from an arbitrary level

x is the distance of the unknown above the same arbitrary level.

Density values reported in Table 7 are an average of three replications, except for 72 and 240 hour UV exposures where two replications were recorded.

Results and Discussion

Table 7 and Figure 25 report average density values obtained for control yarns and those exposed to UV for 72, 142, and 240 hours. There was no significant change in density observed following 72 and 142 hours irradiation at 3500 Å, but a significant increase occurred with 240 hours exposure. This was interpreted to mean that on prolonged exposure to UV under dry oxygen atmosphere there was an increase in crystallinity as measured by an increase in density.

Additional samples were held 240 hours under dry oxygen atmosphere at 52°C. These conditions were identical to UV

exposure conditions with the omission of UV irradiation. In the absence of UV there was no change in density.

TABLE 7

DENSITY AND PERCENT CRYSTALLINITY FOR NYLON 66 YARNS EXPOSED TO ULTRAVIOLET IRRADIATION AT 52°C

Hours Exposed	Density (gm/ml)	Crystallinity (%) (Volume)
0	1.1480	52.4
72	1.1483	52.5
142	1.1482	52.4
240	1.1527	55.4
240-No UV	1.1481	52.4

The relationship between polymer density and crystallinity has been well recognized (96, 109, 118, 122). Density values for the crystalline (1.220 gm/cc) and amorphous (1.069 gm/cc) fractions of nylon 66 as determined by Starkweather and Moynihan (109) were used to determine percent crystallinity by the following relation:

$$\alpha_c = \frac{\rho - \rho_a}{\rho_c - \rho_a} \times 100$$

where α_c = percent crystallinity

ρ = measured density of the sample

ρ_a = density of the amorphous fraction of nylon 66

ρ_c = density of the crystalline fraction of nylon 66

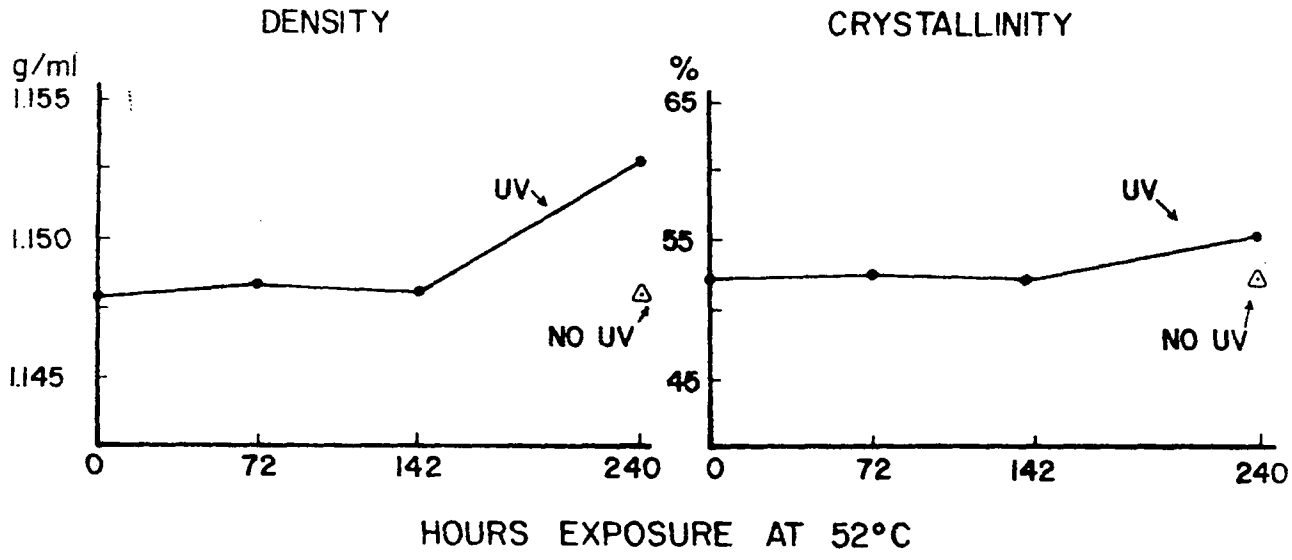

Figure 25 - Density and percent crystallinity for nylon 66 yarns exposed to UV.

This relation yields a crystalline volume fraction rather than a weight fraction of the polymer. If the right hand side of the equation is multiplied by the term ρ_c/ρ a crystalline weight fraction is obtained (3).

There was approximately a 3% increase in crystallinity of nylon 66 yarn as a result of 240 hours exposure to 3500 Å UV irradiation. However, samples held 240 hours under identical atmosphere and temperature but without UV showed no change in crystallinity.

Differential Scanning Calorimetry

In an attempt to further confirm the findings for increased crystallinity some preliminary differential scanning calorimetry (DSC) investigations were initiated. DSC is one of several thermal analytical methods based on the thermodynamic principle that physical changes in polymers are accompanied by changes in enthalpy. In this calorimetric method the heat energy required to maintain two insulated chambers (one containing sample, one reference) equal in temperature over a range of constant temperature increase per unit time is measured. Sample and reference are mounted in holders attached to temperature controls and enclosed in a furnace. Temperature is increased at a constant rate. In series with the heat source to the sample chamber are thermometers registering differences in temperature between sample and reference. Heat is added or withheld to maintain sample and reference at the same temperature. The difference

in heat applied to sample and reference is recorded on a graph where the ordinate represents heat energy and the abscissa temperature increase with time.

The heating rate is critical as interfering thermal effects resulting from the test method itself may cause polymeric change. Generally, a fairly rapid scan (at least $20^{o}C$/min) is employed to avoid the problem as nearly as is possible. If the scan rate is too slow a semicrystalline sample may reorganize its morphology during testing. However, if the heating rate is too high, superheating may occur (60, 115).

Melting behavior of polymers is also sensitive to previous annealing history, the form of the sample (film, fiber, etc.), the manner of packing the sample holder, and decomposition products.

Experimental Procedures

Yarns were chopped into approximately 1/8 inch lengths using a sharp razor blade against a marble surface. This was done in an effort to avoid crushing the ends of the cut filaments as nearly as possible. Samples of approximately 6.5 mg weighed to the nearest 0.01 mg were packed randomly in the sample holder and sealed. Three replications each of the unexposed yarns and those held 240 hours at $52^{o}C$ were prepared. Two replications of each 240 hour UV exposure were prepared.

A Perkin-Elmer DSC-1B calorimeter was used. The

instrument was operated in a sensitivity range R16. It was calibrated at the chosen sensitivity range and scanning rate with a Sn standard (mp 232°C). Preliminary work indicated that a scan rate of 20°C/min gave the most reproducible thermograms and stable base lines. All scans were begun at 60°C and terminated at 280°C.

Results and Discussion

Table 8 reports the melting temperatures (Tm) measured at the center of each discernible peak on the thermogram. The anisotropic nature of semicrystalline polymers accounts for the broad endotherm which does not show the sharp melting point of pure crystalline compounds.

There was no significant difference in Tm of the principle crystalline fraction among the controls, 240 hour UV exposures, and samples held at 52°C for 240 hours without UV. Of particular interest were the smaller melting peaks or shoulders which appeared on thermograms of all 240 hour UV exposures. A typical comparison of thermograms is shown in Figure 26. The shoulders varied in size and shape among the samples but quite consistently appeared near 258°C. In some cases a very small peak also appeared near 254°C.

The presence of multiple melting peaks in DSC endotherms has been observed in studies of polyethylene, polytetrafluoroethylene, polyester and nylon 66. Peterlin and Meinel (82) observed the melting behavior of drawn and rolled polyethylene of high and low crystallinity following

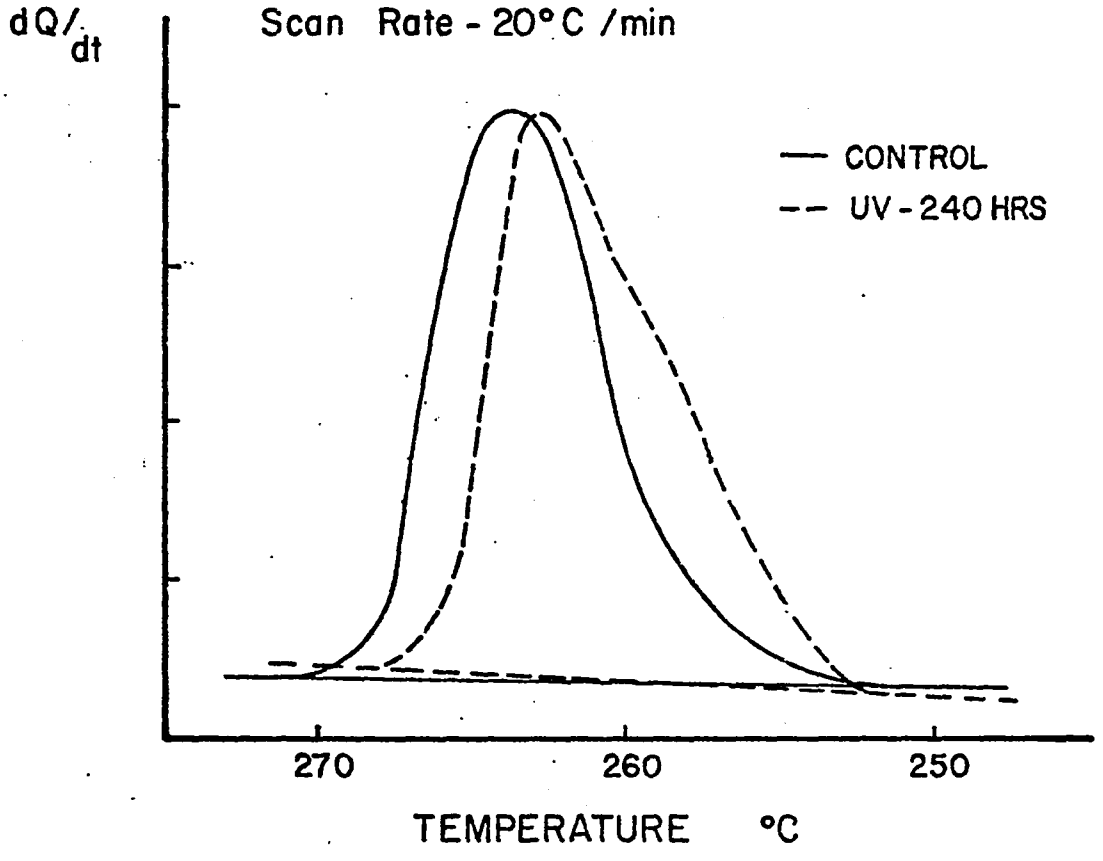

Figure 26 - Typical DSC curves for nylon 66 yarns exposed to UV for 0 and 240 hours.

treatment with fuming nitric acid. Two melting peaks were observed following acid etching of low crystallinity polyethylene. These were interpreted to indicate the presence of two types of crystallites of different thickness in a quenched sample. In an annealed sample, the amount of lower melting material increased with draw ratio in a manner similar to highly crystalline material suggesting the destruction of thick original lamellae and the formation of thinner platelets.

TABLE 8

MAXIMUM MELTING TEMPERATURES FOR NYLON 66 YARNS EXPOSED TO ULTRAVIOLET IRRADIATION AT 52°C AS MEASURED BY DIFFERENTIAL SCANNING CALORIMETRY AT A SCAN RATE OF 20°C/MINUTE

Hours Exposed	Major Melting Peak	Shoulder 1	Shoulder 2
0	261°C		
240-1	260	257°C	255°C
240-2	262	258	257
240-3	260	258*	254
240-No UV			

*Major melting peak. This exposure was actually 264 hours.

Sweet and Bell (115) have recently challenged the theory that multiple endotherms in DSC melting of semi-crystalline polymers are the result of the presence of

different types of crystallites, that is folded chain and partially extended chain crystals. They observed that the relative areas of the double endotherms of polyester and nylon 66 vary with DSC heating rates. As the heating rate is increased the higher temperature endotherm becomes smaller and the lower temperature endotherm larger by the same relative amount. This is interpreted to mean that the high temperature endotherm is merely the result of simultaneous melting and recrystallization of the lower melting crystallites of the low temperature endotherm. At high DSC scan rates less material can recrystallize and hence the area of the high temperature endotherm decreases. The nonrecrystallizable material differs from that which melts and recrystallizes in both crystallite size and perfection rather than crystal morphology.

The effect of γ-irradiation on the shift in Tm of crystalline polytetrafluoroethylene (PTFE) was studied by Kusy and Turner (60). Multiple melting peaks were observed which were attributed to different crystalline regions. The authors noted that lower doses of γ-irradiation have been known to increase PTFE crystallinity. Apparently radiation induced fracture of polymer molecules favors their movement in the amorphous regions and hence their crystallization.

Irradiation damage, that is destruction of crystallites, is known to depress Tm (60). Irradiation sufficient to effect a crosslinked network in polyvinyl chloride was shown to shift Tg and Tm to higher temperatures (10).

In this study DSC data on UV exposed nylon 66 suggest that new crystalline regions which differ from the original crystallites may be formed on prolonged UV exposure. Apparently the temperature in the UV exposure chamber did not cause formation of new crystallites. The findings of Sweet and Bell suggest the necessity of multiple scan rates to rule out any effects of melting and recrystallization in the calorimeter. Unlike their findings a single endotherm was observed initially and on heating at 52°C for 240 hours. Only on UV exposure did multiple peaks appear.

When endotherm area ratios for UV exposed samples and controls were calculated there appeared to be a slight decrease in area on UV exposure suggesting that a slight disruption of initial crystallinity may have occurred as new crystallites were formed. However, these data, shown in Table 9, are inconclusive as area differences do not exceed experimental error.

The DSC experiments suggest that new regions of crystallinity were formed on UV exposure as a result of chain cleavage which allowed molecules to move, primarily in amorphous regions, into a more ordered configuration. However, conclusive evidence would have to exclude any possible effects of annealing history and molecular reorganization in the calorimeter.

TABLE 9

AREA UNDER DIFFERENTIAL SCANNING CALORIMETRY CURVES FOR NYLON 66 YARNS EXPOSED TO ULTRAVIOLET IRRADIATION AT 52°C SCANNED AT 20°C/MINUTE

Hours Exposed	Area (in^2/gm)
0	646.0
240-1	602.2
240-2	607.5
240-3*	610.6
240-No UV	634.0

*This exposure was actually 264 hours.

CHAPTER VI

SUMMARY AND CONCLUSIONS

A multifilament nylon 66 yarn was exposed to 3500 ± 500 Å ultraviolet radiation. Assessments of morphological change were made by dye take-up, wide line nuclear magnetic resonance (NMR), intrinsic viscosity, density, and some preliminary differential scanning calorimetry (DSC) measurements. Viscosity average molecular weight was determined as well as percent change in crystallinity as calculated from density measurements.

Preliminary investigations in yarn preparation and ultraviolet exposure suggested that the objective of the study, to determine the onset and course of ultraviolet effects on the fine structure of a nylon 66 yarn under dry atmospheres of oxygen and nitrogen, could better be met by certain modifications of the original experimental procedure. The yarn was given an aqueous nonionic scour without tension followed by adequate rinsing to remove spinning finish. This procedure was used rather than solvent extraction to avoid possible yarn contamination with photoreactive compounds. Ultraviolet exposure periods of at least 72 hours were required to detect change by measurement techniques employed. Considering the length of time required to obtain measurable

morphological change at 3500 Å, a dry oxygen atmosphere was used for all exposures to the exclusion of a nitrogen atmosphere.

Under the revised experimental procedure the major hypothesis was accepted. Nylon 66 yarn exposed to UV irradiation in the presence of oxygen did exhibit measurable change in fine structure sooner than in a nitrogen atmosphere as determined by dye take-up and intrinsic viscosity. No change was detected by either of these measurements on 72 hours exposure in nitrogen but was detected following 72 hours in oxygen. Exposure periods of 240 hours in oxygen were required for significant change as measured by wide line NMR and density. Intrinsic viscosity and dye measurements detected morphological change following 142 and 72 hour exposure periods, respectively.

The two principal analytical techniques chosen were both useful and complementary in meeting the objective of the work. Anionic dyeing was sensitive to smaller changes in fiber structure and hence detected UV effects in the first exposure period. It revealed constriction of the fiber structure but not the nature of the constriction. Wide line NMR detected significant change in fiber morphology only after 240 hours UV exposure but the shape of the second moment versus temperature plots was useful in determining the manner in which fiber morphology had been affected. The apparent lack of sensitivity of the NMR technique may have been partly due to opposing effects, that is increasing chain

scission which could be expected to enhance molecular motion was occurring as increased crystallinity was restricting it. Density, viscosity, and DSC measurements were used to confirm results from dyeing and NMR experiments.

The findings of the study indicate that photooxidation at a low energy level causes considerable chain scission and reduction in molecular weight as revealed by intrinsic viscosity and reduction in second moment measured at high temperatures. Wide line NMR and preliminary DSC measurements suggest 3500 Å is not sufficiently energetic to cause major chain disruption within crystallites, therefore scission must have occurred primarily in amorphous regions of the fiber.

There was a measurable increase in molecular order on prolonged UV exposure as shown by increased density and percent crystallinity, increased second moment measured at low temperatures, increased line width of the narrow component, and reduction of diffusion rate of Anthraquinone Milling Blue dye. Dyeings with Merpacyl Blue indicated that on 240 hours UV exposure some amine end groups were lost by chemical change or made inaccessible to dye. However, the effect was too small to account for all the change in diffusion rate.

Although high energy irradiation and far ultraviolet are known to effect crosslinking in nylon 66, under the experimental conditions of this study no measurable crosslinking occurred. No insoluble gel was detected in 90% formic acid, nor did wide line NMR indicate crosslinking.

The findings suggest that the newly freed chain ends resulting from photooxidative cleavage of polymers in the amorphous regions of the fiber relax into a crystalline configuration. An irradiation temperature of approximately 52°C was shown not sufficient to cause increased crystallinity in the absence of UV.

Suggestions for Further Study

1. Preliminary Differential Scanning Calorimetry as discussed above was shown to be useful as a measure of increased crystallinity. However, measurements should be made at several scan rates to rule out as nearly as possible interfering effects from annealing in the calorimeter.
2. Measurements of change in polymer crystallinity were attempted by wide angle x-ray. Results were not conclusive by this method presumably because it is insensitive to small changes in crystallinity. If the effects of chain scission and increased crystallinity are cumulative, x-ray studies should be carried out on yarns exposed to UV for periods in excess of 240 hours.
3. Any change in physical structure affects performance of fibers. Therefore, studies of the effect of UV changes in morphology on abrasion resistance, flexural rigidity, tensile properties and other parameters which are related to end use performance could be useful.

4. The role of TiO_2 has been shown to be important in UV degradation of nylon 66 particularly at wavelengths near 3500 Å. It would be of interest to examine the effect of varying form and level of TiO_2 on the parameters measured in this study.
5. It was possible with techniques used in this study to measure an overall increase in fiber crystallinity but it was not possible to determine the location of change within the fiber. It is known that UV affects fiber or film surfaces initially. Therefore, a study of changes in polymer morphology relative to position within the fiber would be of interest.
6. The interrelationships of UV wavelength, temperature, and atmosphere as it influences a particular type of morphological change needs further study. Specifically, a more precise definition of conditions under which crosslinking or chain scission predominate would be useful.

BIBLIOGRAPHY

1. Abbot, E. B., Some Theoretical and Practical Aspects of the Dyeing of Nylon Yarns and Fabrics, J. Soc. Dyers and Colourists 60:55 (1944).

2. Achhammer, B. G., Reinhart, F. W., and Kline, G. M., Mechanism of the Degradation of Polyamides, J. Res. Nat. Bur. Stds. 46:391 (1951).

3. Alexander, L. E. X-Ray Diffraction Methods in Polymer Science. New York: John Wiley and Sons, 1969.

4. American Association of Textile Chemists and Colorists, Rhode Island Section. Doyle, M., chairman. Degradation of Polyamide Fibers Exposed to Various Sources of Radiation, Text. Chem. and Colorist 1:99 (1969).

5. American Association of Textile Chemists and Colorists, Northern New England Section. Knoettner, K. J., chairman. Weathering Degradation of Nylon, Text. Chem. and Colorist 4:57 (1972).

6. American Society for Testing Materials. D 1505-68, Standard Method of Test for Density of Plastics by the Density Gradient Technique. ASTM Book of Standards, Part 27. Philadelphia: American Society for Testing Materials, 1971.

7. American Society for Testing Materials. D 2857-70, Standard Method of Test for Dilute-Solution Viscosity of Polymers. ASTM Book of Standards, Part 27. Philadelphia: American Society for Testing Materials, 1971.

8. Andrew, E. R. Nuclear Magnetic Resonance. Cambridge: Cambridge University Press, 1956.

9. Atherton, E. and Peters, R. H., Studies of the Dyeing of Nylon with Acid Dyes. Part II: Kinetics of the Process, Text. Res. J. 26:497 (1956).

10. Bair, H. E., Matsuo, M., Salmon, W. A. and Kwei, T. K., Radiation-Crosslinked Poly(vinyl chloride). Phase Studies, Macromolecules 5:114 (1972).

11. Bell, J. P., Relation Between Nylon Fiber Mechanical Properties and Dye Diffusion Behavior, J. Appl. Polym. Sci. 12:627 (1968).

12. Bell, J. P., Effect of Fiber and Dyebath Variables on the Rate of Acid Dyeing of Nylon 66, Text. Res. J. 38:984 (1968).

13. Bell, J. P., Carter, W. C. and Felty, D. C., Dye Concentration Profiles within Single Nylon Filaments, Text. Res. J. 37:512 (1967).

14. Bittles, J. A., Brooks, J. A., Iannarone, Jr., J. J. and Landerl, H. P., The Dyeing of Filament Nylon with Acid Dyes, Am. Dyestuff Reptr. 47:138 (1958).

15. Bowen, Jr., J. H. and Rosato, D. V. "Radiation." Environmental Effects on Polymeric Materials, Vol. 1: Environments, edited by D. V. Rosato and R. T. Schwartz. New York: Interscience, 1968.

16. Brauer, G. M. and Horowitz, E. "Systematic Procedures, D. Sodium Fusion for Detection of Sulfur, Nitrogen, and Halogens." Analytical Chemistry of Polymers. Part III. Identification Procedures and Chemical Analysis (High Polymers, Vol. XII), edited by G. M. Kline. New York: Interscience, 1962.

17. British Patent 722,724, E. I. duPont de Nemours and Co. (Through Chem. Abst. 9937 (1957).

18. Burke, J. J. and Orofino, T. A., Nylon 66 Polymers. I. Molecular Weight and Compositional Distribution, J. Polym. Sci. A-2 7:1 (1969).

19. Burnett, G. M. and Riches, K. M., Oxidation of Nylon Model Systems, J. Chem. Soc. B 12:1229 (1966).

20. Carlsson, D. J. and Wiles, D. M., Photooxidation of Polypropylene Films IV: Surface Changes Studied by Attenuated Total Reflection Spectroscopy, Macromolecules 4:174 (1971).

21. Carrington, A. and McLachlan, A. D. Introduction to Magnetic Resonance with Applications to Chemistry and Chemical Physics. New York: Harper and Row, 1967.

22. Carter, M. E. Essential Fiber Chemistry. New York: Marcel Dekker, 1971.

23. Chappell, S. E., Sauer, J. A. and Woodward, A. E., Effects of High Energy Irradiation on Polypropylene, J. Polym. Sci. A 1:2805 (1963).

24. Charlesby, A., Effect of High Energy Radiation on Long Chain Polymers, Nature 171:167 (1953).

25. Charlesby, A. Atomic Radiation and Polymers, Vol. 1 (International Series of Monographs on Radiation Effects in Materials). London: Pergamon Press, 1960.

26. Coblentz, W. W., Correlation of Bioclimatic Ultraviolet and Total Solar Radiation in Washington, D. C., 1941-1948, Bull. Am. Met. Soc. 30:204 (1949).

27. Collins, R. L., Crystallinity in Polyethylene by Nuclear Resonance, Bull. Am. Phys. Soc. 1:216 (1956).

28. Crank, J. and Park, G. S. Diffusion in Polymers. London: Academic Press, 1968.

29. Davis, G. T. and Taylor, H. S., Diffusion Kinetics of Orange II in Nylon 66, Text. Res. J. 35:405 (1965).

30. Dean, J. D., Fleming, C. M. and O'Connor, R. T., Effects of Unfiltered Carbon Arc Light in Accelerated Weathering of Cotton and Other Textiles, Text. Res. J. 22:609 (1952).

31. Deeley, C. W., Woodward, A. E. and Sauer, J. A., Effect of Irradiation on Dynamic Mechanical Properties of 6-6 Nylon, J. Appl. Phys. 28:1124 (1957).

32. Dumbleton, J. H., Bell, J. P. and Murayama, T., The Effect of Structural Changes on Dye Diffusion in Poly(ethylene terephthalate), J. Appl. Polym. Sci. 12:2491 (1968).

33. Egerton, G. S., Attle, E. and Rathor, M. A., Photolytic Degradation of Textile Fibres in the Far Ultraviolet, Nature 5053:1087 (1966).

34. Egerton, G. S. and Fitton, S. L., Formation of Free Radicals in Polymer Films on Irradiation, Nature 178:41 (1956).

35. Egerton, G. S. and Shah, K. M., The Effect of Temperature on the Photochemical Degradation of Textile Materials, Part I: Degradation Sensitized by Titanium Dioxide, Text. Res. J. 38:130 (1968).

36. Flory, P. J. Principles of Polymer Chemistry. Ithaca: Cornell University Press, 1953.

37. Fujiwara, S., Ayao, A. and Shinohara, K., Nuclear Magnetic Resonance in Irradiated Polyethylene, J. Chem. Phys. 26:1343 (1957).

38. Fuschillo, N. and Sauer, J. A., Nuclear Magnetic Resonance and Crystallinity in Polyethylene and Nylon, Bull. Am. Phys. Soc. 2:125 (1957).

39. Fuschillo, N. and Sauer, J. A., Proton Resonance in Neutron and Gamma-irradiated Polyethylene, J. Chem. Phys. 26:1348 (1957).

40. Glick, R. E., Gupta, R. P., Sauer, J. A. and Woodward, A. E., Proton Magnetic Resonance of Poly (hexamethylene adipamide), J. Polym. Sci. 42:271 (1960).

41. Glick, R. E. and Phillips, R. C., Proton Magnetic Resonance Spectra of Variously Treated Nylon 66, J. Polym. Sci. A-2 3:1885 (1965).

42. Gupta, R. P., Nuclear Magnetic Resonance Study of Polyethylene Crystals, Makro. Chemie 42:248 (1960).

43. Gupta, R. P., Nuclear Magnetic Resonance Investigation on Isotactic, Atactic, and Deuterated Isotactic Polypropylene, Kolloid-Zeit. 174:73 (1961).

44. Gupta, R. P., Proton Magnetic Resonance of Neutron Irradiated Polypropylene, Kolloid-Zeit. 174:74 (1961).

45. Gupta, R. P., Proton Magnetic Resonance Investigation of the Orientation of Hydrogen Bonds in Nylon 66, Poly (vinyl alcohol), and Cotton Yarn, J. Appl. Polym. Sci. 10:1535 (1966).

46. Hargreaves, G., Radiative Degradation of Nylon 66 Filaments as Shown with a Polarizing Microscope, Text. Res. J. 32:784 (1962).

47. Hargreaves, G., Molecular Changes in Polyamide and Elastomeric Polymers Due to Nuclear, Ultraviolet, and Thermal Radiation, Aero. Mat. Lab. Found. Res. Proj. NAEC-AML(16)-R360FR101 (1963).

48. Heacock, J. F., Mallory, F. B. and Gay, F. P., Photodegradation of Polyethylene Film, J. Polym. Sci. A-1 6:2921 (1968).

49. Heuvel, H. M. and Lind, K. C. J. R., Electron Spin Resonance Study of the Initial Reaction of the Photodegradation of Nylon 6, J. Polym. Sci. A-2 8:401 (1970).

50. Hill, A. V., Diffusion of Oxygen and Lactic Acid through Tissues, Proc. Royal Soc. London 104B:74 (1928-29).

51. Hirt, R. C. and Searle, N. Z. "Energy Characteristics of Outdoor and Indoor Exposure Sources and their Relation to the Weatherability of Plastics." Weatherability of Plastic Materials (Applied Polymer Symposia No. 4), edited by M. R. Kamal. New York: Interscience, 1967.

52. Hopper, M. E., McGregor, R. and Peters, R. H., Some Observations on the Concentration Dependence of Diffusion Coefficients of Acid Dyes on Nylon, J. Soc. Dyers and Colourists 86:117 (1970).

53. Huggins, M. L., Molecular Weights of High Polymers, Ind. and Eng. Chem. 35:980 (1943).

54. Jellinek, H. H. G. "Fundamental Degradation Processes Relevant to Outdoor Exposure of Polymers." Weatherability of Plastic Materials (Applied Polymer Symposia No. 4), edited by M. R. Kamal. New York: Interscience, 1967.

55. Jellinek, H. H. G. and Chaudhuri, A. K., Inhibited Degradation of Nylon 66 in Presence of Nitrogen Dioxide, Ozone, Air and Near Ultraviolet Radiation, J. Polym. Sci. A-1 10:1773 (1972).

56. Jones, D. W., Proton Magnetic Resonance in Nylon 66, Polymer 2:203 (1961).

57. Kachan, A. A., Sirata, A. G., Chernauvskii, G. V. and Shrubovich, V. A., A Comparison of Radiation and Photochemical Crosslinking of Polyethylene, Vysokomol. soyed. A10(3):471 (1968). (Through Polym. Sci.:USSR 10:546 (1968).

58. Karpov, V. L., Yurkevich, V. G., Kavalerova, L. M., Petrova, N. L., Glazkovskii, Y. V. and Egovrova, E. L., The Radiation Stability of Some Synthetic Fibres, Khim. Volokna 1:30 (1969). (Through Fiber Chem., Vol. 1, 1969.)

59. Kolarik, J. and Janacek, J., Secondary (β) Relaxation Process of Alkaline Polycaprolactam Swollen by Low Molecular Weight Substances, J. Polym. Sci. C 16:441 (1967).

60. Kusy, R. P. and Turner, D. T., Influence of Gamma-irradiation on the Transition Temperatures of Crystalline Poly(tetra fluoroethylene), J. Polym. Sci. A-1 10:1745 (1972).

61. Lawton, E. J., Bueche, A. M. and Balwit, J. S., Irradiation of Polymers by High Energy Electrons, Nature 172:72 (1953).

62. Lenz, R. W. Organic Chemistry of Synthetic High Polymers. New York: Interscience, 1968.

63. Little, A. H. and Parsons, H. L., The Weathering of Cotton, Nylon, and Terylene Fabrics in the United Kingdom, Text. Inst. J. 58:449 (1967).

64. Little, K., Some Effects of Irradiation on Nylon and Polyethylene Terephthalate, Nature 173:680 (1954).

65. Magee, J. L., Theory of Radiation Chemistry. I. Some Effects of Variation in Ionization Density, J. Am. Chem. Soc. 73:3270 (1951).

66. Majury, T. G. and Pinner, S. H., The Irradiation of Polycaprolactam with Gamma-rays and Electrons, J. Appl. Chem. (London) 8:168 (1958).

67. Marek, B. and Lerch, E., Photodegradation and Yellowing of Polyamides, J. Soc. Dyers and Colourists 81:481 (1965).

68. Matsumae, K., Watanabe, M., Nishioka, A. and Ichimiya, T., Viscosity and Elasticity of Gamma-irradiated Polytetrafluoroethylene Resin above the Melting Point, J. Polym. Sci. 28:653 (1958).

69. McCall, D. W. and Anderson, E. W., Molecular Motion in Polyethylene III, J. Polym. Sci. A 1:1175 (1963).

70. McCall, D. S. and Anderson, E. W., Proton Magnetic Resonance in Polyamides, Polymer 4:93 (1963).

71. McGregor, R. and Peters, R. H., The Effect of Rate of Flow on Rate of Dyeing I-The Diffusional Boundary Layer in Dyeing, J. Soc. Dyers and Colourists 81:393 (1965).

72. McGregor, R. and Peters, R. H., Some Observations on the Relation between Dyeing Properties and Fibre Structure, J. Soc. Dyers and Colourists 84:267 (1968).

73. McGregor, R., Peters, R. H. and Petropolous, J. H., Diffusion of Dyes in Polymer Films. Part 3: Naphthalene Scarlet 4R in Nylon 66, Trans. Faraday Soc. 58:1054 (1962).

74. McMahon, P. E., Wide Line Nuclear Magnetic Resonance Studies of Oriented Nylon 66, J. Polym. Sci. A-2 4:639 (1966).

75. McMahon, P. E., Effect of Orientation on Molecular Motion in Nylon 66, Polym. Letters 4:43 (1966).

76. Moore, R. F., The Photochemical Degradation of Polyamides and Related Model N-Alkylamides, Polymer 4:493 (1963).

77. Morton, M. I. "Tensile Behavior of Irradiated Nylon." Ph. D. dissertation, University of Minnesota, 1970.

78. Munden, A. R. and Palmer, H. J., Measurement of Dyeing Properties and Correlation with Orientation in Nylon Yarn, J. Text. Inst. 41:P609 (1950).

79. Olf, H. G. and Peterlin, A., Nuclear Magnetic Resonance Observations of Drawn Polymers II: Segment Mobility (Gamma Process) in Polyethylene Single Crystals, Bulk Material, and Drawn Samples, Kolloid-Zeit, 212:12 (1966).

80. Olf, H. G. and Peterlin, A., Nuclear Magnetic Resonance Observations of Drawn Polymers. VII: Nylon 6.6 Fibers, Preprint No. 294, Camille Dreyfus Laboratory (October 1970).

81. Olf, H. G. and Peterlin, A., Nuclear Magnetic Resonance Observations of Drawn Polymers. IX: Chain Mobilization and Water Mobility in Nylon 66, Preprint No. 317, Camille Dreyfus Laboratory (April 1971).

82. Peterlin, A. and Meinel, G. "Calorimetry of Drawn and Rolled Linear Polyethylene of High and Low Crystallinity." Analytical Calorimetry, Vol. 2, edited by R. S. Porter and J. F. Johnson. New York: Plenum Press, 1970.

83. Peters, H. W. and Turner, J. C., Investigations into the Dyeing of Continuous-filament Nylon with Disperse and Anionic Dyes, J. Soc. Dyers and Colourists 74:252 (1958).

84. Peters, H. W. and White, T. R., The Effect of Heat-setting Treatments on the Dyeing Behaviour of Nylon Yarns and Fabrics, J. Soc. Dyers and Colourists 77:601 (1961).

85. Peters, R. H., Nylon Fibre: A Study of the Mechanism of the Dyeing Process with Acid Dyes, J. Soc. Dyers and Colourists 61:95 (1945).

86. Pomeroy, E. R. and Stevens, H. T., The Effects of Weather on Drapery Lining Fabrics in Two Geographic Regions, J. Home Econ. 56:607 (1964).

87. Rafikov, S. R. and Tsi-pin, S., Chemical Transformations of Polymers--V. Photochemical Transformations of Polycaproamide under Ultra-violet Irradiation in Vacuo, Vysokomol, soyed. 3(1):56 (1961). (Through Polym. Sci.:USSR 3:6 (1961).

88. Rayonet Photochemical Reactor Operating Instructions, The Southern New England Ultraviolet Co., Middletown, Connecticut.

89. Rosenbaum, S., Dyeing of Polyacrylonitrile Fibers: I. Rates of Diffusion with Malachite Green and Diffusion Model, J. Appl. Polym. Sci. 7:1225 (1963).

90. Rosenbaum, S., Role of Sites in Dyeing, Part I: Equilibria, Rates, and their Interdependence, Text. Res. J. 34:159 (1964).

91. Rosenbaum, S., Role of Sites in Dyeing, Part II: Diffusion, Text. Res. J. 34:291 (1964).

92. Rutherford, H. A. "Textiles." Radiation Effects on Organic Materials, edited by R. O. Bolt and J. G. Carroll. New York: Academic Press, 1963.

93. Salvin, V. S., The Effect of Dyes on Light Degradation of Nylon, Am. Dyestuff Reptr. 57:156 (1968).

94. Searle, N. Z. "Photodegradation of Polymers." Analytical Photochemistry and Photochemical Analysis: Solids, Solutions, and Polymers, edited by J. M. Fitzgerald. New York: Marcel Dekker, 1971.

95. Sharkey, W. H. and Mochel, W. E., Mechanism of the Photooxidation of Amides, J. Am. Chem. Soc. 81:3000 (1959).

96. Sharma, R. K. and Mandelkern, L., The Density of Polyethylene Crystallized in the Bulk and from Dilute Solution, Macromolecules 2:266 (1969).

97. Sherwood, P. W., Protecting Textiles from Ultraviolet Degradation, Text. Mfr. 90:54 (1964).

98. Silverstein, R. M. and Bassler, G. C. Spectrometric Identification of Organic Compounds, 2d ed. New York: John Wiley and Sons, 1968.

99. Singleton, R. W. and Cook, P. A. C., Factors Influencing the Evaluation of Actinic Degradation of Fibers, Part II: Refinement of Techniques for Measuring Degradation in Weathering, Text. Res. J. 39:43 (1969).

100. Singleton, R. W., Kunkel, R. K. and Sprague, B. S., Factors Influencing the Evaluation of Actinic Degradation of Fibers, Text. Res. J. 35:228 (1968).

101. Sisman, O., Parkinson, W. W. and Bopp, C. D. "Polymers." Radiation Effects on Organic Materials, edited by R. O. Bolt and J. G. Carroll. New York: Academic Press, 1963.

102. Slichter, W. P., Molecular Motion in Polyamides, J. Polym. Sci. 35:77 (1958).

103. Slichter, W. P., Nuclear Magnetic Resonance Studies of Multiple Relaxations in Polymers, J. Polym. Sci. C 14:33 (1966).

104. Slichter, W. P., Nuclear Resonance Studies of Motion in Polymers, Makro. Chemie 34:67 (1959).

105. Slichter, W. P. and Davis, D. D., Nuclear Magnetic Resonance Studies of Molecular Motion in Natural Rubber, J. Appl. Phys. 34:98 (1963).

106. Slichter, W. P. and Mandell, E. R., Molecular Structure and Motion in Irradiated Polyethylene, J. Phys. Chem. 62:334 (1958).

107. Slichter, W. P. and McCall, D. W., Note on the Degree of Crystallinity in Polymers as found by Nuclear Magnetic Resonance, J. Polym. Sci. 25:109 (1957).

108. Slonim, I. Ya. and Lyubimov, A. N. The NMR of Polymers. New York: Plenum Press, 1970.

109. Starkweather, Jr., H. W. and Moynihan, R. E., Density, Infrared Absorption, and Crystallinity of 66 and 610 Nylon, J. Polym. Sci. 22:363 (1956).

110. Statton, W. O., Segment Mobility in Fibers as Shown by High Temperature Nuclear Resonance, Am. Dyestuff Reptr. 54:P314 (1965).

111. Stephenson, C. V., Moses, B. C., Burks, Jr., R. E., Coburn, Jr., W. C. and Wilcox, W. S., Ultraviolet Irradiation of Plastics. II. Crosslinking and Scission, J. Polym. Sci. 55:465 (1961).

112. Stephenson, C. V., Moses, B. C. and Wilcox, W. S., Ultraviolet Irradiation of Plastics. I. Degradation of Physical Properties, J. Polym. Sci. 55:451 (1961).

113. Stephenson, C. V., Lacey, Jr., J. C. and Wilcox, W. S., Ultraviolet Irradiation of Plastics III. Decomposition Products and Mechanisms, J. Polym. Sci. 55:477 (1961).

114. Subramanian, R. V. R. and Talele, T. V., Photodegradation of Nylon 6, Text. Res. J. 42:207 (1972).

115. Sweet, G. E. and Bell, J. P., Multiple Endotherm Melting Behavior in Relation to Polymer Morphology, J. Polym. Sci. A-2 10:1273 (1972).

116. Szöcs, F., Becht, J. and Fischer, H., On Free Radical Recombination in Irradiated and in Strained Fibres of Polyamides, Eur. Polym. J. 7:173 (1971).

117. Takagi, Y., Studies on the Drawing of Polyamide Fibers VI: Effect of Drawing on the Dye Diffusion Parallel to the Fiber Axis, J. Appl. Polym. Sci. 9:3887 (1965).

118. Tanford, C. Physical Chemistry of Macromolecules. New York: John Wiley and Sons, 1967.

119. Taylor, G. B., The Relation of the Viscosity of Nylon Solutions in Formic Acid to Molecular Weight as Determined by End-Group Measurements, J. Am. Chem. Soc. 69:635 (1947).

120. Taylor, G. B. The Distribution of the Molecular Weight of Nylon as Determined by Fractionation in a Phenol-Water System, J. Am. Chem. Soc. 69:638 (1947).

121. Taylor, H. A., Tincher, W. C. and Hamner, W. F., Photodegradation of Nylon 66. I. Phototendering by TiO_2, J. Appl. Polym. Sci. 14:141 (1970).

122. Tessler, S., Woodbury, N. T. and Mark, H., Application of the Density-Gradient Tube in Fiber Research, J. Polym. Sci. 1:437 (1946).

123. Teszler, O., Wilhart, H. and Rutherford, H. A., The Effect of Nuclear Radiation on Fibrous Materials, Part II: Dyeing Characteristics of Irradiated Cotton and Rayon, Text. Res. J. 28:131 (1958).

124. Thomas, R. J. Personal Communication.

125. Trommer, K. H., Recent Technology in the Dyeing of duPont Nylon Styling Yarns, Canadian Text. J. 85:31 (1968).

126. Vachon, R. N., Rebenfeld, L. and Taylor, H. S., Oxidative Degradation of Nylon 66 Filaments, Text. Res. J. 38:716 (1968).

127. Verma, G. S. P. and Peterlin, A., Electron Spin Resonance Study of Mechanically Stretched Nylon 6 Fibers, Kolloid-Zeit. 236:111 (1970).

128. Vickerstaff, T. The Physical Chemistry of Dyeing. London: Oliver and Boyd, 1954.

129. Wall, M. J. and Frank, G. C., A Study of the Spectral Distribution of Sun-sky and Zenon-arc Radiation in Relation to the Degradation of Some Textile Yarns. Part I: Yarn Degradation, Text. Res. J. 41:38 (1971).

130. Warwicker, J. O., The Structural Causes of the Dyeing Variations of Nylon Subjected to Dry Heat, J. Soc. Dyers and Colourists 86:303 (1970).

131. Wilson, C. W. and Pake, G. E., Nuclear Magnetic Resonance Determination of Degree of Crystallinity in Two Polymers, J. Polym. Sci. 10:503 (1953).

132. Winslow, F. H., Aloisio, C. J., Hawkins, W. L., Matreyek, W. and Matsuoka, S., Oxidative Crystallization of Polythene, Chem. and Ind. 63:1465 (1963).

133. Winslow, F. H. and Hawkins, W. L. "Some Weathering Characteristics of Plastics." Weatherability of Plastic Materials (Applied Polymer Symposia, No. 4), edited by M. R. Kamal. New York: Interscience, 1967.

134. Winslow, F. H., Matreyek, W. and Stills, S. M., Contrasts in Thermal and Photooxidation of Polyethylene, Polym. Preprints 7:390 (1966).

135. Woodward, A. E., Glick, R. E., Sauer, J. A. and Gupta, R. P., Proton Magnetic Resonance of Some Polyamides, J. Polym. Sci. 45:367 (1960).

136. Zimmerman, J., Spectra of Irradiated Polyamides, J. Appl. Polym. Sci. 2:181 (1959).

137. Zimmerman, J., Degradation and Crosslinking in Irradiated Polyamides and the Effect of Oxygen Diffusion, J. Polym. Sci. 46:151 (1960).

APPENDIX

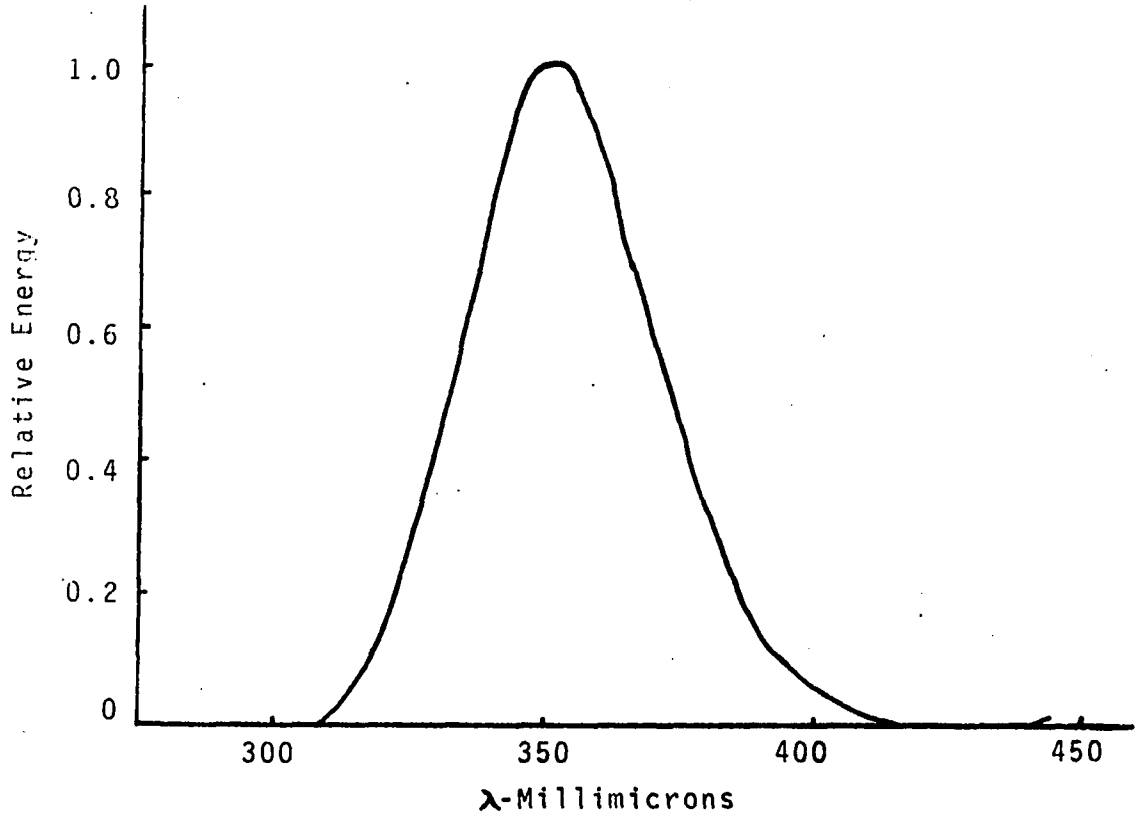

Figure 27 - Spectral distribution of RPR-3500 A lamps used in the Rayonet Reactor (88). Approximately 24 watts of "black light," about 90% in the 3500 Å range; approximately 1.5 to 5 x 10^{16}/sec/cm^3 photons of "black light;" and an intensity at the center of the reactor for new lamps of 9.2 mw/cm^2 were recorded at a reactor temperature of 44°C.

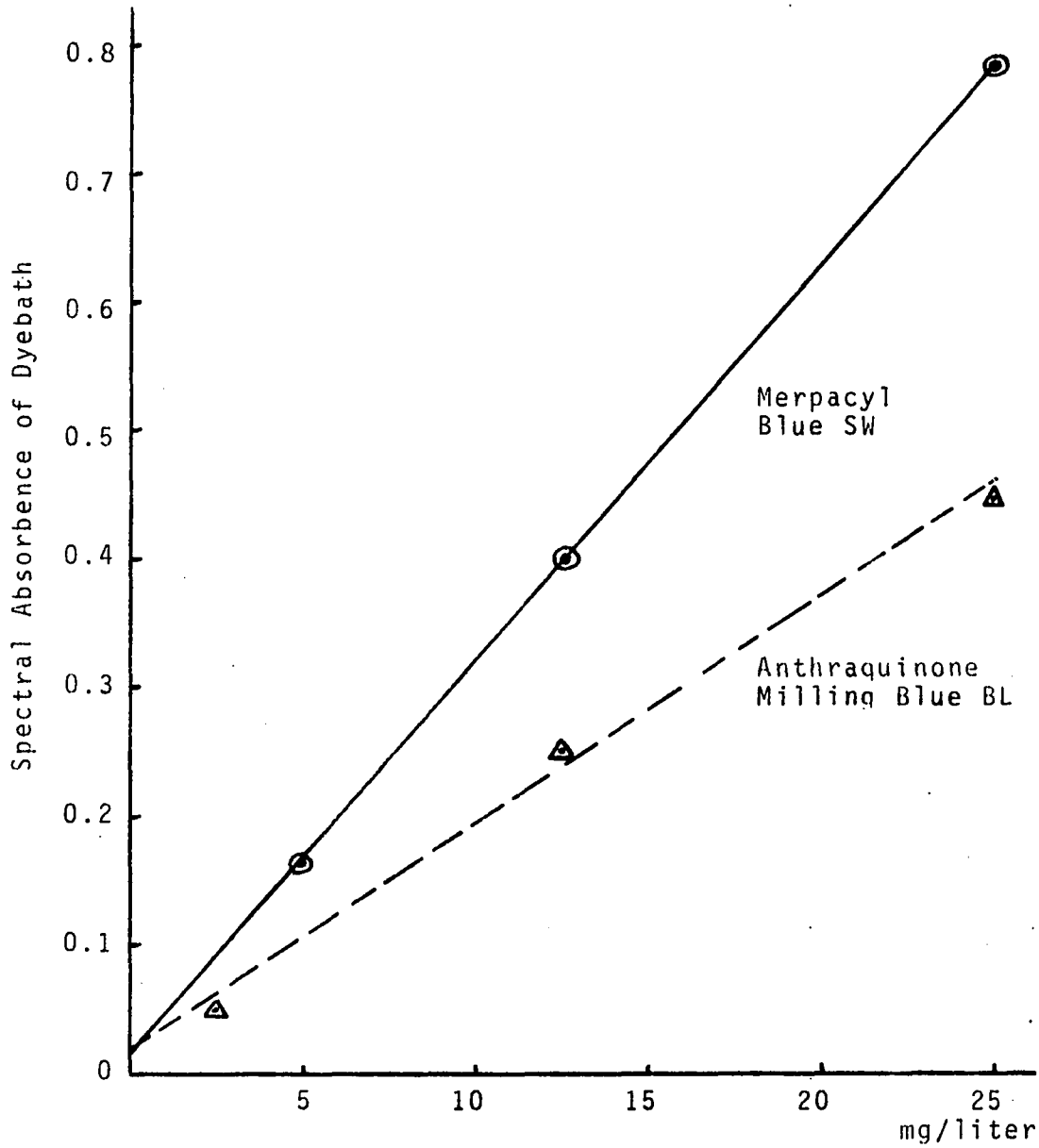

Figure 28 - Relationship of spectral absorbence and dyebath concentration for two diagnostic dyes.

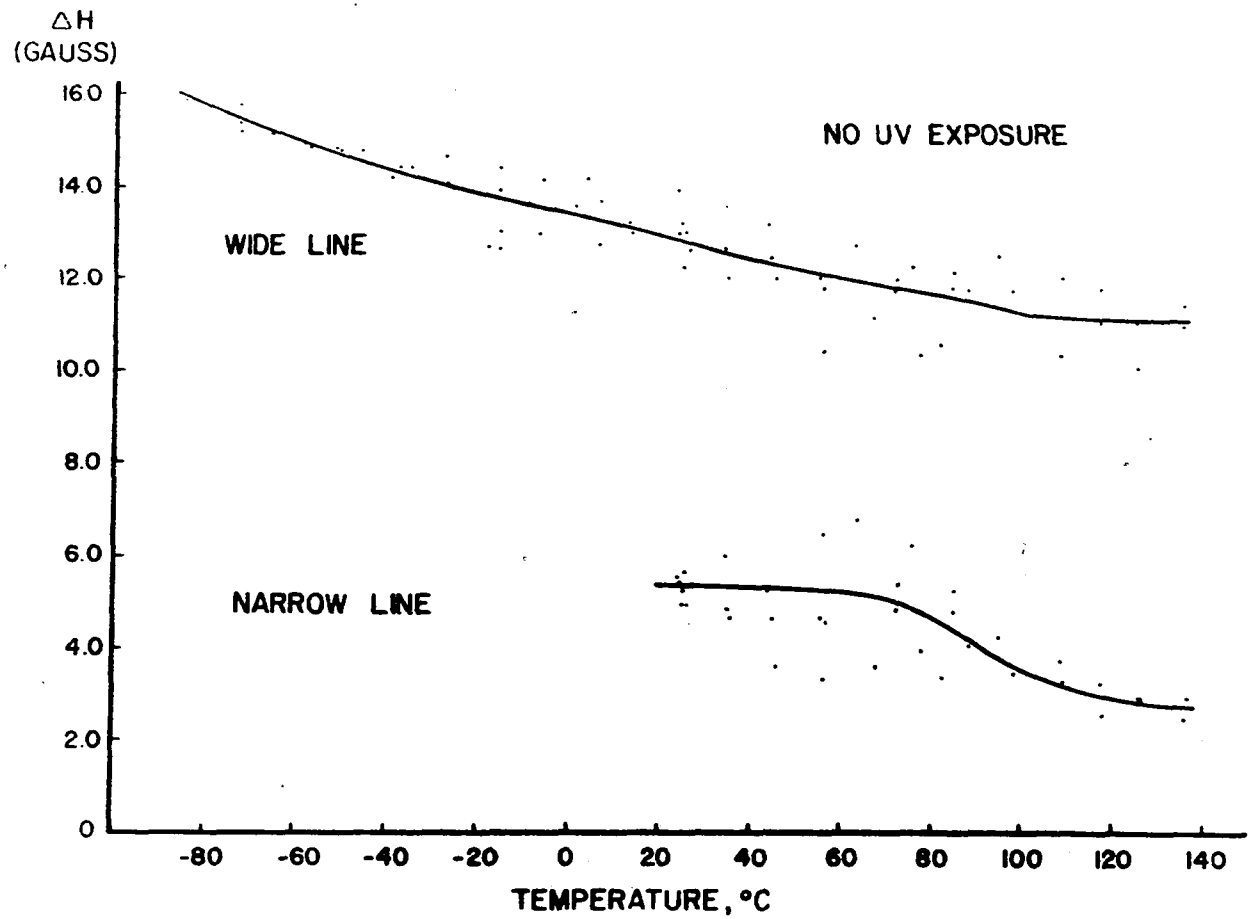

Figure 29 - Line width of wide and narrow components of the NMR line for nylon 66 exposed to UV for 0 hours.

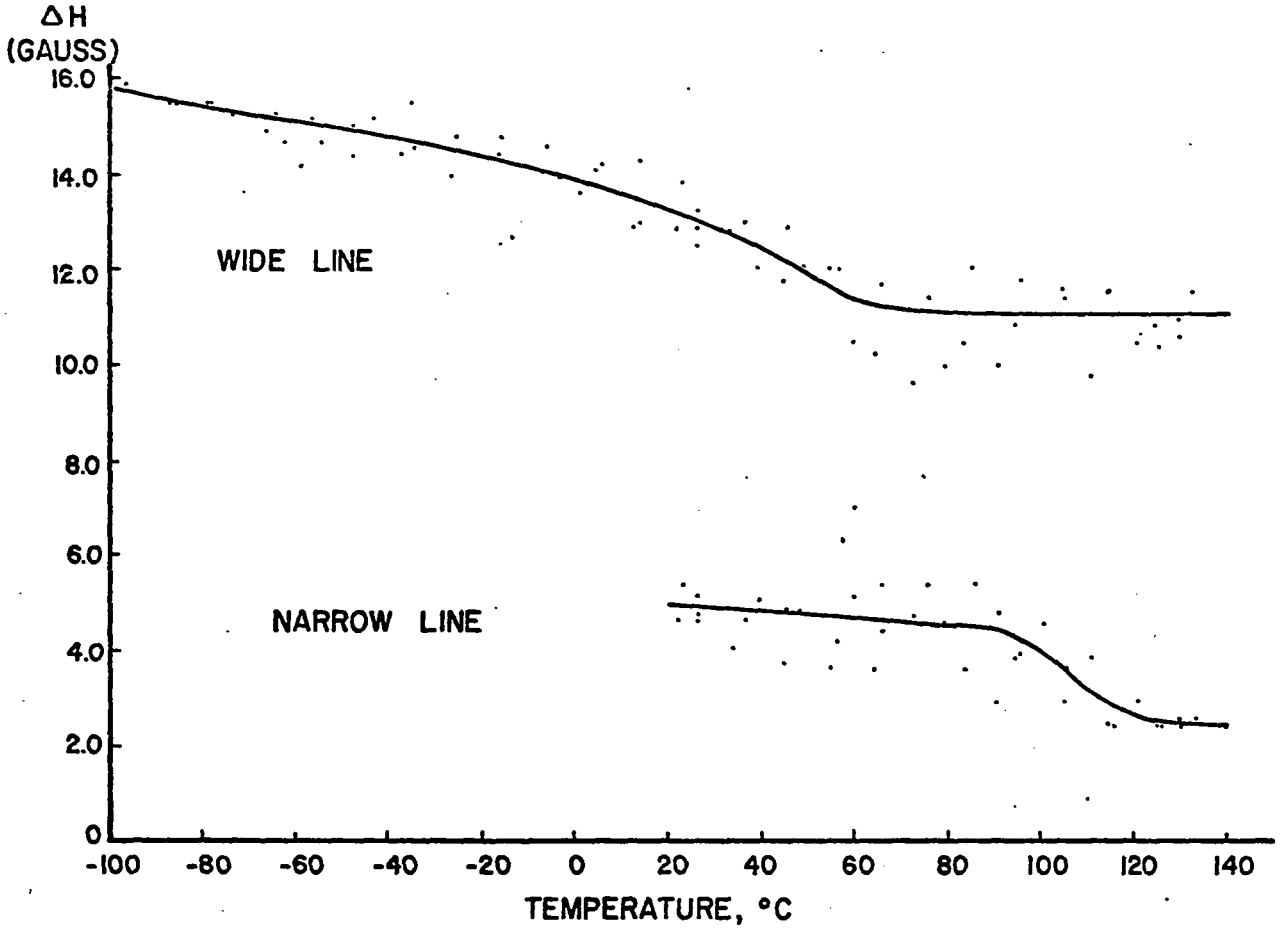

Figure 30 - Line width of wide and narrow components of the NMR line for nylon 66 exposed to UV for 240 hours.

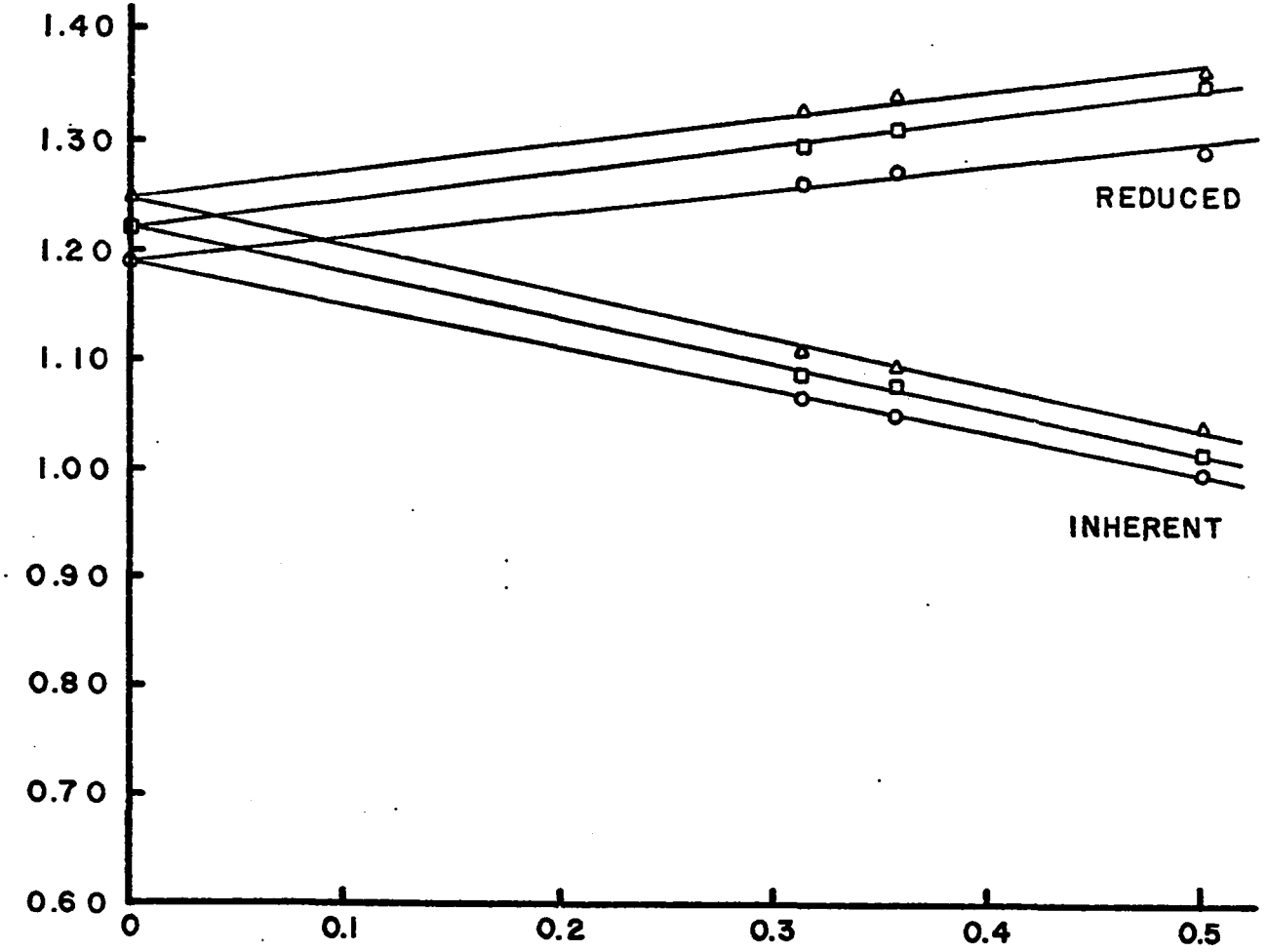

Figure 31 - Intrinsic viscosity for three nylon 66 control samples obtained by extrapolation of reduced and inherent viscosities to zero concentration.

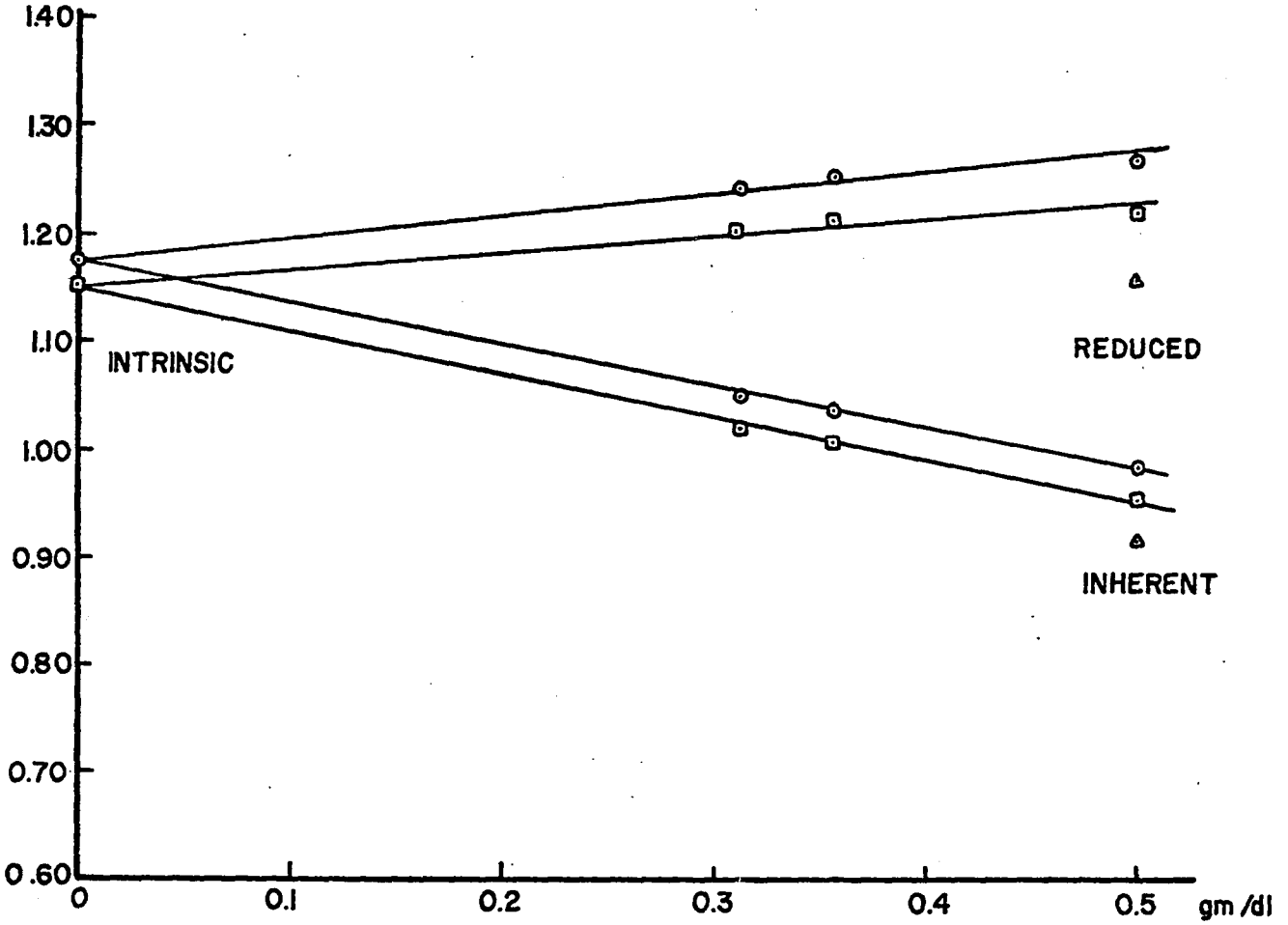

Figure 32 - Intrinsic viscosity for two nylon 66 yarns exposed to UV for 72 hours obtained by extrapolation of reduced and inherent viscosities to zero concentration.

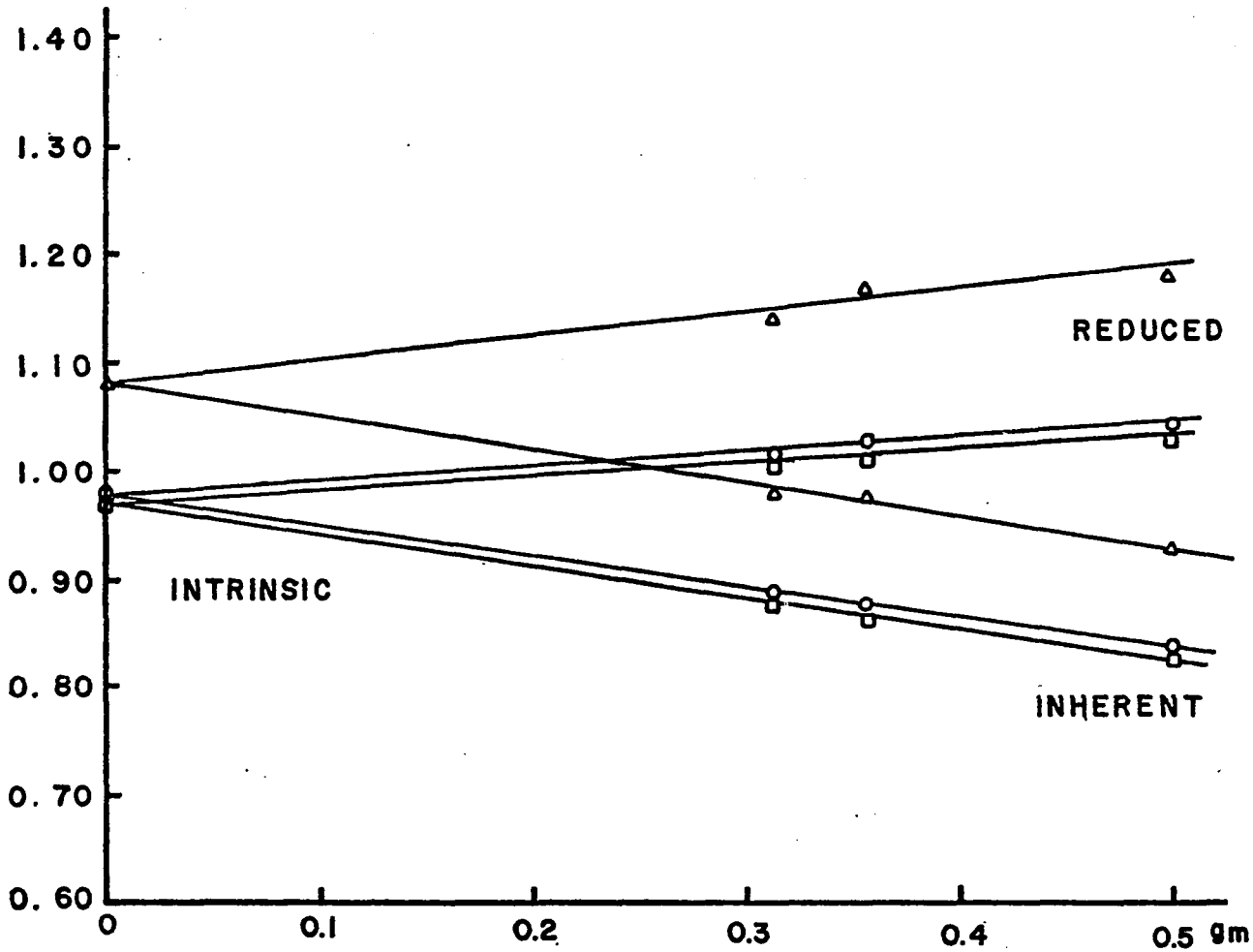

Figure 33 - Intrinsic viscosity for three nylon 66 yarns exposed to UV for 142 hours obtained by extrapolation of reduced and inherent viscosities to zero concentration.

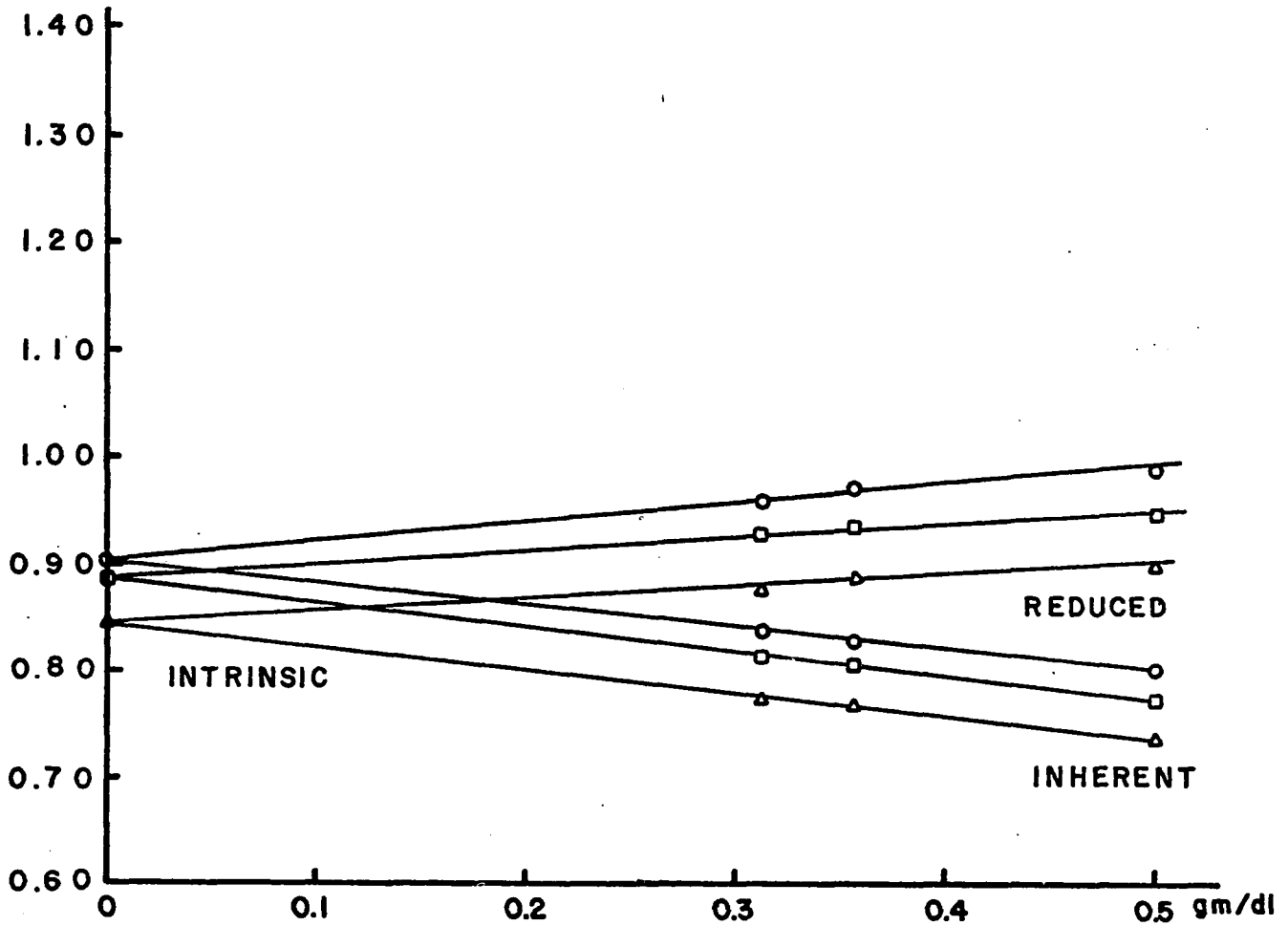

Figure 34 - Intrinsic viscosity for three nylon 66 yarns exposed to UV for 240 hours obtained by extrapolation of reduced and inherent viscosities to zero concentration.

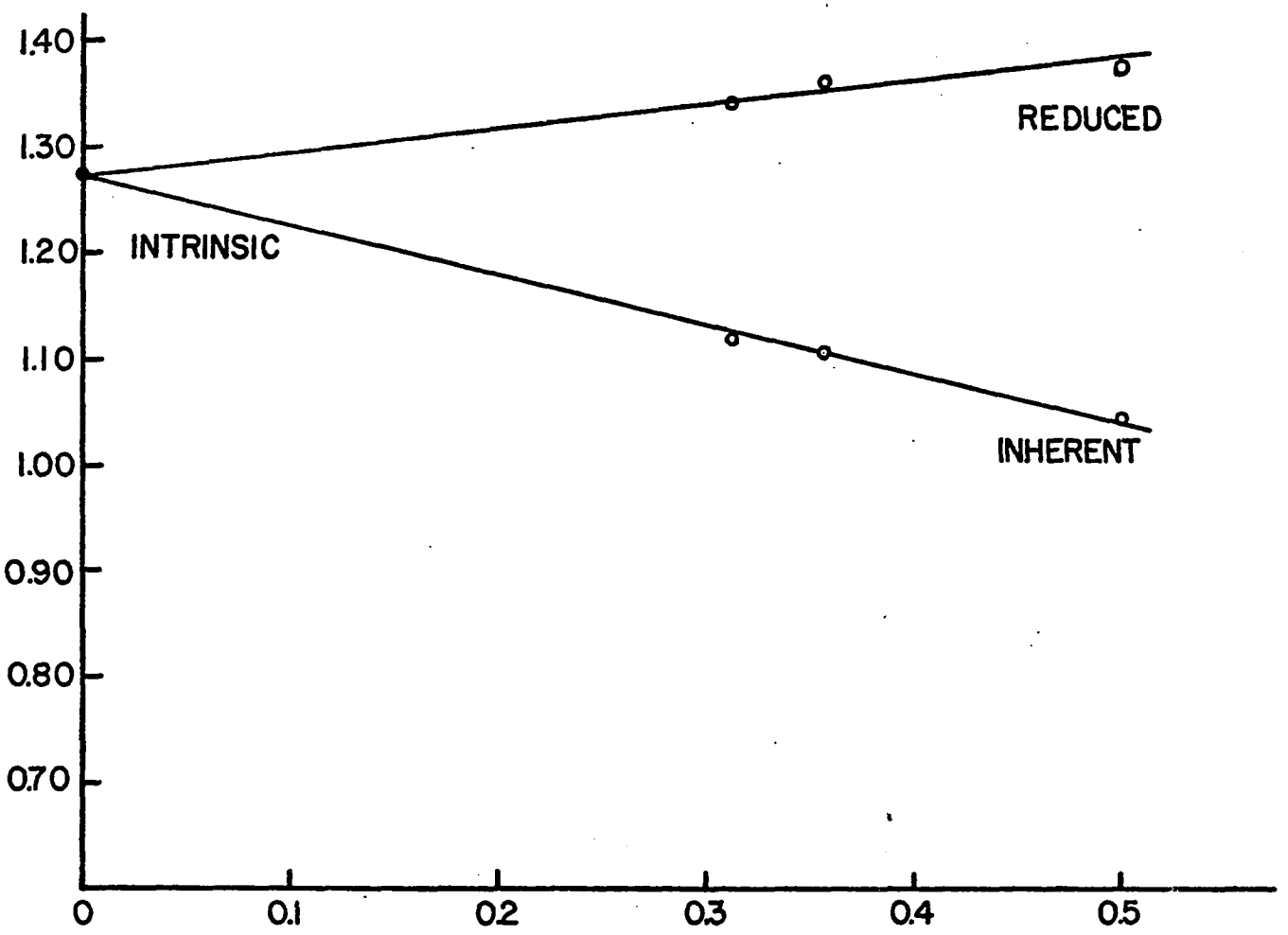

Figure 35 - Intrinsic viscosity for a nylon 66 yarn exposed 240 hours at 52°C with no UV obtained by extrapolation of reduced and inherent viscosities to zero concentration.

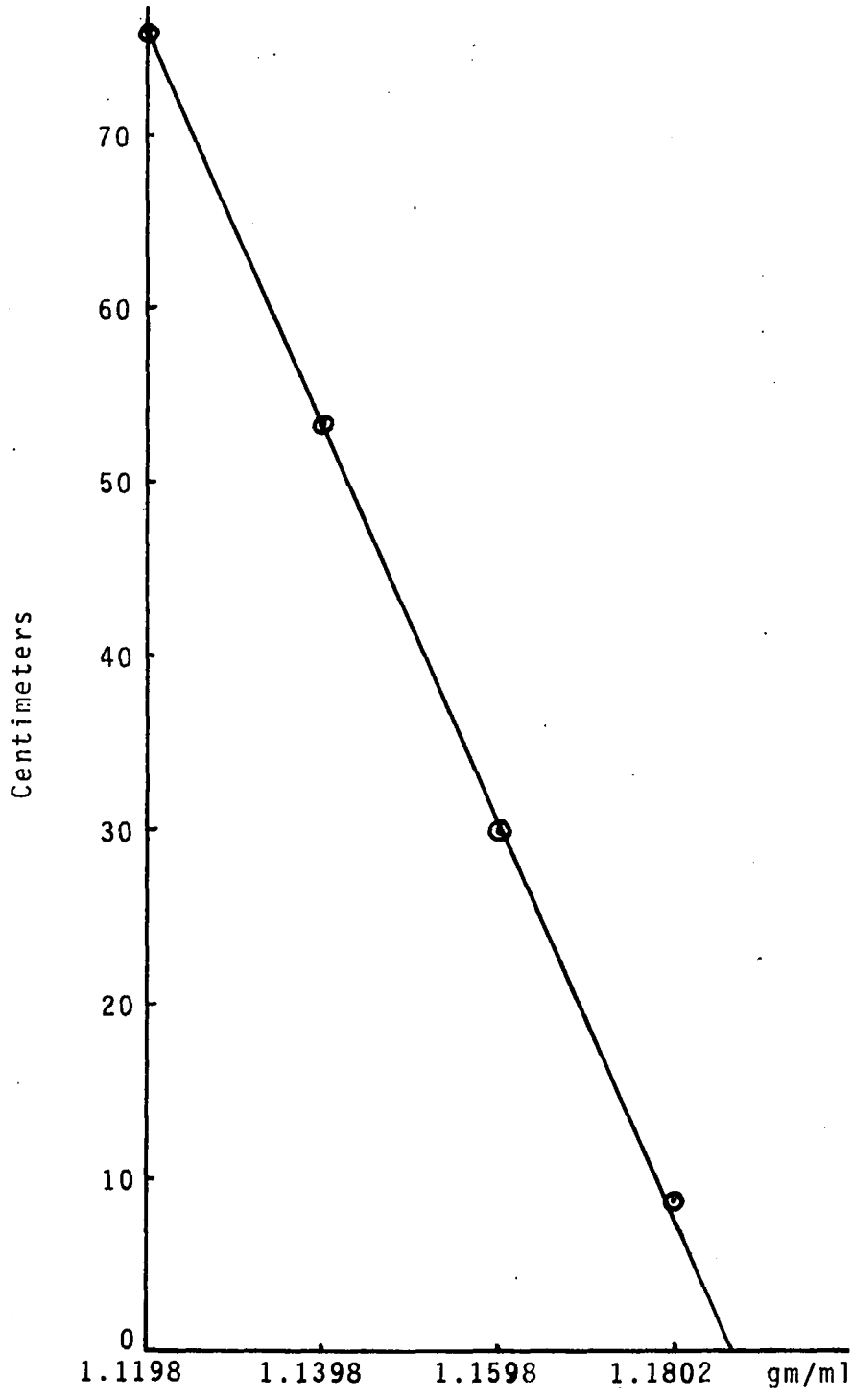

Figure 36 - Calibration of density gradient column.